3. El catió Ag^+ com a model en l'estudi de Cu-MT

3.1. Introducció

Amb l'objectiu principal d'esbrinar la similitud de comportament de Ag(I) i Cu(I) en coordinar-se a les MT, primerament s'han valorat amb Ag(I) les formes Zn-MT i les apo-formes corresponents, tant de la MT sencera com dels seus dominis α i β per separat. Un cop coneguts els tres sistemes Ag-MT, s'ha comparat el comportament de Ag(I) i Cu(I) envers aquestes proteïnes considerant les dades publicades sobre la coordinació de Cu(I) a MT recombinant [14].

Aquest capítol consta de dos treballs. El primer és un article, ja publicat, en el qual l'autor d'aquesta tesi doctoral únicament va participar en la part corresponent als estudis amb Ag(I). En aquest treball es va realitzar un primer estudi comparatiu Ag-Cu enfront el fragment β de MT utilitzant únicament les dades obtingudes mitjançant espectroscòpia òptica. Cal destacar que en el moment de la realització del treball esmentat, l'estudi de la coordinació metàl·lica al fragment β de MT era pràcticament inexistent degut als inconvenients associats amb la seva obtenció ja sigui per síntesi química o a partir de la digestió parcial de la proteïna nativa. Això va provocar que aquest treball es publiqués separadament i constituís així el primer article dedicat a l'estudi de la coordinació de metalls monovalents al fragment β de MT recombinant de mamífer. El segon treball que s'inclou en aquest capítol és un manuscrit en vies de publicació, en el qual s'ha estudiat en profunditat la coordinació de la Ag(I) tant a la MT com als seus fragments α i β. Aquest treball, on s'han emprat tant dades d'espectroscòpia òptica com d'espectrometria de masses, ha permès comparar amb detall els sistemes Ag-MT i Cu-MT.

Article 3

A new insight into the Ag^+ and Cu^+ binding sites in the metallothionein β domain

Journal of Inorganic Biochemistry, 1999, **73(1,2)**, 57-64

ELSEVIER

Journal of Inorganic Biochemistry 73 (1999) 57–64

JOURNAL OF Inorganic Biochemistry

A new insight into the Ag^+ and Cu^+ binding sites in the metallothionein β domain

Roger Bofill [a], Òscar Palacios [a], Mercè Capdevila [a], Neus Cols [b],, Roser González-Duarte [b], Sílvia Atrian [b], Pilar González-Duarte [a,*]

[a] *Departament de Química, Facultat de Ciències, Universitat Autònoma de Barcelona, Bellaterra, E-08193 Barcelona, Spain*
[b] *Departament de Genètica, Facultat de Biologia, Universitat de Barcelona, Avinguda Diagonal 645, E-08071 Barcelona, Spain*

Received 23 July 1998; received in revised form 23 October 1998; accepted 16 November 1998

Abstract

The copper(I) and silver(I) binding properties of the β fragment of recombinant mouse metallothionein 1 have been studied by electronic absorption and circular dichroism spectroscopy. When possible, the stoichiometry of the species formed was confirmed by electrospray mass spectrometry. The behaviour observed differs from that reported for the native protein. Titration of either Zn_3-βMT at pH 7 or apo-βMT at pH 3 with Cu^+ leads to the formation of species having the same stoichiometry and structure: Cu_6-βMT, Cu_7-βMT and Cu_{10}-βMT. In the first stage of the titration of Zn_3-βMT with Cu^+ at pH 7 one additional species of formula Cu_4Zn_1-βMT was detected. In contrast, the titration of Zn_3-βMT at pH 7.5 and of apo-βMT at pH 2.5 with Ag^+ proceeds through different reaction pathways, affording Zn_xAg_3-βMT, Ag_6-βMT and Ag_9-βMT or Ag_3-βMT, Ag_6-βMT and Ag_9-βMT, respectively. The CD envelope corresponding to species with the same stoichiometric ratio, Ag_6-βMT and Ag_9-βMT, indicates that they have a different structure at each pH value. On the basis of the differences observed, the postulated similarity between copper and silver binding to metallothionein may be questioned.

Keywords: Recombinant β-metallothionein; Metallothionein; Copper(I) binding; Silver(I) binding; β Fragment

1. Introduction

Metallothioneins (MT) constitute a well-defined group of low-molecular-weight cysteine-rich metal-binding proteins, widely distributed in nature and generally considered responsible for metal homeostasis and detoxification [1,2]. To date most spectroscopic and chemical studies on the metal-binding properties of MT have been carried out with proteins isolated from mammalian organs. Relatively few studies have been undertaken with synthetic MT, and even fewer with the protein obtained by genetic engineering. With the aim of laying the groundwork for primary structural modifications of MT [3], we used the recombinant DNA approach to synthesize mouse Zn_7-MT and the corresponding α (Zn_4-αMT) and β (Zn_3-βMT) domains. Synthesis in *E. coli* rendered preparations of high purity and allowed us to report the bioproduction of the β domain for the first time [4]. In addition, cadmium titrations of recombinant mouse Zn_7-MT and Zn_4-αMT, followed by absorption and CD spectroscopy, showed that they reproduce the behaviour observed for the native proteins [4,5]. Titration of Zn_3-βMT with $CdCl_2$ afforded Cd_3-βMT, Cd_4-βMT and Cd_9-βMT species, which we reported for the first time [4,6].

The synthesis of well-defined, separate α and β domains, particularly the latter, seems to be very promising. Recent studies suggest that the two domains of mammalian MT have evolved to perform different functional roles and that they have distinctive kinetic features. It has been proposed that the kinetically labile β domain may function in metal-exchange processes, whereas the kinetically more stable α domain may be important in detoxification [7]. Detailed knowledge of the behaviour of the isolated domains should contribute significantly to our understanding of the entire MT and corroborate the proposed independent behaviour of the α and β domains [8]. In addition, it has recently been reported that the structure of the β domain in mammalian MT bears close resemblance to the 3D structure in solution of the same domain in crab MT 1 [7]. Accordingly, our understanding of the main functions of crustacean MT is likely to be enhanced by the study of the mammalian β fragment behav-

* Corresponding author. Fax: +34-93-581-3101; E-mail: iqipilar@cc.uab.es

0162-0134/99/$ - see front matter
PII S0162-0134(98)10091-0

iour. However, until recently, the study of the β domain was hindered by the difficulties associated with its synthesis by means of the solid-phase or solution fragment-condensation techniques, or with its recovery and purification from living organisms.

Despite the high level of similarity found between the behaviour of native versus recombinant MT towards Cd(II) [4,5], the results obtained with Hg(II) [9] were different from those reported for the native proteins [10]. This finding prompted us to extend our studies to monovalent metal ions such as Cu(I) and Ag(I). Copper metallothioneins have been most extensively studied, mainly in vitro, yielding a variety of results on the Cu-binding stoichiometry [11–13]. Moreover, the spectral data for silver binding are claimed to be of interest, as they are believed to provide information on copper binding to MT. According to the literature, the close similarities displayed by Cu(I) and Ag(I) in their interaction with MT support the use of Ag^+ as an NMR-active analogue of Cu^+ in structural studies [13]. In this paper, we examine and compare the Cu(I) and Ag(I) binding abilities of the recombinant mouse β fragment at different pH values through the pattern of the CD and UV–Vis absorption spectra recorded during the corresponding titrations. Although little information is available on M^I-βMT (M^I=Cu, Ag) species, there appear to be differences in the behaviour of recombinant protein and native protein in their presence.

2. Experimental

2.1. Protein preparation and characterization

Expression assays, fermentator-scale cultures, purification of the fusion protein and recovery and analysis of the recombinant mouse Zn_3-βMT 1 fragment were performed as previously described [4]. Accordingly, the Zn_3-βMT species was obtained in a Tris–HCl buffer (50 mM, pH=7) except for those samples to be used in the Ag(I) titrations, which were obtained in Tris–$HClO_4$ (50 mM, pH=7), to avoid precipitation of AgCl. All protein solutions had a final concentration of about 300 μM. These were diluted and titrated with freshly prepared solutions of $[Cu(CH_3CN)_4]^+$ in CH_3CN/H_2O or Ag^+ in Milli-Q purified water at 25°C.

The apo-βMT proteins were prepared by acidification of the recombinant material with 10^{-2} M HCl until the pH was 3 for the Cu(I) titrations and with $ClCH_2COOH/ClCH_2COONa$ buffer at pH 2.5 for the Ag(I) titrations. At pH lower than 3.5 the Zn_3-βMT is entirely demetalled, according to the CD spectrum. In contrast, Cu(I) and Ag(I) can bind to S-Cys at low pH down to 1.5.

2.2. Metal solutions

Glassware, solutions and Chelex-100 used in metal-ion-binding studies were prepared as described [4]. Due to the known sensitivity of Cu(I) to both oxidation and disproportionation, the solutions of Cu^+ were prepared from $[Cu(CH_3CN)_4]ClO_4$ [14], in 30% (v/v) CH_3CN/H_2O. The concentration of copper was quantified by AAS using a Perkin-Elmer 2100 atomic absorption spectrometer. The absence of detectable Cu^{2+} in the freshly prepared Cu(I) solution, and after use as a titrating agent, was confirmed by the lack of EPR signal (Bruker ESP 300E; at 77 K). To avoid hydrolysis, Ag^+ solutions were prepared by dissolving $AgClO_4$ in aqueous $HClO_4$ of pH 0.5 and standardized by potentiometric titrations against standard NaCl solution [15]. The concentration of the Cu^+ or Ag^+ solution used as titrating agent was in the range 10^{-2}–10^{-3} M.

2.3. Metal-ion-binding reactions

Metal-binding experiments were carried out by sequentially adding molar ratio aliquots of concentrated Cu^+ or Ag^+ solution to a single solution of either Zn_3-βMT or apo-βMT. For each addition, the protein sample was allowed to react with the metal ion until the CD features became stable. Thus, the CD spectra were recorded every 10 min until subsequent CD spectra were fully coincident. Absorption studies were conducted in parallel with CD studies. At some points during the titrations, a 10 μl aliquot was withdrawn and saved for mass determination.

All manipulations involving the metal and protein solutions were performed in argon atmosphere and titrations were carried out at least in duplicate to ensure the reproducibility of each single point.

The pH for all experiments remained constant throughout. This was achieved differently in the case of Cu(I) or Ag(I) titrations. In Cu^+ titrations no buffers were needed to maintain the initial pH of the protein solution, 7 or 3. In contrast, the acidity of the Ag(I) solution required the addition of appropriate buffer solutions of Tris–$HClO_4$ (250 mM, pH 7.5) or $ClCH_2COOH/NaOH$ (20 mM, pH 2.5).

The electronic absorption measurements were performed in 1 cm capped quartz cuvettes on an HP-8452A diode array UV–Vis spectrophotometer. A Jasco spectropolarimeter (model J-715) interfaced to a computer was used for CD measurements. A Peltier PTC-351 S was used to maintain the temperature constant at 25°C in all the experiments. Both types of spectrum were corrected for the dilution effects and processed using the program GRAMS 32.

2.4. Chelex-100 experiments

The possibility that Zn(II) was bound to the protein in the M^I-βMT species (M^I=Cu or Ag) formed in the titrations of Zn_3-βMT at pH=7 was considered. In order to determine the zinc content in the $Zn_xM_y^I$-βMT species, a second titration was carried out until the suspected mixed-metal species was formed. Then, a small quantity of Chelex-100 was added to the solution following a procedure described elsewhere [4] and the sulfur, zinc and copper or silver contents of the supernatant and of the solutions obtained after treatment of the

resin with 2 M HNO_3 were analysed. Total sulfur, zinc and copper contents were measured by inductively coupled plasma atomic emission spectrometry (ICP-AES) [16] using a Thermo Jarrell Ash, Polyscan 61E at 182.040 nm (S), 213.856 nm (Zn) and 324.754 nm (Cu). For Ag(I)-containing samples, analogous elemental analyses were performed by inductively coupled plasma mass spectrometry (ICP-MS) on a Perkin-Elmer, Elan-6000 at 33.9679 uma (S) and 106.905 and 108.905 uma (Ag).

2.5. Molecular mass determination

The molecular mass of the Cu-βMT species contained in aliquots withdrawn from the titration experiments was determined by electrospray ionization mass spectrometry (ESI-MS) on a Fisons Platform II Instrument (VG Biotech) equipped with the Mass Lynx software provided by the manufacturer, calibrated using horse heart myoglobin (0.1 mg/ml). Two sets of conditions were required depending on the sample. For the Cu-βMT samples at pH 7: 10 μl of the βMT solution was injected at 25 μl/min; source temperature, 180°C; capillary counter electrode voltage, 4500 V; lens counter electrode voltage, 1000 V; cone potential, 30 V; *m/z* range, 1000 to 1800; scanning rate, 4 s/scan; interscan delay, 0.2 s. The liquid carrier was a 5:95 mixture of methanol and 3 mM ammonium formiate/ammonia at pH 7. For samples at pH 3: 10 μl of the βMT solution was injected at 30 μl/min; source temperature, 100°C; capillary counter electrode voltage, 4000 V; lens counter electrode voltage, 500 V; cone potential, 70 V; *m/z* range, 1000 to 1800; scanning rate, 3 s/scan; interscan delay, 0.4 s. The liquid carrier was a 50:50 mixture of acetonitrile and formic acid at pH 3. The ease of oxidation of Cu^+ in acidic media was avoided by adding mercaptoethanol (0.01%).

Unfortunately, the high concentrations of buffer required by the silver solutions to maintain the pH hampered the characterization of Ag-βMT species by ESI-MS. Studies to overcome this problem are now being performed.

Throughout this paper we refer to the mol equivalents of metal added in terms of 'x M^+' to stand for 'x mol equivalents of M^+' or 'a molar ratio M^+:protein of x'.

3. Results and discussion

The present study aims to determine the binding abilities of the recombinant βMT fragment in the presence of differing concentrations of Cu^+ and Ag^+. The M^I-βMT species, M^I = Ag(I), Cu(I), have been identified from saturation of the chiral intensity, changes in the UV–Vis absorption spectra and mass determination as increasing amounts of metal ions are added to the protein. The analysis of the behaviour of recombinant Zn_3-βMT at pH 7 towards M^I requires knowledge of the role played by the Zn atom. In other words, the interpretation of the spectral changes accompanying the addition of M^I to Zn_3-βMT must take into account the spectral signals due to the SCys → Zn^{2+} LMCT bands, which can overlap with the new bands related to copper- or silver-thiolate interactions. By using apo-βMT, we ensure that the binding site structure depends only on the incoming metal. Thus, titrations at two different pH values were carried out. These have allowed not only the evaluation of the masking effect of the Zn–SCys coordination but also determination of the stoichiometry of mixed-metal $Zn_xM^I_y$-βMT species.

3.1. Apo-βMT fragment

Parts (a)–(c) of Fig. 1 show the CD, electronic absorption spectra and the difference spectra of the latter recorded during the titration of the recombinant apo-βMT fragment with Cu(I), while parts (a)–(c) of Fig. 2 show those recorded during the titration with Ag(I). As expected, the apo-βMT fragment does not have a pronounced CD spectrum (Figs. 1(a) and 2(a), line 0) with no signal above 250 nm.

3.1.1. Reaction of recombinant mouse apo-βMT with Cu^+

Upon the addition of Cu(I) to apo-βMT, a derivative-like envelope, 303(+) nm and 326(−) nm, and a very intense band at 263(+) nm develop isodichroically (311 nm) (see Fig. 1(a)) and the absorption at 255 nm increases linearly (Fig. 1(b)). The CD bands reach their maxima at 6 Cu and the linearity in absorbance is kept until the same number of equivalents of copper are added. Also, the difference spectra (Fig. 1(c)) show that every Cu(I) added between 1 and 6 contributes equally to the formation of a species with a Cu_6S_9 unit that probably contains a unique type of coordination geometry about Cu. Moreover, the molecular weight obtained by ESI-MS of 3532.93 is consistent with the expected molecular weight for a Cu_6-βMT species of 3533.82 (apo-βMT + 6Cu − 6H).

The addition of increments of Cu(I) to Cu_6-βMT up to one Cu(I) reveals an extensive rearrangement of the Cu_6-βMT aggregate with the incorporation of the seventh Cu(I) (Fig. 1(a)). Thus, there is a development of new bands at 237(+), 336(+), 368(+) and 400(−) nm and the intense band centred at 263(+) nm decreases in intensity, while it shifts to 259(+) nm. The absorption spectra and the difference absorption spectra (Fig. 1(b) and (c), respectively) show that during this phase there are significant contributions at wavelengths not observed before: 235, 285 and 335 nm. These are consistent with the changes observed in the CD spectra and indicate formation of new Cu–S coordination environments, which give rise to a new species, of stoichiometry Cu_7-βMT. The presence of this species was confirmed by ESI-MS yielding a molecular weight of 3595.86, in comparison with the expected value for Cu_7-βMT species of 3596.36 (apo-βMT + 7Cu − 7H).

Over 7 Cu^+ added, the absorption spectra, with an isosbestic point at 320 nm, and their difference spectra are indicative of copper binding to Cu_7-βMT until 10 Cu^+ added (see Fig. 1(b) and (c)). These show the contribution of the Cu–S bonds in the high energy region and also a loss of

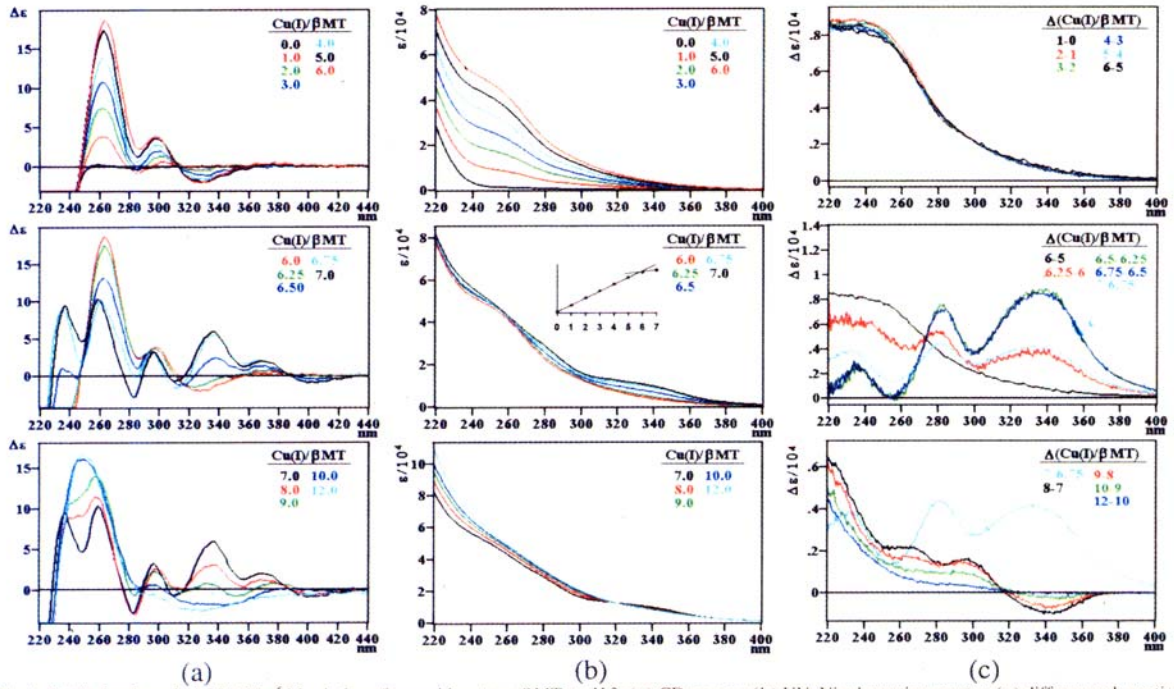

Fig. 1. Cu(I) titration of a 1.98×10^{-5} M solution of recombinant apo-βMT at pH 3: (a) CD spectra; (b) UV–Vis absorption spectra; (c) difference absorption spectra obtained by subtracting the successive spectra of (b). For comparison, their intensities have been normalized with respect to one molar addition. The Cu^+ to MT molar ratios are indicated within each frame. The inset in (b) shows the variation of the absorbance at 255 nm between 0 and 7 equivalents of Cu^+ added.

absorbance centred at 340 nm, which could indicate the loss of a particular type of copper coordination constituted in the anterior phase. The CD spectra during this phase show that the bands at 297(+), 336(+), 368(+) and 400(−) collapse, while the two bands at 237(+) and 259(+) nm give rise to a unique band centred at 245(+) nm (Fig. 1(a)).

3.1.2. Reaction of recombinant mouse apo-βMT with Ag^+

The spectral data shown for the apo-βMT fragment titration with Ag^+ (Fig. 2) are unusually weak although the protein concentration was doubled to enhance the signal-to-noise ratio. The low intensities of these spectra contrast with the data we obtained when Ag^+ binds to Zn_3-βMT, but are consistent with those reported for the titration of the apo form of native fragments with silver [17]. Moreover, CD and UV–Vis data obtained in this work do not resemble those recorded for Cu^+ either in the shape of the spectral envelopes or in their intensities. The CD data (Fig. 2(a)) show formation of Ag_3-βMT with bands at 250(+) and 290(+) nm. Ag_3-βMT is replaced by a new species, Ag_6-βMT, which is characterized by a CD spectrum with maxima at 246(+), 270(+) and 295(+) nm. Finally, we can associate the broad bands at 276(+) and 350(−) with formation of Ag_9-βMT.

UV–Vis absorption spectra show a broad envelope that starts at about 380 nm and extends into the far-UV (Fig. 2(b)). The intensity of the absorption in the 250–290 nm region increases linearly with increasing Ag(I) equivalents up to 6 Ag^+. The slope of the absorbance intensity clearly changes with the addition of the seventh equivalent. This finding is corroborated by the difference spectra (Fig. 2(c)) which indicate a cooperative effect for the first 3 Ag(I) equivalents added, similar behaviour from 3 to 6 Ag^+, and a smaller increment in absorbance due to the last equivalents. Saturation is reached for 9 Ag^+. Unfortunately, the difference spectra are not well resolved and they only reveal a generalized absorption between 230 and 400 nm, with a maximum centred at 230 nm, which could indicate the same type of Ag–S coordination environment in all the species formed.

3.2. Zn_3-βMT fragment

Parts (a)–(c) of Fig. 3 show the CD, electronic absorption spectra and the difference spectra of the latter recorded during the titration of the recombinant Zn_3-βMT fragment with Cu(I), while parts (a)–(c) of Fig. 4 show those recorded during the titration with Ag(I). As expected, the Zn_3-βMT species shows the characteristic CD feature (Figs. 3(a) and 4(a), line 0), already described elsewhere [4].

3.2.1. Reaction of recombinant mouse Zn_3-βMT with Cu^+

Intense dichroic bands develop in the CD spectrum during the addition of the first 4 Cu(I) equivalents to Zn_3-βMT. Fig. 3(a) shows that the 247(+) nm CD band characteristic of Zn_3-βMT increases its intensity and red-shifts up to 258(+)

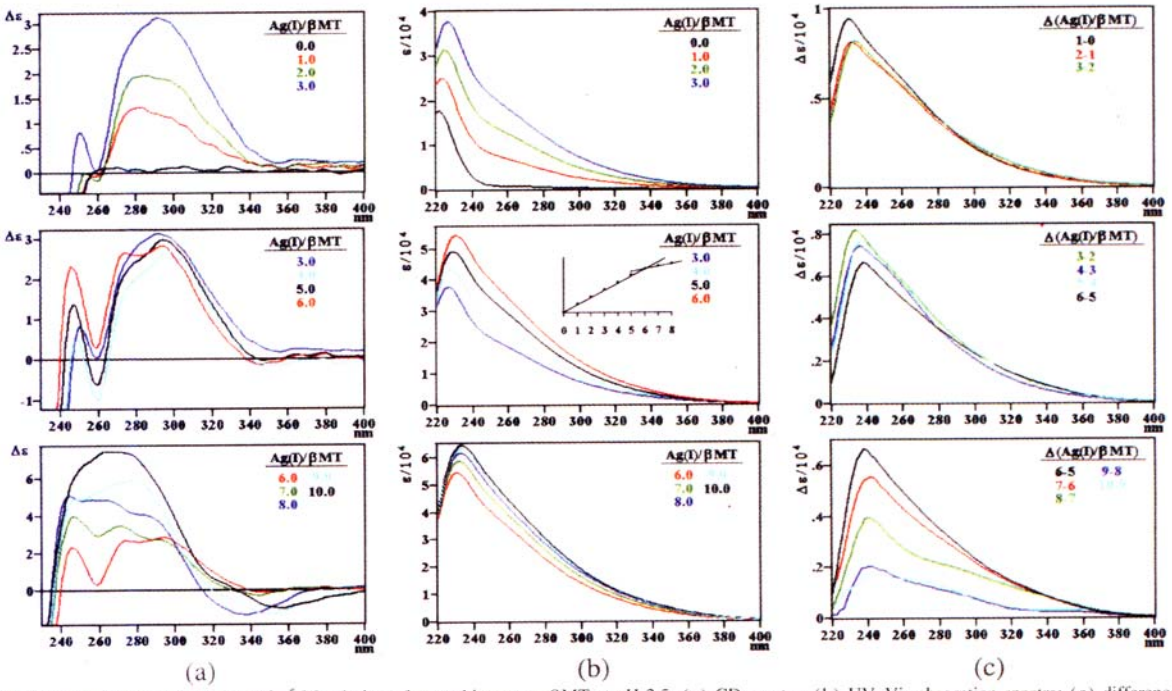

Fig. 2. Ag(I) titration of a 4.00×10^{-5} M solution of recombinant apo-βMT at pH 2.5: (a) CD spectra; (b) UV–Vis absorption spectra; (c) difference absorption spectra obtained by subtracting the successive spectra of (b). The Ag^+ to MT molar ratios are indicated within each frame. The inset in (b) shows the variation of the absorbance at 250 nm between 0 and 8 equivalents of Ag^+ added.

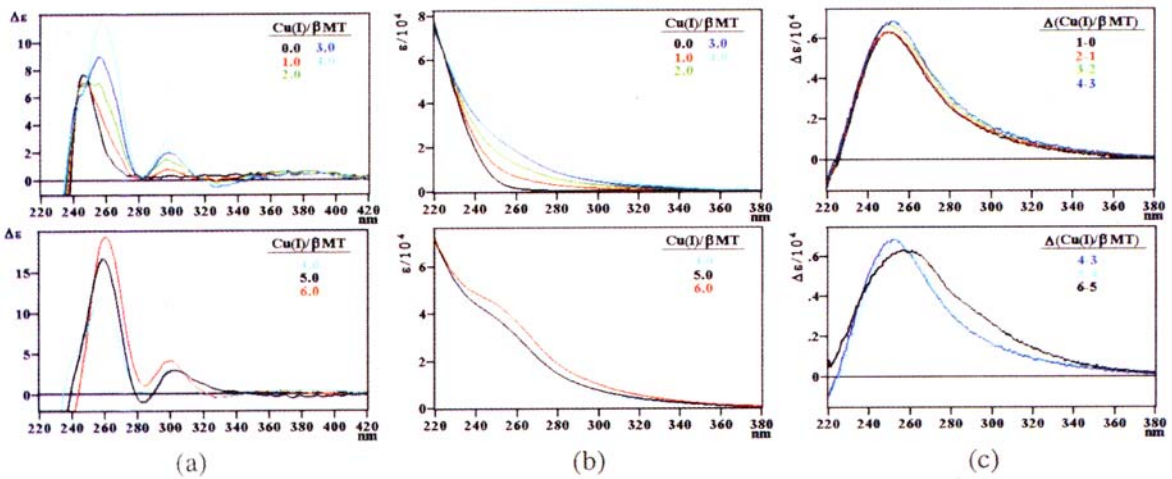

Fig. 3. Cu(I) titration of a 1.95×10^{-5} M solution of recombinant Zn_7-βMT at pH 7: (a) CD spectra; (b) UV–Vis absorption spectra; (c) difference absorption spectra obtained by subtracting the successive spectra of (b). The Cu^+ to MT molar ratios are indicated within each frame. The spectra corresponding to the last phases of the titration have been omitted as they coincide with the last two of Fig. 1(a)–(c).

maintaining a shoulder at about 240 nm, while two bands at 297(+) and 327(−) nm gradually intensify through isodichroic points at 248, 282 and 315 nm. The absorption UV–Vis spectra (Fig. 3(b)) and their difference spectra (Fig. 3(c)) indicate an isosbestic (224 nm) increase in absorbance at about 250 nm and also a cooperative effect in the binding of these 4 Cu(I). The negative increase in absorbance below 230 nm can be attributed to the superposition of the loss of Zn–S chromophores (240 nm) over the gain due to the newly formed Cu–S chromophores. In a parallel titration, Chelex-100 was added after incorporation of the first four Cu^+ in order to bind the displaced Zn^{2+} ions (data not shown), according to the method described previously [4]. Analytical results indicated that the chelating resin sequestered 2 Zn^{2+}

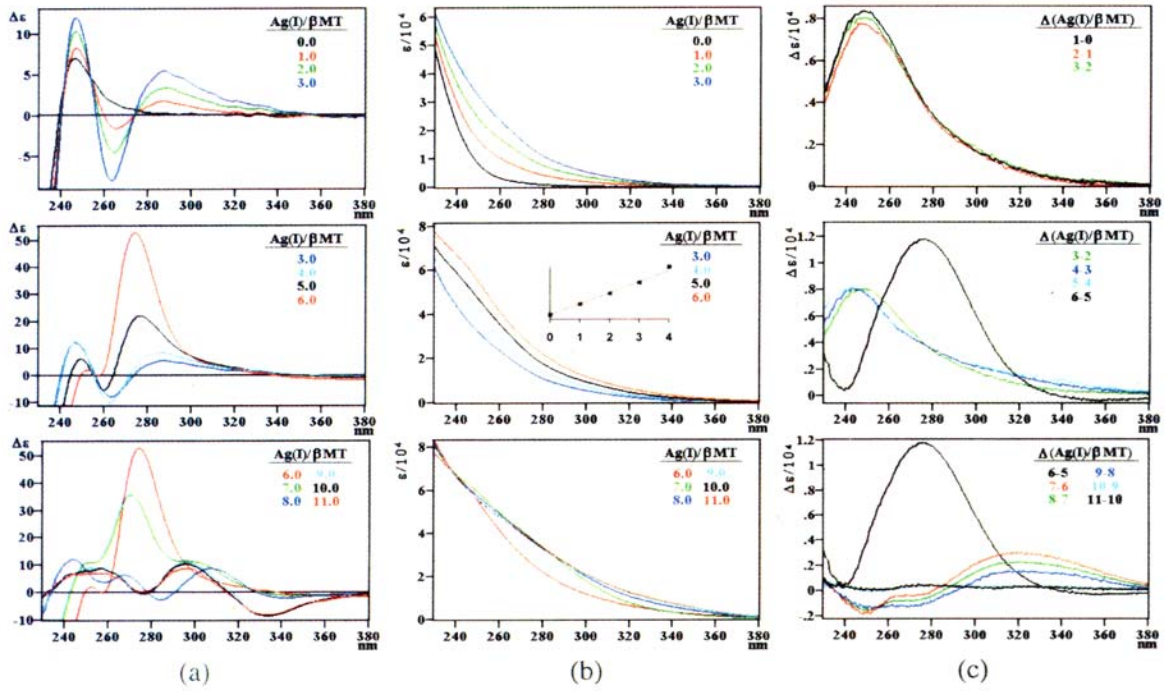

Fig. 4. Ag(I) titration of a 1.99×10^{-5} M solution of recombinant Zn_3-βMT at pH 7.5: (a) CD spectra; (b) UV–Vis absorption spectra; (c) difference absorption spectra obtained by subtracting the successive spectra of (b). The Ag^+ to MT molar ratios are indicated within each frame. The inset in (b) shows the variation of the absorbance at 263 nm between 0 and 4 equivalents of Ag^+ added.

of the three initially bound in Zn_3-βMT, and that the protein coordinated 4 Cu^+ and 1 Zn^{2+}. In addition, the CD and UV–Vis absorption spectra remained unchanged after this treatment. All these data allow us to postulate a stoichiometric ratio of Zn_1Cu_4-βMT for the species that forms cooperatively in the first stage of the titration.

Further addition of copper, from 4 to 6 Cu^+, results in the isodichroical (346 nm) formation of a new species, which is characterized by an increase in intensity of the bands at 258(+) and 297(+) nm, and the disappearance of the shoulder at about 240 nm (Fig. 3(a)). Interestingly, this spectrum is practically identical to that recorded for Cu_6-βMT in the titration of apo-βMT with 6 Cu^+ and thus indicative of identical stoichiometries and structures for the species present in solution after the addition of 6 Cu^+ to either apo-βMT (pH 3) or Zn_3-βMT (pH 7). This coincidence is corroborated by the UV–Vis and difference spectra. Moreover, subsequent additions of Cu(I) to Cu_6-βMT give rise to nearly identical spectral patterns (CD, UV–Vis absorption and difference spectra) regardless of the pH (7 or 3) of the titration. Molecular weight measurements for Cu_6-βMT and Cu_7-βMT species are in good agreement with the values found in the titration of the apo-βMT fragment (see above). Accordingly, titrations carried out at pH 3 and pH 7 reveal that the series of species Cu_6-βMT, Cu_7-βMT, Cu_{10}-βMT form in sequence as Cu^+ is added to either apo-βMT or Zn_3-βMT, respectively. The similarity of the CD spectral traces indicates that not only the stoichiometry of the Cu_x-βMT species ($x=6$, 7 and 10) but also their structures are independent of the pH (3 or 7). As the last two stages of the titration at pH 7 coincide with the last two of Fig. 1(a)–(c) neither the spectra nor the corresponding descriptions have now been included.

3.2.2. Reaction of recombinant mouse Zn_3-βMT with Ag^+

Again, as found with the apo form of this fragment, the spectral data with Ag^+ differ from those recorded in the titration of Zn_3-βMT with Cu^+. Fig. 4 shows the spectra obtained as aliquots of Ag^+ were added to a solution of recombinant Zn_3-βMT held at pH 7.5. Addition of Ag^+ results in a steep growth in the intensity of the 247(+) nm CD band characteristic of Zn_3-βMT up to 3 Ag^+, while a derivative-like envelope (263(−) and 288(+) nm) centred at 274 nm develops isodichroically (253, 273 nm). Concurrently, the UV–Vis absorbance at 263 nm increases linearly up to 3 Ag^+ (Fig. 4(b)) and the corresponding difference spectra (Fig. 4(c)) are coincident. All these data show a high cooperativity at this stage of the titration.

To analyse the influence of Zn^{2+} ions on the Ag-βMT species formed, Chelex was added to the Zn_3-βMT solution after the addition of 3 Ag^+ in a parallel titration. Surprisingly, unlike the behaviour observed in the Cu^+ titration, the UV–Vis absorption and CD spectra changed considerably after addition of the resin: the 247(+) CD band decreased in intensity while the exciton coupling disappeared to give rise

to a band centred at 279(+) nm (data not shown). This was attributed to the removal not only of the displaced Zn(II) ions but also of those still bound to the fragment, as ICP analyses confirmed the presence of 3 Zn(II) ions in the resin and 3 Ag^+ in the supernatant. Therefore, on the basis of the spectroscopic and analytic data, a stoichiometric ratio of Zn_xAg_3-βMT, where $1 \leq x \leq 3$, can be proposed for the first species cooperatively formed in the titration. In addition, the absorption at 247 nm, which has traditionally been assigned exclusively to Zn–S chromophores, remains when all the Zn(II) ions coordinated to the protein in the Zn_xAg_3-βMT ($1 \leq x \leq 3$) species are removed with the aid of Chelex-100. The same absorption can be seen in the titration of apo-βMT with Ag(I) (Fig. 2). Accordingly, it can be deduced that the spectral data recorded at pH 7.5 in the 247 nm region are a superposition of at least two bands: the first is from the Zn–S chromophore and the second reflects the absorption of a particular type of Ag–S coordination.

On addition from 3 to 6 Ag^+, the characteristic exciton coupling signal of Zn_xAg_3-βMT centred at 274 nm vanishes to give rise to a very intense band at the same wavelength. Also, the band observed at 247(+) nm loses intensity and disappears, indicating the loss of the coordinated Zn(II) ions. The new Gaussian-shaped band can be taken as the fingerprint of the Ag_6-βMT species. Although the UV–Vis spectra are not conclusive in this phase of the titration, their difference spectra show a very intense and clearly defined absorption at 276 nm.

The last phase of the titration corresponds to subsequent additions up to 11 Ag^+. The spectra are indicative of the complexity of the changes that take place in solution and show that saturation is achieved for 9 Ag^+. The Ag_9-βMT species is characterized by a spectral envelope that shows a broad band centred at 259(+) nm and a derivative envelope centred at 317 nm. The difference spectra indicate the loss of the Ag–S chromophores formed in the previous phases and the appearance of a third Ag–S environment characterized by an absorption centred at 319 nm. Comparison of the CD envelopes corresponding to species with the same stoichiometric ratio with those obtained in the titration of the apo-βMT strongly suggests that each Ag-βMT species adopts a distinct structure at each pH value (compare Figs. 2(a) and 4(a)).

In summary, on the basis of the spectroscopic data and their comparison at neutral and acidic pH, we propose the reaction pathways given in Fig. 5. These show that the recombinant βMT fragment binds Ag^+ and Cu^+ in several stages, with distinct species forming at Ag_6 and Ag_9, whose structure depends on the pH (2.5 or 7.5), and Cu_6, Cu_7 and Cu_{10} as pH-independent structures (in the range 3 to 7). Also, two mixed-metal species have been characterized, Zn_1Cu_4 and Zn_xAg_3 ($1 \leq x \leq 3$), which introduces interesting questions about the charge compensation-based displacement of Zn^{2+} from MT by monovalent metal ions [18] and about the ability of silver to afford mixed-metal MT species [13]. These results clearly indicate that the behaviour of copper towards

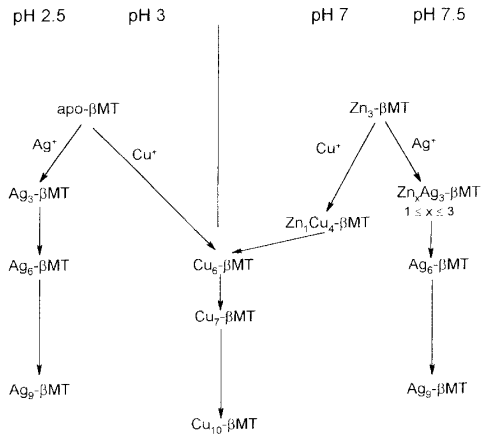

Fig. 5. Series of proposed binding pathways followed when Cu^+ or Ag^+ is added to both recombinant apo-βMT and recombinant Zn_3-βMT.

MT cannot necessarily be inferred from that of silver. The spectral data we report here show the development of maxima at molar ratios (3, 6 and 9) that appear to be reasonable for Ag-βMT complexes, differing from those values determined for Cu^+ binding to the β fragment (6, 7 and 10).

Up to now literature data on the copper-binding stoichiometry in mammalian MT are not conclusive. Thus, the titration of the chemically synthesized β domain of rat liver MT 2 with Cu(I) at pH 2.5 allowed characterization of a single species, Cu_6-βMT. This was detected by emission spectroscopy; but CD maxima intensities were reached with only three to four coppers. The two to three coppers added after reaching the maxima appeared to be CD-silent [12]. On the other hand, the stoichiometries we have found for the species with more than 6 Cu^+, Cu_7-βMT and Cu_{10}-βMT, are consistent with the early work of Nielson and Winge [8], where similar ratios of copper to protein in the β domain obtained by partial enzymic digestion were determined using metal-dependent proteolysis. In addition, recent results have shown that the recombinant expression of the βMT domain in Cu-supplemented media affords mixtures of Cu_6-βMT (25%) and Cu_7-βMT (75%) [19]. With respect to Ag(I), CD spectral data recorded during the titration with Ag^+ of apo-βMT 1 and Zn_3-βMT 1, both obtained by partial digestion of the native protein, allowed characterization of the Ag_3-βMT and Ag_6-βMT, and Ag_6-βMT species, respectively [17,18]. However, the number of species, their stoichiometry and corresponding spectral envelopes do not coincide with those found with the recombinant protein. We have observed that the pH plays a significant role in the metallothionein metal-binding pathways. Moreover, reactions of recombinant MT fragments with Cu^+ and Ag^+, like the reaction of recombinant MT with Hg^{2+} [9], are not as instantaneous as those reported for Cd^{2+} [4,5]. Thus, provision of the required stabilization time for the formation of complex species and constancy of pH during the titration are fundamental to

achieve a precise indication of the stoichiometric ratios of the Ag- and Cu-MT species.

Due to the differences observed in the abilities of Cu(I) and Ag(I) to bind to recombinant βMT, the αMT and the entire MT have also been studied. Again, the results differ from those reported in the literature for the native proteins and show that the recombinant proteins bind copper and silver differently. A detailed report on these findings is in preparation.

The CD, UV and, above all, difference absorption spectra have allowed us to identify precise UV–Vis absorptions during the titrations of the recombinant βMT fragment with monovalent metal ions. In the case of silver, absorptions at three distinct wavelengths have been recorded: 248 (formation of Zn_xAg_3-βMT), 276 (formation of Ag_6-βMT) and 319 nm (formation of Ag_9-βMT), the positions of which clearly parallel the features observed in the CD spectrum (Fig. 4). Interestingly, the appearance of each of these absorptions implies the disappearance of the previous one. Thus, it is tempting to speculate that each energy corresponds to a different geometry of coordination about silver, which in turn may be related to the metal-to-SCys molar ratio. As a general pattern, with increasing M(I)/βMT stoichiometry the stereochemistry around the metal might change from tetrahedral to diagonal through trigonal-planar coordination. Conversely, the addition of copper to recombinant βMT gives rise to a more complex pattern of difference spectra: a broad absorption centred at 235 (formation of Cu_6-βMT), three simultaneous absorptions at 235, 285 and 335 (formation of Cu_7-βMT) and weak absorptions at 265 and 295 nm (formation of Cu_{10}-βMT) (Fig. 1). Traditionally, in the Cu(I)-containing mammalian metallothioneins it has been proposed that the Cu(I) is trigonally coordinated by the SCys ligands [20,21]. However, the structural diversity of copper and silver thiolates [22], the lack of established correlations between their structure and physical properties [23] and the few conclusive assignments of the different absorption energies associated with the manifold coordination numbers of these metal ions in protein environments [11] do not give us enough evidence to support a specific type of coordination for the M^I-βMT species reported in this study.

4. Abbreviations

EPR	electron paramagnetic resonance
ESI-MS	electrospray ionization mass spectrometry
ICP-AES	inductively coupled plasma atomic emission spectrometry
ICP-MS	inductively coupled plasma mass spectrometry

Acknowledgements

This work was supported through Projects PB97-0216 and PN96-0225. M.C. is indebted to the Fundación Caja de Madrid for a post-doctoral fellowship and R.B. to the Comissionat per a Universitats i Recerca de la Generalitat de Catalunya (CIRIT) for a pre-doctoral scholarship. We acknowledge the Serveis Científico-Tècnics, UB (ESI-MS, ICP-AES, ICP-MS), the Servei d'Anàlisi Química, UAB (AAS, CD) and the ICMAB (EPR) for allocating instrument time.

References

[1] J.H.R. Kägi, A. Schäffer, Biochemistry 27 (1988) 8509.
[2] D.M. Templeton, M.G. Cherian, Methods Enzymol. 205 (1991) 11.
[3] N. Romero-Isart, N. Cols, M.K. Termansen, J.L. Gelpí, R. González-Duarte, S. Atrian, M. Capdevila, P. González-Duarte, Eur. J. Biochem. 259 (1999) 519.
[4] M. Capdevila, N. Romero-Isart, R. González-Duarte, S. Atrian, P. González-Duarte, Cell Mol. Life Sci. 53 (1997) 681.
[5] N. Cols, N. Romero-Isart, M. Capdevila, B. Oliva, P. González-Duarte, R. González-Duarte, S. Atrian, J. Inorg. Biochem. 68 (1997) 157.
[6] M. Capdevila, N. Romero-Isart, N. Cols, S. Atrian, M.J. Stillman, R. González-Duarte, P. González-Duarte, An. Quim. Int. Ed. 92 (1996) 199.
[7] S.S. Narula, M. Brouwer, Y. Hua, I.M. Armitage, Biochemistry 34 (1995) 620.
[8] K.B. Nielson, D.R. Winge, J. Biol. Chem. 260 (1985) 8698.
[9] S. Atrian, R. Bofill, M. Capdevila, N. Cols, P. González-Duarte, R. González-Duarte, A. Leiva, O. Palacios, N. Romero-Isart, in: C. Klaassen (Ed.), Metallothionein IV, Birkhäuser, Basel, 1998, p. 55.
[10] W. Lu, M.J. Stillman, J. Am. Chem. Soc. 115 (1993) 3291.
[11] D.L. Pountney, I. Schauwecker, J. Zarn, M. Vašák, Biochemistry 33 (1994) 9699.
[12] Y.J. Li, U. Weser, Inorg. Chem. 31 (1992) 5526.
[13] H. Li, J.D. Otvos, Biochemistry 35 (1996) 13929.
[14] G.J. Kubas, Inorg. Synth. 19 (1979) 90.
[15] I.M. Kolthoff, E.B. Sandell, E.J. Meehan, S. Bruckenstein, Quantitative Chemical Analysis, Macmillan, New York, 1969.
[16] J. Bongers, C.D. Walton, D.E. Richardson, J.U. Bell, Anal. Chem. 60 (1988) 2683.
[17] A.J. Zelazowsky, Z. Gasyna, M.J. Stillman, J. Biol. Chem. 264 (1989) 17091.
[18] A. Zelazowski, M.J. Stillman, Inorg. Chem. 31 (1992) 3363.
[19] N. Cols, N. Romero-Isart, R. Bofill, M. Capdevila, P. González-Duarte, R. González-Duarte, S. Atrian, Protein Eng. (1999) in press.
[20] G.N. George, D. Winge, C.D. Stout, S.P. Cramer, J. Inorg. Biochem. 27 (1986) 213.
[21] A. Presta, A.R. Green, A. Zelazowski, M.J. Stillman, Eur. J. Biochem. 227 (1995) 226.
[22] I.G. Dance, K. Fisher, G. Lee, in: M.J. Stillman, F.C. Shaw III, K.T. Suzuki (Eds.), Metallothioneins, VCH, New York, 1992, pp. 284–323.
[23] H.G. Fijolek, P. González-Duarte, S.H. Park, S.L. Suib, M.J. Natan, Inorg. Chem. 36 (1997) 5299.

Manuscrit

Is Ag(I) an adequate probe for Cu(I) in structural copper-metallothionein studies?
The binding features of Ag(I) to mammalian metallothionein 1

Is Ag(I) an adequate probe for Cu(I) in structural copper-metallothionein studies? The binding features of Ag(I) to mammalian metallothionein 1

Òscar Palacios, Mercè Capdevila, Pilar González-Duarte✉

Departament de Química, Facultat de Ciències, Universitat Autònoma de Barcelona, E-08193 Bellaterra, Barcelona, Spain
Phone: + 34 935 811 363; Fax: + 34 935 813 101; E-mail: Pilar.Gonzalez.Duarte@uab.es

Abstract

The binding abilities of silver(I) to mammalian MT 1 have been studied and compared with those of copper(I), recently reported [1], with the aim of analyzing the suitability of Ag(I) as a probe of Cu(I) in Cu-MT studies. The Zn/Ag replacement in recombinant mouse Zn_7-MT 1 and corresponding Zn_4-αMT 1 and Zn_3-βMT 1 fragments, as well as the stepwise incorporation of Ag(I) to the corresponding apo-MTs, have been followed in parallel by various spectroscopic techniques including electronic absorption (UV-vis), circular dichroism (CD) and electrospray mass spectrometry coupled to capillary zone electrophoresis (CZE-ESI-MS). A comparative analysis of the sets of data obtained in the titrations of the three proteins with $AgClO_4$ at pH 7.5 and 2.5 has led to the corresponding reaction pathways and given evidence of unprecedented stoichiometries and structural features for the species formed during the above processes. Thus, the Zn/Ag replacement in Zn_7-MT 1 at pH 7.5 has revealed the subsequent formation of the following MT species: Ag_4Zn_5–MT, Ag_7Zn_3–MT, Ag_8Zn_3–MT, $Ag_{10}Zn_2$–MT, $Ag_{12}Zn_1$–MT, Ag_x-MT, x = 14-19, whose structure consists of two additive domains only if Zn(II) remains coordinated to the protein. A second structural role for Zn(II) has been deduced from the different folding found for the Ag_x-MT species of the same stoichiometry formed at pH 7.5 or 2.5. Comparison of the binding features of Cu(I) and Ag(I) to the entire MT at pH 7.5 shows that among all the M_xZn_y-MT ($0 \le y < 7$) species found only $M^I_4Zn_5$-MT $[(Zn_4)^\alpha(M_4Zn_1)^\beta]$ and $M^I_7Zn_3$-MT $[(M_3Zn_2)^\alpha(M_4Zn_1)^\beta]$, which form during the first stages of the Zn(II)/M(I) metal replacement, show comparable 3D structures and thus they are the only species where Ag(I) ions can be predicted to be an adequate probe for Cu(I).

***Keywords**:* Silver metallothionein · αMT · βMT · CZE-ESI-MS · Silver as probe of copper

Introduction

Metallothioneins (MTs) are ubiquitous low molecular weight cysteine-rich metalloproteins that exist naturally with zinc and/or copper bound to them. While the search for the precise function of these unconventional proteins prompts most of the present research on this field, full knowledge of their 3D structure is only available for a small number of MTs containing Zn and/or Cd ions. Concerning mammalian MTs, all actually structurally-characterized MT 1 and MT 2 consist of a C-terminal (α) and a N-terminal (β) domains, which enfold the $M_4(SCys)_{11}$ and $M_3(SCys)_9$ aggregates, respectively[2]. Conversely, the failure to obtain single crystals and the unsuitability of the ^{63}Cu and ^{65}Cu isotopes for NMR studies [3] account for the scarcity of structural information on copper-containing MTs. Thus, *S.cerevisae* CUP1*,* is the only reported structure of a copper metallothionein, also unique for an Ag-substituted derivative. The NMR solution structure of both forms allowed conclusion that yeast binds seven Cu(I) or Ag(I) ions in a single cluster [2, 4]. However, a recent NMR reinvestigation of yeast Cu_7-MT has shown that a number of different arrangements of the seven copper ions is consistent with the highly refined structure of the polypeptide fold [5]. This, together with the unequal coordination preferences of Cu(I) and Ag(I) with thiolate sulfur ligands [2], casts doubts on the Cu/Ag isomorphous replacement in MTs and thus on the suitability of the ^{107}Ag isotope as a probe for the study of Cu-containing MTs [5, 6].

The study of the binding features of Ag(I) to MT has attracted much less attention than that of Cu(I). With the exception of those aiming at the structural determination of yeast Cu-MT by using Ag(I) as a probe [4, 7, 8], and one devoted to the binding of Ag(I) to phytochelatins [9], or class III metallothioneins, most of the publications refer to mammalian MTs [10, 11, 12, 13]. These, which include native and chemically synthesized proteins in their M_7-MT (M= Zn, Cd) or apo-MT forms, led to the following commonly accepted features: a) Ag(I) binding to MT gives rise to a small number of metallated species, none of them containing heterometallic Ag_xM_y aggregates within the α or β domains; b) Ag(I) binds preferentially to the β domain, which yields Ag_6-βMT; from this point the Ag(I) cations start binding to the α domain, which also reaches saturation for 6 Ag(I) equivalents; c) the Ag_{12}-MT species with a $(Ag_6)^\alpha(Ag_6)^\beta$ occupancy is of special relevance; d) saturation of the protein is accomplished for 17-18 Ag(I) eq, both Ag_{12}-MT and $Ag_{17\text{-}18}$-MT containing digonally coordinated Ag(I) cations. However, some of these features were apparently too distant to the results we obtained in the Cu(I)-MT 1 system [1].

The analysis of the Ag(I) binding abilities of MTs by the standard titration procedures is more complex not only than that of Zn(II) or Cd(II) but also than Cu(I). On the one hand, the acidity of the Ag(I) solutions used as titrating agents require high buffer concentrations in the protein sample to maintain its pH invariable, but the presence of such concentrations hinders the use of spectrometric techniques [14]. Besides, only certain counterions accompanying the Ag(I) cations assure the solubility

of the silver salt while allowing spectrophotometric measurements in the wavelength range usually studied. On the other hand, monitoring of the titration only by optical spectroscopy provides limited information mainly due to the lack of well established correlations between the observed absorption wavelengths and the possible tetrahedral, trigonal or digonal coordination environments of Ag(I) to $SCys^-$ thiolate ligands in MTs. In addition, on the basis of the diversity and complexity found in silver thiolates [2], the coexistence of different coordination geometries about silver in polynuclear MT species should be considered.

The detailed knowledge on the Cu(I) binding abilities to recombinant mouse MT 1 [1] and the use of spectrometric techniques coupled to efficient separation methods such as CZE, as applied to the Cd-MT system [15], have been recently reported. Both studies provide an adequate base to extend our previous work with Cu(I) to the Ag(I)-MT system with the final purpose of comparing the behavior of both monovalent metal ions towards the same protein. In the present work the Ag(I) binding to recombinant mouse MT 1 and corresponding α and β fragments has been monitored in parallel by electronic absorption and mass spectroscopies. A comparative analysis of the results obtained for the three proteins at both pH 7.5 and 2.5 gives a new insight on the binding features of Ag(I) to this isoform of mammalian MT. Also, comparison of these features with those previously reported for Cu(I) binding to the same MT shows that Ag(I) ions can be taken as a probe of Cu(I) binding only for a limited number of heterometallic Cu_xZn_y-MT species. Spectroscopic data for all homometallic M_x-MT species observed with the same stoichiometry are consistent with different 3D structures for M = Cu and Ag.

Materials and Methods

Protein Preparation and Characterization. Expression assays, fermentator-scale cultures, purification of the fusion protein and recovery and analysis of the recombinant mouse Zn_7-MT, Zn_4-αMT and Zn_3-βMT fragments were performed as previously described [16,17], and obtained in a Tris-$HClO_4$ pH= 7 buffer [14]. The apoproteins were prepared by acidification of the recombinant material with $ClCH_2COOH/ClCH_2COONa$ buffer until pH 2.5. All protein solutions had a final concentration of about 300 μM, which were appropriately diluted to 20 μM with Milli-Q-purified and Ar-degased water before being titrated at 25ºC with freshly prepared and standardized solutions of $AgClO_4$ [14].

Metal Ion Binding Reactions. Metal binding experiments were carried out by sequentially adding molar ratio aliquots of concentrated Ag^+ solutions to a single solution of either Zn_7-MT, Zn_4-αMT or Zn_3-βMT. Several counterions accompanying the Ag(I) cation were tested as titrating agents (NO_3^-, BF_4^-, PF_6^- and ClO_4^-). Among them, $AgClO_4$ was chosen as it afforded less interferences in the optical measurements. Three different techniques were used to monitor the binding reaction of Ag(I) to the corresponding protein: UV-vis absorption, CD spectroscopy and mass spectrometry, through the CZE-ESI-MS coupling. For each addition of Ag(I), the protein sample was allowed to react with the metal ion until the CD features became stable, as already indicated [14]. The mean stabilization time required for each addition ranged between 1.5 to 2 hours. Absorption and spectrometric studies were conducted in parallel with CD studies.

All manipulations involving the metal and protein solutions were performed in an argon atmosphere, and titrations were carried out at least in duplicate to assure the reproducibility of each single point.

The pH for all experiments remained constant throughout. The acidity of Ag(I) solution required the buffering of the protein containing solutions with either Tris/$HClO_4$ at pH 7.5 or $ClCH_2COOH$/NaOH at pH 2.5 [14].

Instrumentation. The electronic absorption and CD measurements were performed, corrected and processed as already described [14]. Mass data were recorded with a PE-SCIEX API 300 Ion-spray triple-quadrupole mass spectrometer (Thornhill, ON, Canada). A BioToolBox software was used of the interpretation of CID (collision induced dissociation) MS spectra. The CZE separations were carried out with a Beckmann P/ACE 2200 (Beckmann, Fullerton, CA). For the CZE-ESI-MS coupling the design described by Corr and Anacleto was used [18]. The capillary threaded through the ion-spray needle to end 1 mm back its orifice. A sheathflow was supplied coaxially to merge with the electrophoretic capillary flow just before the orifice. The makeup flow of 2 μl min-1 (5 mM ammonium acetate buffer in 50% methanol) was supplied by means of a Harvard Apparatus Model 22 syringe pump. The potential applied to the ionspray needle was 4.2 kV. The resulting potential difference across the separation capillary was 12-20 kV, depending on the Ag(I) concentration, in order to allow a current between 12 and 25 μA and the running buffer concentration ranged between 30-45 mM of ammonium acetate at pH 7, depending on the Ag:MT ratio, higher amount of buffer required for higher Ag(I) concentration. The ionspray nebulizer gas flow was 1.00 L min-1.

Results and Discussion

Coupling of spectroscopic and spectrometric techniques for the study of the silver-binding abilities of recombinant mouse MT 1 and corresponding α and β fragments

Optical spectroscopies (CD and UV-vis) provide information on the number of metal-MT species formed during the titration of the MT protein with a specific metal ion, their corresponding stoichiometry and degree of folding. However, the accuracy of the

data retrieved is inversely related to the number of species simultaneously present in the sample. On the basis of the successive equilibria involved in the formation of a specific aggregate it should not be exceptional the coexistence of several species in solution. Accordingly, knowledge of the metal binding features of MTs can be greatly improved if complementary techniques to optical spectroscopies are used. In recent years, ESI-MS has shown to be an adequate choice as it affords knowledge on the molecular distribution of the various complex species coexisting within the sample [15]. While earlier studies on recombinant mouse Zn_3-βMT showed that silver and copper bind to this protein differently, they also evidenced that ESI-MS measurements required previous separation of the high buffer concentration in the Ag(I)-MT samples [14]. A recently reported method based on the coupling of CZE separation with ESI-MS detection has shown the possibility of the on-line removal of significant amounts of buffer that would otherwise mask the electrospray signals of the protein [15].

With the aim of extending the actual understanding of the Ag-MT system, and establishing a detailed comparison with Cu-MT, we have combined CZE-ESI-MS with optical techniques in order to study the Ag(I) binding abilities of recombinant mouse Zn_3-βMT, Zn_4-αMT and Zn_7-MT at two pH values, 7.5 and 2.5. The final results for each protein arise from a comparative analysis of three sets of data: CD, UV-vis and CZE-ESI-MS. For the sake of brevity, only CD data corresponding to the titration of Zn_7-MT (Fig. 1) and Zn_4-αMT (Fig. 2) with $AgClO_4$ are shown, while the remaining optical data recorded in these titrations are given as supplementary material in Fig. S1-S4; those of Zn_3-βMT have already been reported [14]. Following a comparable methodology to that applied in our previous studies [1, 14, 16, 17], the analysis o f the optical data has led to the reaction pathways shown in Scheme 1. On the other hand, although the difference in migration of the silver-containing MT complexes is too small to allow their separation by CZE, the CZE-ESI-MS coupling has allowed a satisfactory separation of the metal-MT species from the Tris buffer at pH 7.5, revealing the exact nature of the aggregates present in solution at each point of the titrations, as given in Table 1. Representative MS spectra are shown in Fig. S5-S7. The CZE-ESI-MS electropherograms are similar in the three titrations and consist of a major peak followed by a back shoulder. Unfortunately, at pH 2.5 it has not been possible to record comparable data.

Comparison of optical (Scheme 1) and mass (Table 1) sets of data allows conclusion that CZE-ESI-MS not only confirms but also extends the information obtained from CD and UV-vis spectroscopies about the number of species and corresponding stoichiometries. In summary, consideration of the mass data allows: a) determination of the Zn(II) content in all the heterometallic species found, b) completion of the reaction pathways with totally unpredictable species (denoted with * in Scheme 2) if only the optical data had been taken into account, and c) verification of the absence of cooperative processes during the Zn/Ag

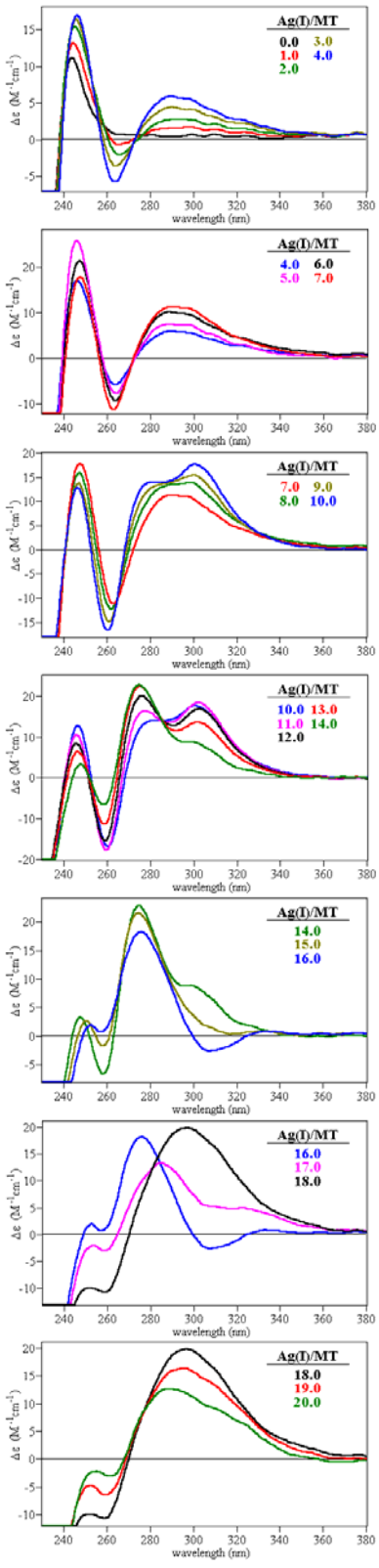

Figure 1. CD spectra recorded during the Ag(I) titration of a 20.21 μM solution of recombinant Zn_7-MT at pH 7.5. The Ag^+ to MT molar ratios are indicated within each frame.

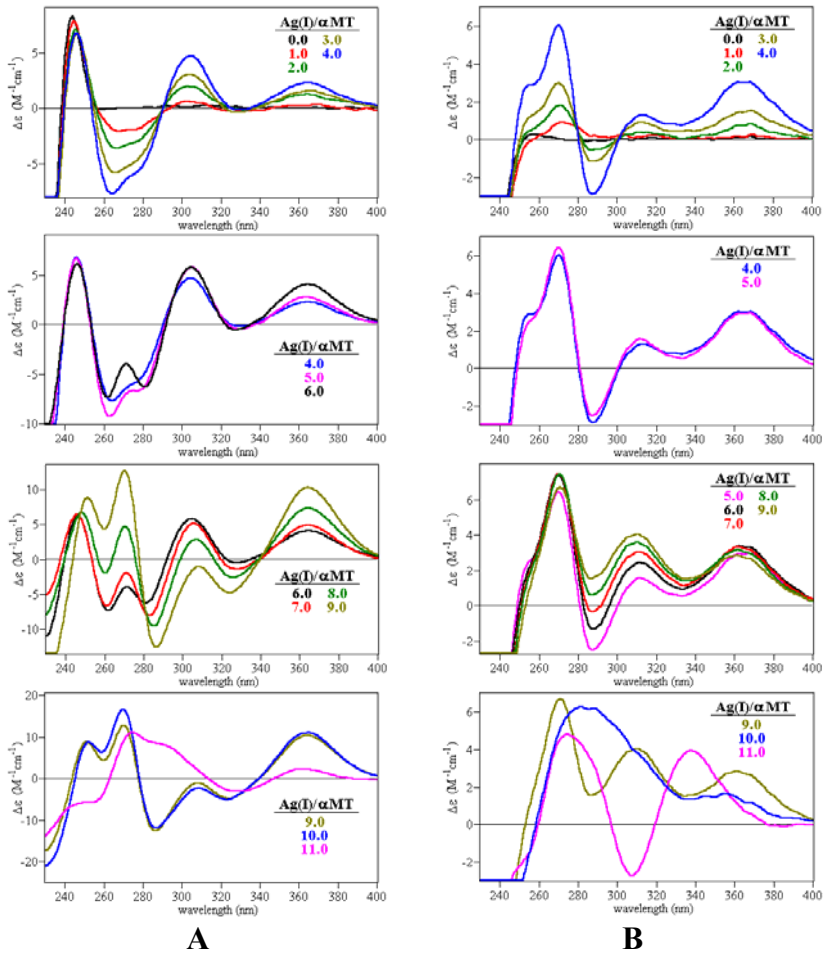

Figure 2. CD spectra recorded during the Ag(I) titration of a 20.08 μM solution of mammalian Zn_4-αMT at pH 7.5 (**A**) and of a 19.96 μM solution of mammalian apo-αMT at pH 2.5 (**B**). The Ag^+ to MT molar ratios are indicated within each frame.

replacements in both domains of MT and of its presence in the two first steps of the titration of the entire protein. The overall results, which have allowed us to propose the reaction pathways accompanying the Zn/Ag replacement in the three Zn-MT species, Scheme 2, or the stepwise incorporation of Ag(I) to the corresponding apo-MTs, are discussed below.

Remarkably, the analysis of the spectrometric data (Table 1) along the three titrations provides valuable information concerning the CD fingerprint of the existing metal-MT species. Thus, on the basis of the ESI-MS data, only very few additions of Ag(I) to the Zn-MT proteins give rise to a unique species in solution. In these cases, the CD fingerprint of the species formed is readily available as it corresponds to the CD spectrum of the solution (Table 2A). Conversely, most of the additions of Ag(I) lead to mixtures of Ag,Zn-MT and/or Ag-MT species and thus the electronic absorption spectra represent an average of the optical features of the different species coexisting in solution. Fortunately, in some titration points the high predominance of a particular species allows the assumption that its CD fingerprint should be similar to the CD spectrum obtained from the mixture. This occurs most frequently in the entire protein, where the silver stoichiometry in the predominant species usually matches the number of

Scheme 1. Reaction pathways proposed on the basis of the optical spectroscopic data retrieved from the titrations of Zn_3-βMT [14], Zn_4-αMT and Zn_7-MT with $AgClO_4$ at pH 7.5 and 2.5, respectively.

β domain:

$$Zn_3\text{-}\beta MT \rightarrow Ag_3Zn_x\text{-}\beta MT \rightarrow Ag_6\text{-}\beta MT \rightarrow Ag_9\text{-}\beta MT$$

$$apo\text{-}\beta MT \rightarrow Ag_3\text{-}\beta MT \rightarrow Ag_6\text{-}\beta MT \rightarrow Ag_9\text{-}\beta MT$$

α domain:

$$Zn_4\text{-}\alpha MT \rightarrow Ag_4Zn_x\text{-}\alpha MT \rightarrow Ag_6Zn_y\text{-}\alpha MT \rightarrow Ag_9\text{-}\alpha MT \rightarrow Ag_{11}\text{-}\alpha MT$$

$$apo\text{-}\alpha MT \rightarrow Ag_4\text{-}\alpha MT \rightarrow Ag_5\text{-}\alpha MT \rightarrow Ag_9\text{-}\alpha MT \rightarrow Ag_{10}\text{-}\alpha MT \rightarrow Ag_{11}\text{-}\alpha MT$$

entire MT:

$$Zn_7\text{-}MT \xrightarrow{coop} Ag_4Zn_x\text{-}MT \xrightarrow{coop} Ag_7Zn_y\text{-}MT \rightarrow Ag_{10}Zn_z\text{-}MT \rightarrow Ag_{14}\text{-}MT \rightarrow Ag_{16}\text{-}MT \rightarrow Ag_{18}\text{-}MT$$

$$apo\text{-}MT \rightarrow Ag_6\text{-}MT \rightarrow Ag_{10}\text{-}MT \rightarrow Ag_{13}\text{-}MT \rightarrow Ag_{16}\text{-}MT$$

Ag(I) eq added (Table 2B). This is not a common scenario for the αMT and βMT fragments. However, in these cases, the distribution of species obtained from ESI-MS data allows identification of the titration point whose CD spectrum should resemble the CD fingerprint of a particular metal-MT species. Thus, the CD features of Ag_4Zn_1-βMT, Ag_6-βMT and Ag_3Zn_2-αMT, should be close to the CD spectra recorded after the addition of 3 or 4 Ag(I) eq to Zn_3-βMT, and 4 Ag(I) eq to Zn_4-αMT, respectively. Finally, due to its minor presence in solution, it is not possible to assign a CD spectrum and thus to know the CD features of some of the species formed during the Zn/Ag replacement in Zn_7-MT (Table 2C).

The silver-binding abilities of recombinant mouse MT 1 and corresponding α and β fragments

The combined evidence from the optical (Fig. 1, 2A, S1 and S3) and mass data (Table 1) obtained during the titrations of the recombinant mouse Zn_7-MT, Zn_4-αMT and Zn_3-βMT [14] at pH 7.5 with $AgClO_4$ leads to the reaction pathways given in Scheme 2. A deeper insight into these data provides significant information on the Ag(I)-MT system, the more relevant issues being discussed immediately after.

One main conclusion refers to the coexistence of several Ag,Zn-MT and/or Ag-MT species in the vast majority of the titration points (Table 1). The exceptions (Table 2A) are found either in the last stages of the titrations of the three proteins, as they achieve saturation, or in the titration points corresponding to the cooperative formation of Ag_4Zn_5-MT and Ag_7Zn_3-MT. While this coexistence is unprecedented according to earlier Ag(I) binding studies to MT, the combination of mass and optical data has disclosed a similar situation in Cd-MT systems [15, 19]. To this novelty, otherwise unexceptional on the basis of the successive formation constants of complex species, the predominance of certain species in solution is also remarkable. This is the case for Ag_4Zn_1-βMT, Ag_7-βMT, Ag_3Zn_2-αMT, Ag_6Zn_1-αMT, and Ag_9-αMT, the latter being an outstanding example. Thus, Ag_9-αMT appears in solution after the addition of 2 Ag(I) eq to Zn_4-αMT, it becomes the predominant species for 7 Ag(I) eq, it exists as a unique species between 8 and 10 Ag(I) eq and evolves to Ag_{11}-αMT after the addition of the 11th Ag(I) eq. Regarding the Zn/Ag replacement in Zn_7-MT, it proceeds according to the stepwise formation of Ag,Zn-MT and Ag-MT species with no experimental evidence showing a higher stability of some species over the others.

Other relevant features deserve special consideration. First, the entire protein and also the

Table 1. Distribution of the metal aggregates present in solution, according to ESI-MS data, during the titration of Zn_3-βMT (**A**), Zn_4-αMT (**B**) and Zn_7-MT (**C**) with Ag(I) at pH 7.5 as a function of the number of Ag(I) equivalents added

A

	Ag(I) equivalents added*									
	0	1	2	3	4	5	7	8	9	10
Zn_3-βMT	**X**	**X**	**X**							
Ag_3Zn_1-βMT			x	x						
Ag_4Zn_1-βMT		x	**X**	**X**						
Ag_5-βMT				x	x	x	x	x		
Ag_6-βMT				x	**X**	x	x	x		
Ag_7-βMT						**X**	**X**	**X**		
Ag_8-βMT						x		x		
Ag_9-βMT									**X**	**X**

*Several attempts to record the ESI-MS spectrum after the addition of 6 Ag(I) eq were unsuccessful

B

	Ag(I) equivalents added										
	0	1	2	3	4	5	6	7	8	9	10	11
Zn_4-αMT	**X**	**X**	**X**	**X**								
Ag_1Zn_3-αMT		x	x									
Ag_2Zn_3-αMT			x	x								
Ag_3Zn_2-αMT			**X**	**X**	**X**	x	x	x				
Ag_4Zn_2-αMT			x	x	x	x	x					
Ag_6Zn_1-αMT					x	**X**	**X**	x				
Ag_9-αMT			x	x	x	x	x	**X**	**X**	**X**	**X**	
Ag_{11}-αMT												**X**

C

	Ag(I) equivalents added																				
	0	1	2	3	4	5	6	7	8	9	10	11	12	13	14	15	16	17	18	19	20	22
Zn_7-MT	**X**	**X**	**X**	x																		
Ag_4Zn_5-MT		x	**X**	**X**	x	**X**	**X**															
Ag_7Zn_3-MT					x	**X**	**X**															
Ag_8Zn_3-MT								**X**														
$Ag_{10}Zn_2$-MT								x	**X**	**X**	**X**	x										
$Ag_{12}Zn_1$-MT									x	x	**X**	**X**	**X**	x								
Ag_{14}-MT														**X**	x	x						
Ag_{15}-MT															**X**	**X**						
Ag_{16}-MT															x	x	**X**	x	x			
Ag_{17}-MT																	x	**X**	**X**			
Ag_{18}-MT																			x	x		
Ag_{19}-MT																				**X**	**X**	**X**

X: major species x: minor species

Scheme 2. Reaction pathways corresponding to the subsequent replacement of Zn(II) by Ag(I) at pH 7.5 in (**A**) Zn_4-αMT, (**B**) Zn_3-βMT and (**C**) Zn_7-MT, on the basis of both optical and mass data. The existence of the species highlighted by * would not have been deduced if only optical data had been considered

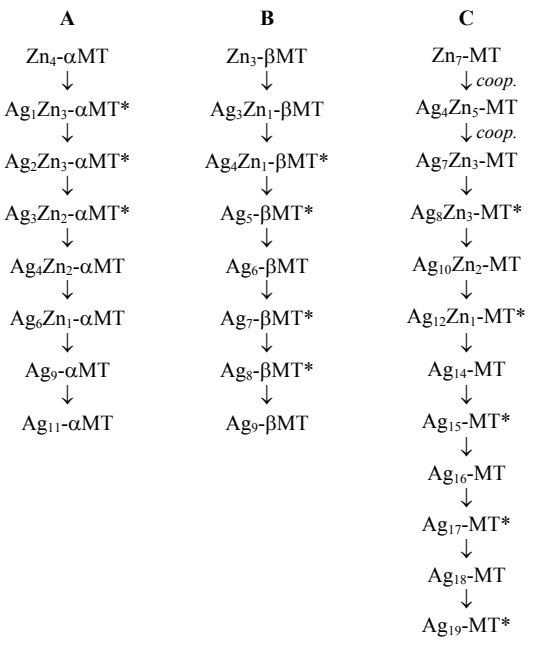

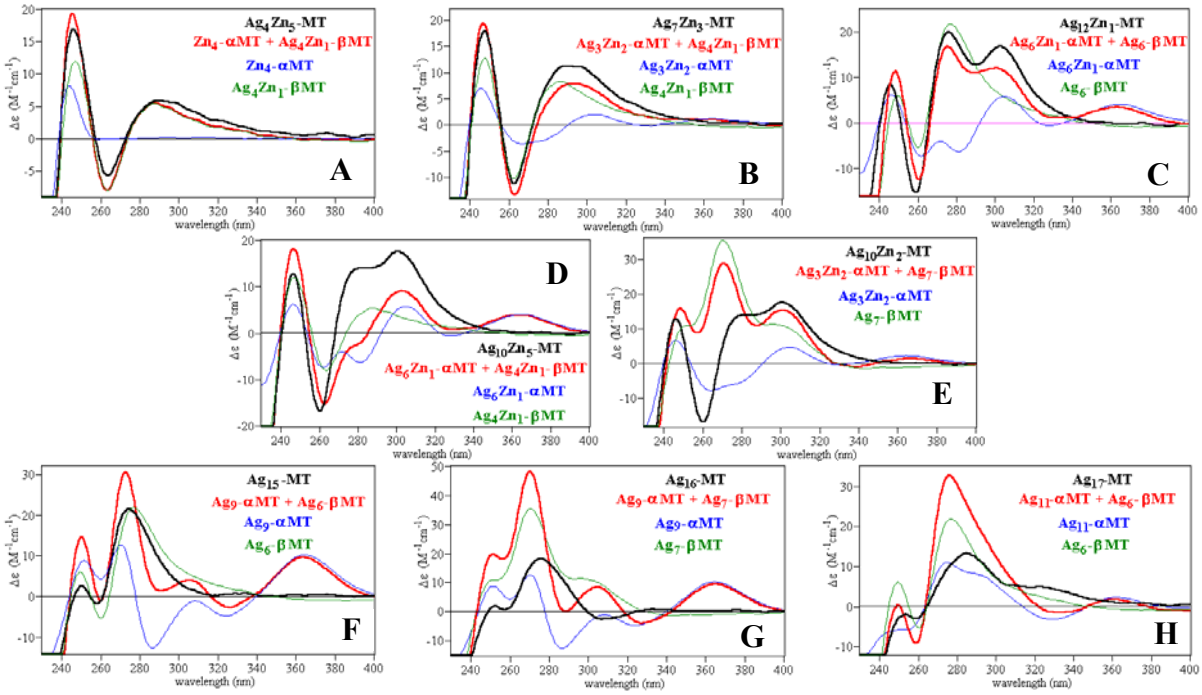

Figure 3. Comparison of the CD spectra of the heterometallic Ag_4Zn_5-MT (**A**); Ag_7Zn_3-MT (**B**); $Ag_{12}Zn_1$-MT (**C**); $Ag_{10}Zn_5$-MT (**D** and **E**), and homometallic Ag_{15}-MT (**F**), Ag_{16}-MT (**G**) and Ag_{17}-MT (**H**) species formed during the Ag(I) titration of Zn_7-MT at pH 7.5 with the sum of the CD spectra of some of the species obtained in the Ag(I) titrations of the αMT and the βMT fragments at the same pH value (Table 3)

separate α and β fragments produce a significant number of heterometallic Ag,Zn-MT species. Prior to these results it was accepted that Ag_6Zn_4–MT was the only heterometallic species formed, which consisted of homometallic $(Zn_4)^{\alpha}$ and $(Ag_6)^{\beta}$ aggregates [20]. A second unprecedented issue refers to the formation of species such as Ag_1Zn_3-αMT, Ag_3Zn_2-αMT, Ag_3Zn_1-βMT or Ag_7Zn_3-MT, whose stoichiometry is not consistent with the 1:2 replacement rule of Zn(II) by Ag(I) established on a charge compensation basis [21]. Significantly, some of the previous species are more relevant -regarding predominance and maintenance in solution- than others that follow the 1:2 substitution pattern. Once saturation of the proteins is achieved, only homometallic Ag-MT species are found with Ag:S ratios close to 1 (19:20 MT, 11:11 αMT and 9:9 βMT), the 19Ag(I)/MT occupancy not being consistent with the 17.3 ratio proposed for the estimation of the concentration of MT in tissue samples by the silver-saturation method [22].

Unfortunately, comparison of the results obtained at both pH values, 7.5 and 2.5, is restricted to the optical data owing to the unsuccessful attempts to record ESI-MS spectra at pH 2.5, as already noted. The different metal-MT species proposed along the six titrations (Scheme 1) have been identified from saturation of the chiral intensity (Fig. 1, 2 and S4) and changes in the UV-vis absorption spectra (Figures S1-S4), as described for the Ag(I) titration of Zn_3-βMT [14]. A further insight into these data reveals different CD envelopes for species with the same Ag(I):MT ratio at pH 7.5 and 2.5 (Ag_9-αMT, Ag_{11}-αMT, Ag_6-βMT, Ag_9-βMT and Ag_{16}-MT) strongly suggesting that their structure is pH-dependent. This would be consistent with a template effect of the Zn(II) ions as already proposed for the related Cu(I)-MT system [1]. Thus, the final folding of the Ag-MT aggregates is probably determined by the Zn(II) ions initially bound to the proteins at pH 7.5 but not at 2.5.

Main features of the difference UV-vis absorption spectra recorded during the titrations of Zn_7-MT, Zn_4-αMT and Zn_3-βMT at pH 7.5 (Fig. S1, S3 and [14]) can be generalized as follows: a) the binding of the first Ag(I) eq to the three proteins causes the appearance of an absorption band at *ca*. 250 nm

Table 2. Classification of the metal aggregates formed during the titration of Zn_3-βMT, Zn_4-αMT and Zn_7-MT with Ag(I) at pH 7.5 according to their CD fingerprints. Species whose CD fingerprint: A) can be definitely known, B) can be only approximately known, and C) is unavailable. The CD fingerprint of species in italics have been obtained from solutions where the total Ag(I) content does not match the silver stoichiometry in the corresponding formula (See text).

		MT	αMT	βMT
A	Definite CD fingerprint	Ag_4Zn_5-MT Ag_7Zn_3-MT Ag_{19}-MT	Ag_9-αMT Ag_{11}-αMT	Ag_9-βMT
B	Approximate CD fingerprint	Ag_8Zn_3-MT $Ag_{10}Zn_2$-MT $Ag_{12}Zn_1$-MT Ag_{15}-MT Ag_{16}-MT Ag_{17}-MT	*Ag_3Zn_2-αMT* Ag_6Zn_1-αMT	*Ag_4Zn_1-βMT* *Ag_6-βMT* Ag_7-βMT
C	Unavailable CD fingerprint	Ag_{14}-MT Ag_{18}-MT	Ag_1Zn_3-αMT Ag_2Zn_3-αMT Ag_4Zn_2-αMT	Ag_3Zn_1-βMT Ag_5-βMT Ag_8-βMT

Table 3. Possible metal distributions between domains in the Ag_xZn_y-MT ($0 \le y < 7$) species found in the Ag(I) titration of Zn_7-MT at pH 7.5. Species with definite CD fingerprint are highlighted in bold, with approximate CD fingerprint in black, and with unavailable CD fingerprint in gray. Metal distributions whose CD features nicely match those of the corresponding MT species are enclosed within a solid line, those distributions that can only be assumed to describe the entire MT (see text) are enclosed within a thin line, while the CD features of those enclosed within a dotted line do not have a good fit and thus they should be disregarded.

Ag_4Zn_5-MT	⇒	**$(Zn_4)^\alpha$ $(Ag_4Zn_1)^\beta$**	$(Ag_4Zn_2)^\alpha$ **$(Zn_3)^\beta$**		
Ag_7Zn_3-MT	⇒	$(Ag_4Zn_2)^\alpha$ $(Ag_3Zn_1)^\beta$	**$(Ag_3Zn_2)^\alpha$ $(Ag_4Zn_1)^\beta$**	$(Ag_2Zn_3)^\alpha$ $(Ag_5)^\beta$	$(Ag_1Zn_3)^\alpha$ $(Ag_6)^\beta$
Ag_8Zn_3-MT	⇒	$(Ag_4Zn_2)^\alpha$ $(Ag_4Zn_1)^\beta$	$(Ag_2Zn_3)^\alpha$ $(Ag_6)^\beta$	$(Ag_1Zn_3)^\alpha$ $(Ag_7)^\beta$	
$Ag_{10}Zn_2$-MT	⇒	$(Ag_6Zn_1)^\alpha$ $(Ag_4Zn_1)^\beta$	$(Ag_4Zn_2)^\alpha$ $(Ag_6)^\beta$	$(Ag_3Zn_2)^\alpha$ $(Ag_7)^\beta$	
$Ag_{12}Zn_1$-MT	⇒	$(Ag_6Zn_1)^\alpha$ $(Ag_6)^\beta$	**$(Ag_9)^\alpha$** $(Ag_3Zn_1)^\beta$		
Ag_{14}-MT	⇒	**$(Ag_9)^\alpha$** $(Ag_5)^\beta$			
Ag_{15}-MT	⇒	**$(Ag_9)^\alpha$** $(Ag_6)^\beta$			
Ag_{16}-MT	⇒	**$(Ag_9)^\alpha$** $(Ag_7)^\beta$	**$(Ag_{11})^\alpha$** $(Ag_5)^\beta$		
Ag_{17}-MT	⇒	**$(Ag_9)^\alpha$** $(Ag_8)^\beta$	**$(Ag_{11})^\alpha$** $(Ag_6)^\beta$		
Ag_{18}-MT	⇒	**$(Ag_9)^\alpha$** **$(Ag_9)^\beta$**	**$(Ag_{11})^\alpha$** $(Ag_7)^\beta$		
Ag_{19}-MT	⇒	**$(Ag_{11})^\alpha$** $(Ag_8)^\beta$			

sometimes accompanied by a less intense contribution at *ca*. 300 nm, b) further additions of Ag(I) provoke absorptions at *ca*. 275 and 320 nm for the entire protein and its α fragment, but only at 275 nm for the β fragment, and c) the final additions of Ag(I) give rise to a very broad absorption in the range 300-380 nm in the case of the entire MT and its β fragment, which differs from the unique envelope of the α fragment. Remarkably, the difference absorption data obtained for the Ag(I) binding to apo-MT, apo-αMT and apo-βMT [14] at acidic pH only reveal a generalized absorption between 230 and 400 nm with a maximum centered at *ca*. 240 nm, thus indicating that the coordination environments about Ag(I) in all the species formed should be comparable. Unfortunately, all the patterns observed through the analysis of the optical data cannot be extended to assigning a specific type of coordination environment for the silver centers, owing to the scarcity of well established correlations between the stereochemistry around Ag(I) in silver thiolates and the corresponding absorption energies.

One further issue concerning the CD features of Ag(I) binding to MT deserves consideration. Remarkably, while most of the CD spectra recorded during the Ag(I) titration of the Zn_4-αMT fragment either at pH 7.5 (Fig. 2A) or 2.5 (Fig. 2B) show an unprecedented absorption at *ca*. 360 nm, this is absent in the titrations of Zn_3-βMT and Zn_7-MT. The exceptional stability and maintenance in solution of the Ag_9-αMT species and the low-energy region of the band suggest the assignment of the previous absorption to metal cluster-centered transitions brought about by Ag(I)-Ag(I) interactions, which could be indicative of an specific Ag(I) polyhedron in Ag_9-αMT [23].

Metal distribution between the α and β domains of MT

Knowledge of the Ag_xZn_y-MT stoichiometries and CD features of the observed species in the entire protein allows determination of the silver and/or zinc content in its corresponding α and β fragments provided the same information is available for the two separate α and β domains. The procedure used entails the addition of the CD fingerprints of the individual fragments and comparison with that of the particular species of the entire protein [1]. Consequently, it will provide information on the metal distribution as long as the constituting α and β domains in this species maintain an independent behavior. Conversely, a non additive behavior will give evidence of their mutual dependence.

Based on these premises, all the possible combinations of the individually identified α and β aggregates whose total metal content matches that of the characterized Ag_xZn_y-MT species have been considered (Table 3). The main drawback in order to follow the above mentioned procedure comes from the absence of an specific CD fingerprint for those aggregates which are not either unique or clearly predominant in solution at a certain stage of the titration (Table 2C). This limitation accounts for enabling consideration of only eight out of the twenty-three possible combinations depicted in Table 3. Remarkably, the unique cases in which the

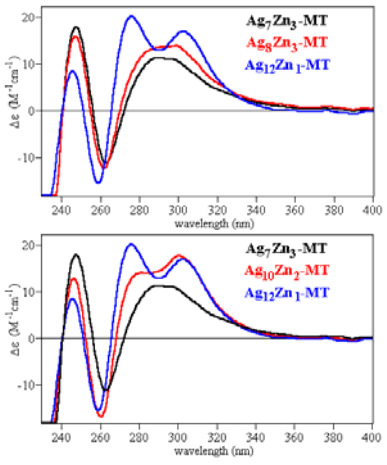

Figure 4. Comparison of the CD spectra of Ag_8Zn_3-MT (**A**) and $Ag_{10}Zn_5$-MT (**B**) with those of Ag_7Zn_3-MT and $Ag_{12}Zn_1$-MT.

Scheme 3. Proposed reaction pathways for Ag(I) and Cu(I) binding to mammalian Zn_7-MT 1. The metal distribution between domains in the heterometallic Ag_xZn_y-MT species is based on the comparison of the separate α and β fragments with the entire protein as discussed in the text.

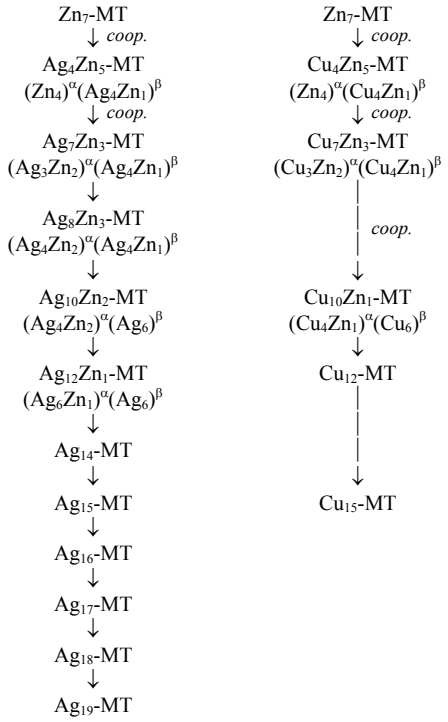

structure of the entire MT appears to be built from the addition of the independent fragments (Fig. 3) correspond to three heterometallic species, Ag_4Zn_5-MT, Ag_7Zn_3-MT and $Ag_{12}Zn_1$-MT (Table 3). A particular case is found for the two remaining heterometallic aggregates. The analysis of their metal distribution is hampered either by the lack of CD information referring to the α fragment or by the non additive behavior of the corresponding fragments (Table 3, Fig. 3). Notwithstanding this, the metal disposition in Ag_8Zn_3-MT and $Ag_{10}Zn_2$-MT can be proposed if taking as reference the species formed before (Ag_7Zn_3-MT) and after ($Ag_{12}Zn_1$-MT) them. The similarities between the CD fingerprints of Ag_8Zn_3-MT *vs*. Ag_7Zn_3-MT and of $Ag_{10}Zn_2$-MT *vs*. $Ag_{12}Zn_1$-MT, Fig. 4, provide the main clues to fit all the experimental data, which lead to the proposal of $(Ag_4Zn_2)^\alpha(Ag_4Zn_1)^\beta$ and $(Ag_4Zn_2)^\alpha(Ag_6)^\beta$ metal distributions for Ag_8Zn_3-MT and $Ag_{10}Zn_2$-MT, respectively.

The sequence of steps accompanying the Zn/Ag replacement in Zn_7-MT that is consistent with a comprehensive analysis of the optical and mass data recorded in this work is given in Scheme 3. Thus, the first four Ag(I) eq added to Zn_7-MT bind to the β domain by displacing two of the three Zn(II) ions initially bound to it. The remaining Zn(II) ions in this domain are not replaced by Ag(I) until four new Ag(I) eq have entered the α domain giving thus rise to the $(Ag_4Zn_2)^\alpha(Ag_4Zn_1)^\beta$ distribution in the Ag_8Zn_3-MT species. While the next two Ag(I) eq give rise to $(Ag_6)^\beta$ in the $Ag_{10}Zn_2$-MT species, the $(Ag_6)^\beta$ aggregate remains unchanged by the subsequent additions of silver leading to $(Ag_6Zn_1)^\alpha(Ag_6)^\beta$ in the $Ag_{12}Zn_1$-MT species. Further addition of Ag(I) eq causes formation of a series of homometallic species Ag_x-MT, $14 \le x \le 19$, but provides no experimental evidences in order to find out their metal distribution between domains or to ascertain if they consist of a unique domain. Overall, the presence of at least one Zn(II) ion bound to the protein seems to be a requirement for the Ag-MT system to have a bidominial structure, as already found in the Cu-MT system [1].

Comparison of the Ag(I) and Cu(I) binding abilities of recombinant mouse MT 1

Comparison of the binding features of Ag(I) and Cu(I) [1] toward recombinant mouse Zn_7-MT 1, Scheme 3, shows that both M(I) ions follow exactly the same pattern during the first steps of the Zn/M(I) replacement, but from this stage their behavior

Scheme 4. Proposed reaction pathways for Ag(I) and Cu(I) binding to mammalian Zn_3-βMT 1 (**A**) and Zn_4-αMT 1 (**B**). Species with the same stoichiometry for Ag(I) and Cu(I) are highlighted in bold, those in italics coincide on the M(I) content but differ on that of Zn(II).

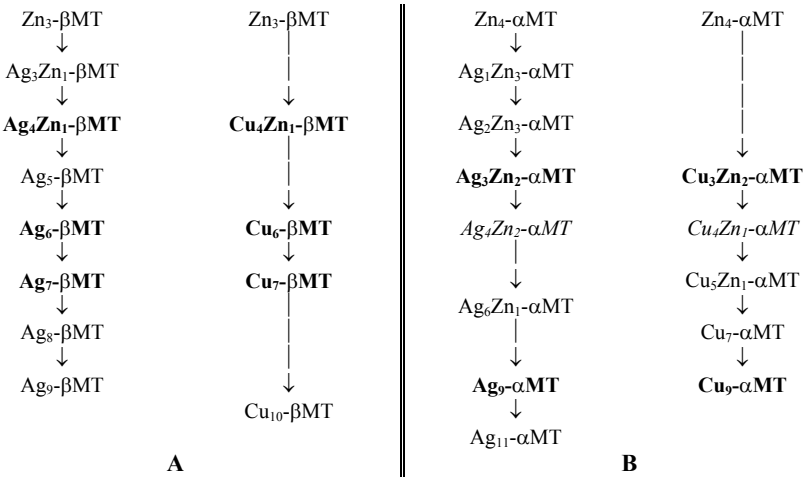

Scheme 5. Proposed reaction pathways for Ag(I) and Cu(I) binding to mammalian apo-αMT 1 (**A**) and apo-MT 1 (**B**). Species with the same stoichiometry for Ag(I) and Cu(I) are highlighted in bold

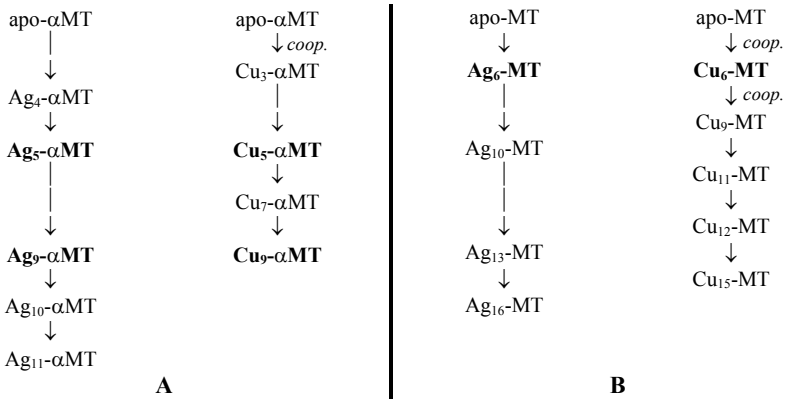

differentiates increasingly as more M(I) eq are bound to the protein.

The initial parallel behavior is evidenced by the cooperative formation of aggregates of the same stoichiometry, $M^I_4Zn_5$-MT and $M^I_7Zn_3$-MT, which show equivalent metal distributions between domains and comparable CD spectra, Fig. 5A and 5B, all these data being indicative of isostructural M(I)-MT complexes. Differences start appearing with the addition of M(I) ions to the $M^I_7Zn_3$-MT species. Thus, while Ag_7Zn_3-MT gives rise first to Ag_8Zn_3-MT and then to $Ag_{10}Zn_2$-MT, both with a $(Ag_4Zn_2)^\alpha$ occupancy, the Cu_7Zn_3-MT analog cooperatively evolves to $Cu_{10}Zn_1$-MT $[(Cu_4Zn_1)^\alpha(Cu_6)^\beta]$. Further additions cause the previous $M^I_{10}Zn_y$-MT aggregates to yield respectively $Ag_{12}Zn_1$-MT $[(Ag_6Zn_1)^\alpha (Ag_6)^\beta]$ and Cu_{12}-MT. The differences observed in the stoichiometries of the heterometallic aggregates formed after $M^I_7Zn_3$-MT, as well as in their corresponding structure (Fig. 5C, 5D), evidence the greater reluctance of Zn(II) to be displaced by Ag(I) than by Cu(I). Once $Ag_{12}Zn_1$-MT and Cu_{12}-MT are formed, the evolution of the M^I_x-MT species shows increasing dissimilarities until the saturation of the protein is achieved, which occurs for Ag_{19}-MT and Cu_{15}-MT, respectively (Scheme 3).

The differences observed in the binding of Ag(I) and Cu(I) to recombinant Zn_7-MT 1 do not hamper extending previous findings in the Cu-MT 1 system [1] to the silver analog. First, both monovalent metal ions show only a partial preference for the β domain, and not absolute as proposed in earlier studies [24]. Consistently, for M(I) = Ag, Cu, the first four M(I) eq added to Zn_7-MT lead to $(M_4Zn_1)^\beta$ occupancies, but the evolution of this domain to the corresponding homometallic $(M_6)^\beta$ species requires previous binding of four M(I) ions to the α counterpart (Scheme 3). Second, also for both M(I) = Ag, Cu, the 3D structure of M(I)-containing MT species follows a common pattern. Thus, only the 3D structure of heterometallic species -those of formula $M^I_xZn_y$-MT with $y \neq 0$- can be considered as formed by the addition of two independent α and β domains, as discussed for the Ag_xZn_y-MT species in the previous section. Conversely, the folding observed for the homometallic M^I_x-MT species cannot be described on the basis of a bi-dominial structure.

A glance over the reaction pathways accompanying the Zn/M(I), M= Ag, Cu, replacement in Zn_4-αMT and Zn_3-βMT (Scheme 4) suggests more similarities in the stoichiometry of the M(I)-

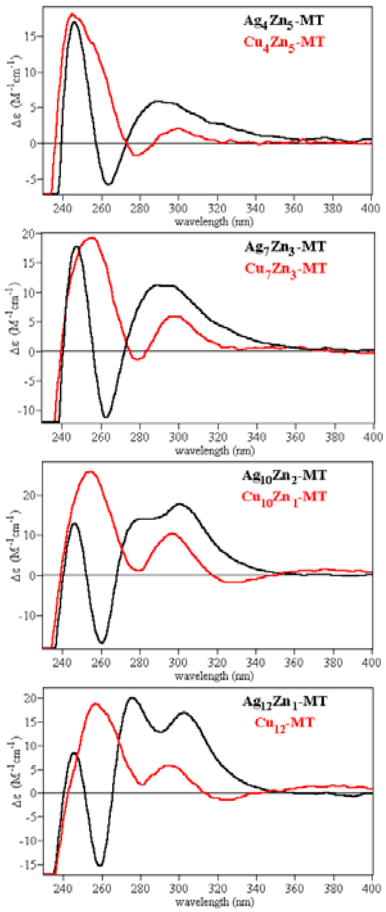

Figure 5. Comparison of the CD spectra of several Ag_xZn_y-MT species formed during the titration of Zn_7-MT 1 with Ag(I) [Ag_4Zn_5-MT (**A**), Ag_7Zn_3-MT (**B**), $Ag_{10}Zn_2$-MT (**C**), $Ag_{12}Zn_1$-MT (**D**)] with the closest analogs found in the titration of the same protein with Cu(I).

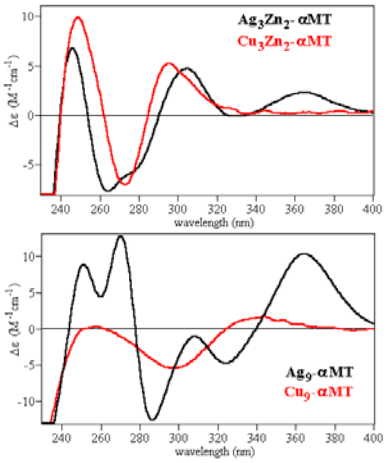

Figure 6. Comparison of the CD spectra of Ag_3Zn_2-αMT (**A**) and Ag_9-αMT (**B**), formed during the titration of Zn_4-αMT 1 with Ag(I), with the stoichiometric analogs found in the titration of the same protein with Cu(I).

containing species for the βMT than for the αMT domain. However, the analysis of the optical data is clearly indicative that the binding of Ag (Fig. 2 and S1) or Cu [1] to Zn_4-αMT has closer resemblance than that to the Zn_3-βMT domain [14]. In fact, the behavior of Zn_4-αMT toward Ag(I) and Cu(I) reproduces at a smaller scale that of Zn_7-MT just described. Thus, the addition of the first three M(I) eq causes formation of the $M^I_3Zn_2$-αMT species through parallel spectral evolutions and with CD fingerprints that suggest comparable 3D structures (Fig. 6A). Subsequent additions induce an increasing differentiation until achieving saturation for Ag_{11}-αMT or Cu_9-αMT, respectively. Remarkably, the M^I_9-αMT (M= Ag, Cu) species have the same stoichiometry but different folding as evidenced in Fig. 6B. On the other hand, the replacement mechanism of Zn(II) in Zn_3-βMT by addition of Ag(I) and Cu(I) had been object of previous studies [14]. The different behavior we reported for both metal ions is fully consistent with the present results, which afford a more detailed picture of the reaction pathway (Scheme 2B). The combined used of CD, UV-vis and CZE-ESI-MS in the present work shows that $M^I_4Zn_1$-βMT, M^I_6-βMT and M^I_7-βMT have the same stoichiometry, Scheme 4A, but a different structure for M= Ag and Cu [14]. This finding suggests that Ag(I) and Cu(I) bind differentially to the βMT fragment and that the Zn(II) ions initially bound to the protein fail to determine formation of structurally related species even in the first stages of the titrations. Conversely, the observed similarities in the behavior of Zn_4-αMT and Zn_7-MT during the first steps of Zn/M(I) replacement are consistent with a template effect of the Zn(II) ions, which determine the folding of these proteins while being replaced by M(I).

The incorporation of M(I) ions, M = Ag, Cu, to the apo-forms of the entire MT and corresponding αMT and βMT fragments gives additional information on the different binding features of Ag(I) and Cu(I) to these proteins. The reaction pathways followed by apo-MT and apo- αMT are given in Scheme 5, while those corresponding to apo-βMT can be found elsewhere [14]. On the basis of the stoichiometries and CD features of the species formed by the addition of Ag(I) and Cu(I) to the apoproteins, their behavior can be summarized as follows: a) apo-MT and apo- βMT show a common behavior as they both bind differently these monovalent metal ions (Fig. 7A), b) notwithstanding this, the first M(I) ions added to apo-MT bind to the β domain, and c) Ag(I) and Cu(I) bind similarly to the α domain but only in the first stages of metal loading, which lead to structurally related M^I_5-αMT species, Fig. 7B and 7C.

Conclusions

The results obtained in this work give a new insight on the Zn/Ag(I) replacement mechanism in mammalian Zn_7-MT 1 and constitutive Zn_4-αMT and Zn_3-βMT fragments as well as on the Ag(I) loading to the corresponding apoforms. The study of the separate fragments has shown to be essential for the understanding of the metal binding properties of the entire MT protein. Also, the coupling of mass (CZE-ESI-MS) to optical (CD and UV-vis) spectroscopies has allowed a detailed analysis of the reaction pathways accompanying the above processes.

Main unprecedented findings on the Ag(I) binding to Zn_7-MT at pH 7.5 refer to the high number and structural features of the silver-containing MT species. Thus, those of general formula Ag_xZn_y-MT, unlike the homometallic Ag_x-MT, can be considered

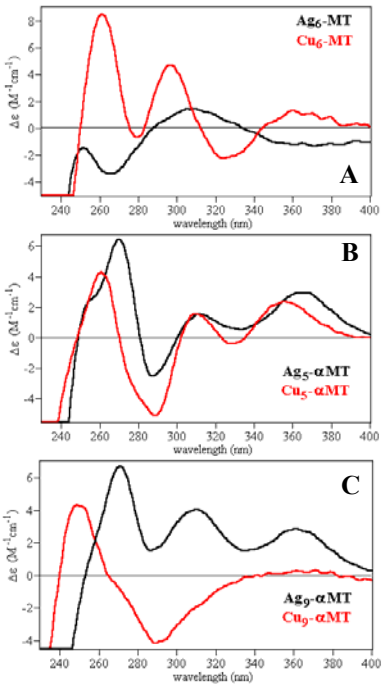

Figure 7. Comparison of the CD spectra of Ag_6-MT (**A**), Ag_5-αMT (**B**) and Ag_9-αMT (**C**), formed during the titration of apo-MT 1 and apo-αMT 1 with Ag(I), with the stoichiometric analogs found in the titration of the same proteins with Cu(I).

as formed by two independent α and β domains, each having an specific metal distribution. In addition, on the basis of the stoichiometries and folding of the Ag_x-MT species formed at pH 2.5, which differ from those found at pH 7.5, it can be concluded that Zn(II) ions are responsible for a template effect pre-conditioning the structure of the protein before they are displaced by Ag(I).

In order to address the question about the suitability of Ag(I) as a probe in the study of Cu(I) containing MT we have compared the binding features of both M(I) ions (M = Ag, Cu) toward the same Zn_7-MT protein under analogous conditions. One of the important conclusions is that the binding of Cu(I) and Ag(I) to the entire MT at pH 7.5 is totally comparable for a limited number of MT species, which remarkably enfold at least one Zn(II) ion within each of the two constituting α and β domains. This occurs for $M^I_4Zn_5$-MT $[(Zn_4)^\alpha(M_4Zn_1)^\beta]$ and $M^I_7Zn_3$-MT $[(M_3Zn_2)^\alpha(M_4Zn_1)^\beta]$, which are the only species where Ag(I) ions can be predicted to be an adequate probe for Cu(I). As the subsequent Zn/M(I) replacement in $M^I_7Zn_3$-MT is concomitant with increasing differentiation in the binding features of Cu and Ag, it seems likely that the latter is not a good model for the study of homometallic mammalian Cu-MT 1 species.

Another conclusion is based on the observation that the binding of M(I) ions to apo-MT at pH 2.5 leads to M(I)-MT species of different stoichiometries and structures for M = Ag or Cu, which evidences that they have specific coordination preferences towards the same protein ligand. These do not show while Zn(II) ions remain bound to the protein but become apparent when they are being displaced and thus cannot counterbalance the unequal preferences of Ag(I) and Cu(I). The results here reported are fully consistent with a further conclusion: copper has a greater affinity than silver towards the entire mammalian MT 1 and its separate α and β fragments. Thus, on the one hand the formation of $Ag_{12}Zn_1$-MT $[(Ag_6Zn_1)^\alpha(Ag_6)^\beta]$ *vs* Cu_{12}-MT is one of the examples of the greater efficiency of Cu to displace Zn from the protein. On the other, the fact that the stoichiometry and folding of the homometallic Cu_x-βMT species, unlike the silver analogs, is not dependent on the pH value indicates that the Zn(II) ions initially bound in Zn_3-βMT at pH 7.5 fail to play the structural role they perform when silver binds to the same protein. Overall, the spectroscopic data reported in the present paper can serve as a guideline for the design of structural studies in silver-reconstituted copper-containing metallothioneins.

Acknowledgements

Research reported from the corresponding author's laboratory was supported by a grant from the Spanish Ministerio de Ciencia y Tecnología (BQU2001-1976). Dra. Sílvia Atrian, who kindly provided us with the recombinant proteins used in this work, acknowledges the Spanish Ministerio de Ciencia y Tecnología for financial support (BIO2000-0910). We also acknowledge the Servei d'Anàlisi Química, Universitat Autònoma de Barcelona (CD, UV-vis) for allocating instrument time and Sandra Mounicou for technical assistance.

References

1. Bofill R, Capdevila M, Cols N, Atrian S, González-Duarte P (2001) J Biol Inorg Chem 6 : 408-417
2. González-Duarte P (2003) In: McCleverty JA, Meyer TJ (eds) Comprehensive Coordination Chemistry II. Pergamon, New York, Vol. 8, in press
3. Li YJ, Weser U(1992) Inorg Chem 31 : 5526-5533
4. Peterson CW, Narula SS, Armitage IM (1996) FEBS Letters 379 : 85-93
5. Bertini I, Hartman HJ, Klein T, Liu G, Luchinat C, Weser U (2000) Eur J Biochem 267 : 1008-1018
6. Romero-Isart N, Vašák M (2002) J Inorg Biochem 88 : 388-396
7. Narula SS, Mehra RK, Winge DR, Armitage IM (1991) J Am Chem Soc 113 : 9354-9358
8. Narula SS, Winge DR, Armitage IM (1993) Biochemistry 32 : 6773-6787
9. Mehra RK, Tran KT, Scott GW, Mulhandani P, Saini S (1996) J Inorg Biochem 61 : 125-142
10. Stillman MJ (1999) Metal-Based Drugs 6 : 277-290 and references therein
11. Nielson KB, Winge DR (1985) J Biol Chem 260 : 8698-8701 and references therein
12. Kull FJ, Reed HF, Elgren TE, Ciardelli TL, Wilcox DE (1990) J Am Chem Soc 112 : 2291-2298
13. Li H, Otvos JD (1998) J Inorg Biochem 70 : 187-194 and references therein
14. Bofill R, Palacios O, Capdevila M, Cols N, González-Duarte R, Atrian S, González-Duarte P (1999) J Inorg Biochem 73 : 57-64
15 Polec K, Palacios O, Capdevila M, González-Duarte P, Lobinski R (2002) Talanta 57 : 1011-1017
16. Capdevila M, Cols N, Romero-Isart N, González-Duarte R, Atrian S, González-Duarte P (1997) CMLS Cell Mol Life Sci 53 : 681-688
17. Cols N, Romero-Isart N, Capdevila M, Oliva B, González-Duarte P, González-Duarte R, Atrian S (1997) J Inorg Biochem 68 : 157-166
18. Corr JJ, Anacleto JF (1996) Anal Chem 68 : 2155-2163
19. Domenech J, Palacios O, Villarreal L, González-Duarte P, Capdevila M, Atrian S (2003) FEBS Letters 533 : 72-78
20. Li H, Otvos JD (1996) Biochemistry 35 : 13929-13936
21 Zelazowski A, Stillman MJ (1992) Inorg Chem 31 : 3363-3370
22. Scheuhammer AM, Cherian MG (1986) Toxicol Appl Pharmacol 82: 417-425
23. Roschitzki B, Vasak M (2002) J Biol Inorg Chem 7 : 611-616
24. Winge DR (1991) Methods Enzymol 205 : 438-447

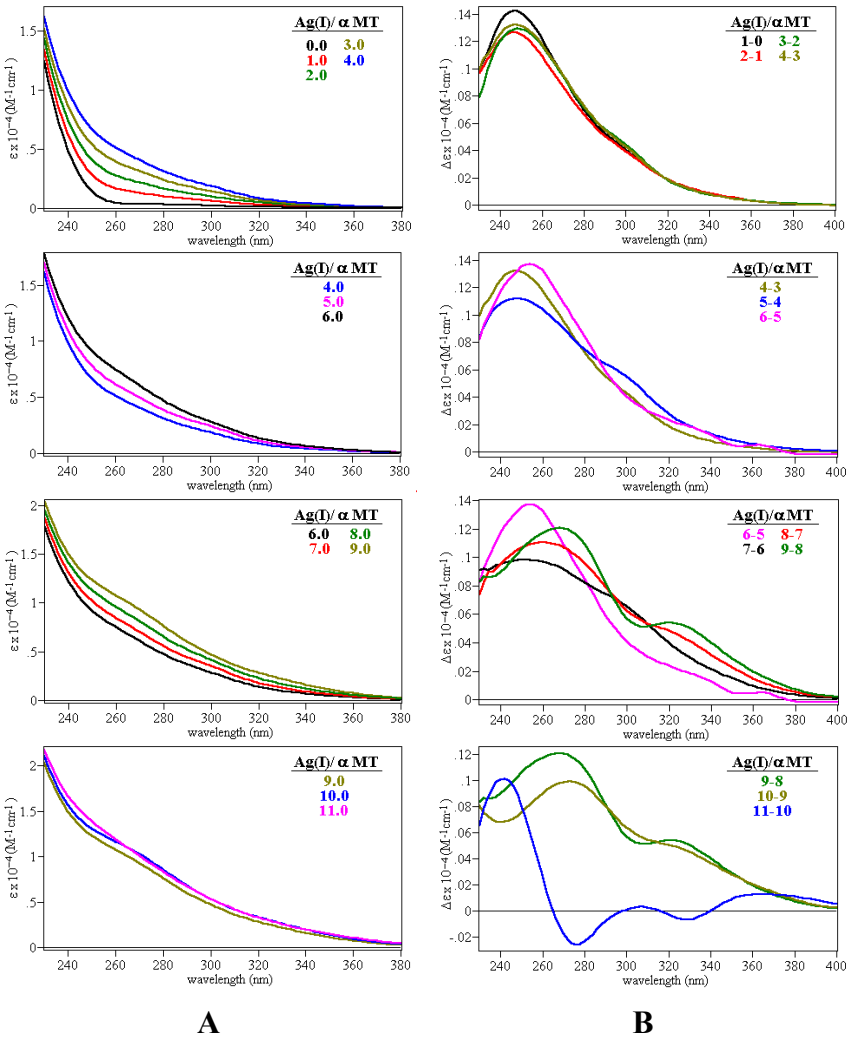

Figure S1. Ag(I) titration of a 20.08 μM solution of recombinant Zn_4-αMT at pH 7.5: (**A**) UV-vis absorption spectra; (**B**) difference absorption spectra obtained by subtracting the successive spectra of (**A**). The Ag^+ to MT molar ratios are indicated within each frame.

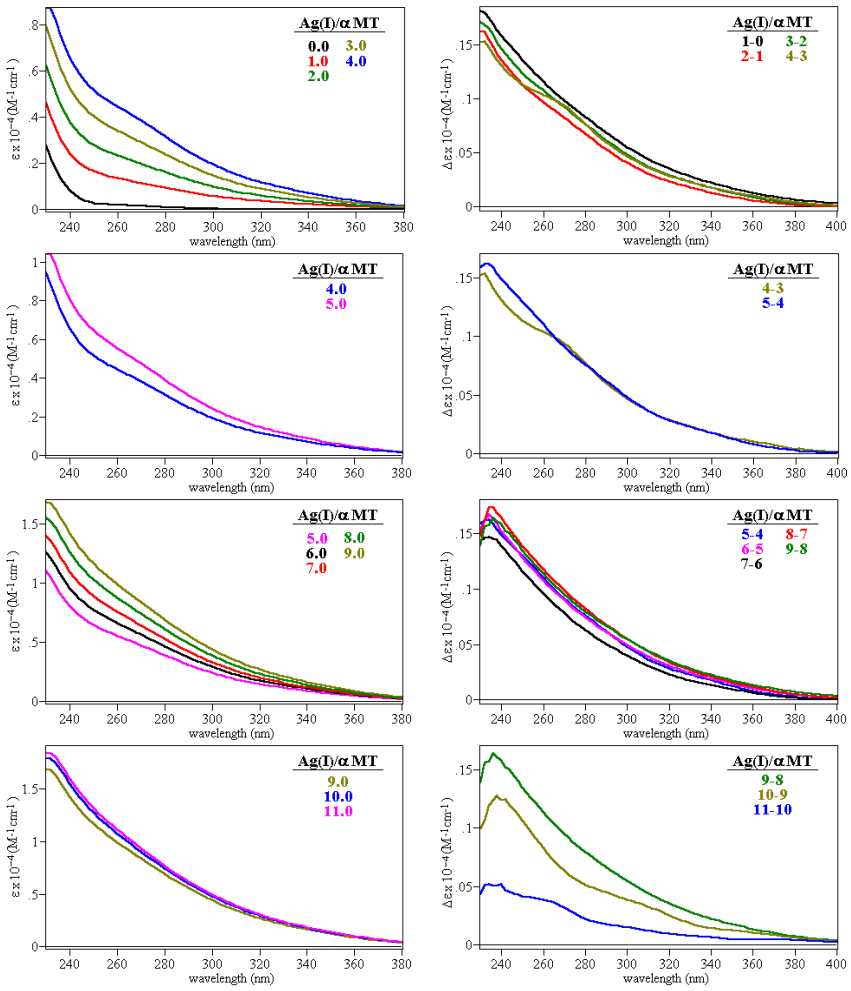

Figure S2. Ag(I) titration of a 19.96 μM solution of recombinant apo-αMT at pH 2.5: (**A**) UV-vis absorption spectra; (**B**) difference absorption spectra obtained by subtracting the successive spectra of (**A**). The Ag^+ to MT molar ratios are indicated within each frame.

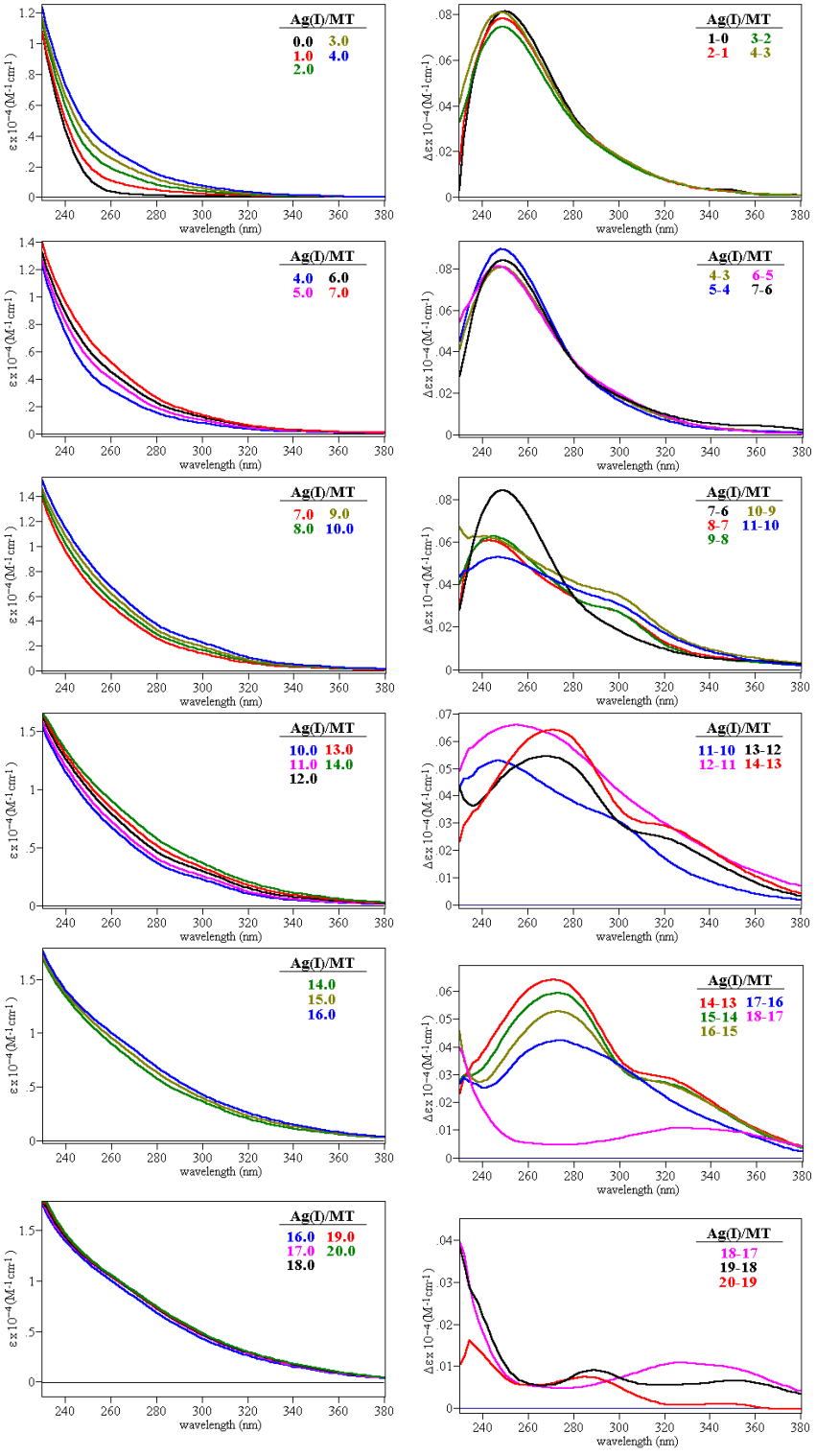

Figure S3. Ag(I) titration of a 20.21 μM solution of recombinant Zn_7-MT at pH 7.5: (**A**) UV-vis absorption spectra; (**B**) difference absorption spectra obtained by subtracting the successive spectra of (**A**). The Ag^+ to MT molar ratios are indicated within each frame.

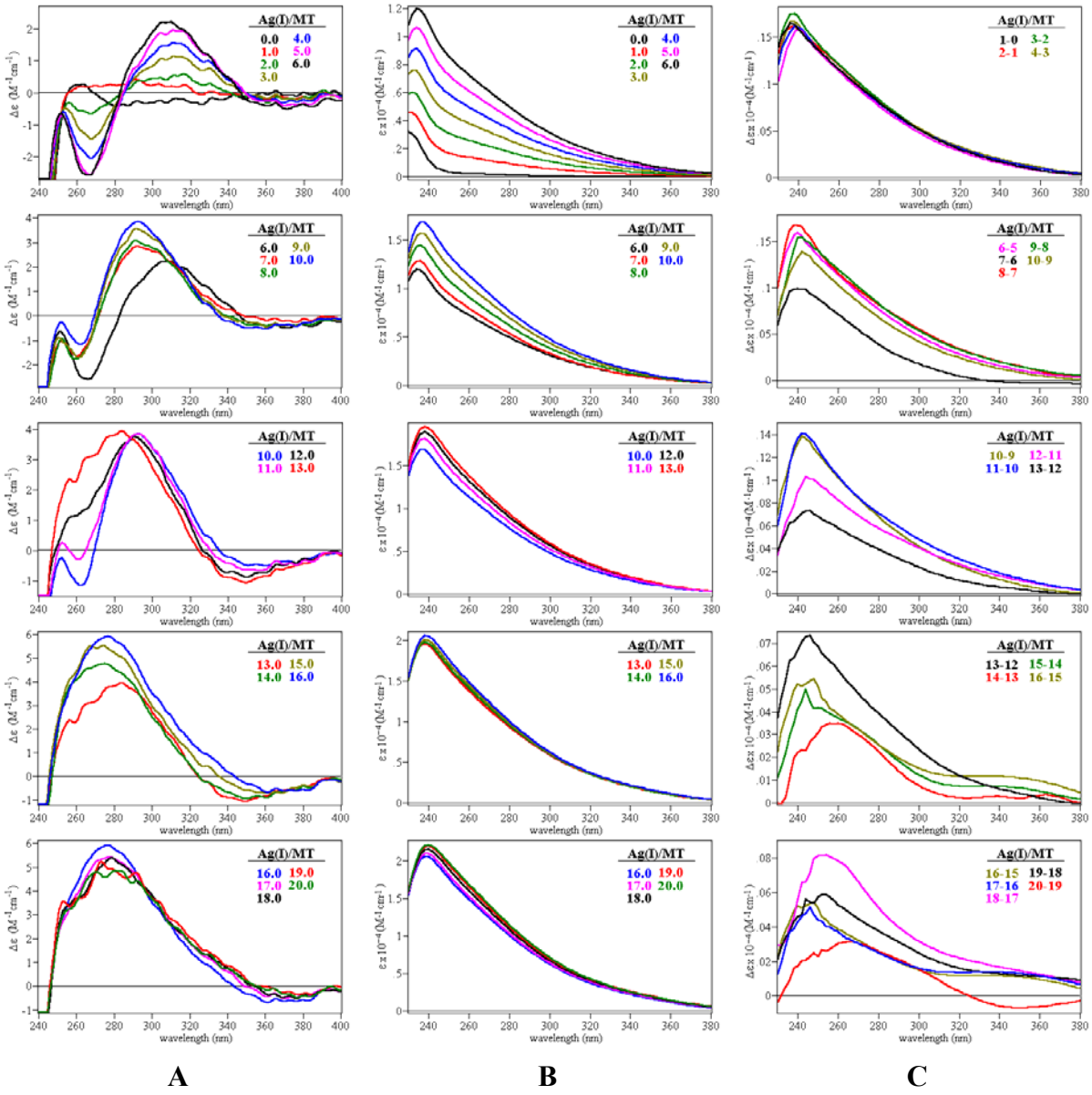

Figure S4. Ag(I) titration of a 20.29 μM solution of recombinant apo-MT at pH 2.5: (**A**) CD spectra; (**B**) UV-vis absorption spectra; (**C**) difference absorption spectra obtained by subtracting the successive spectra of (**C**). The Ag^+ to MT molar ratios are indicated within each frame.

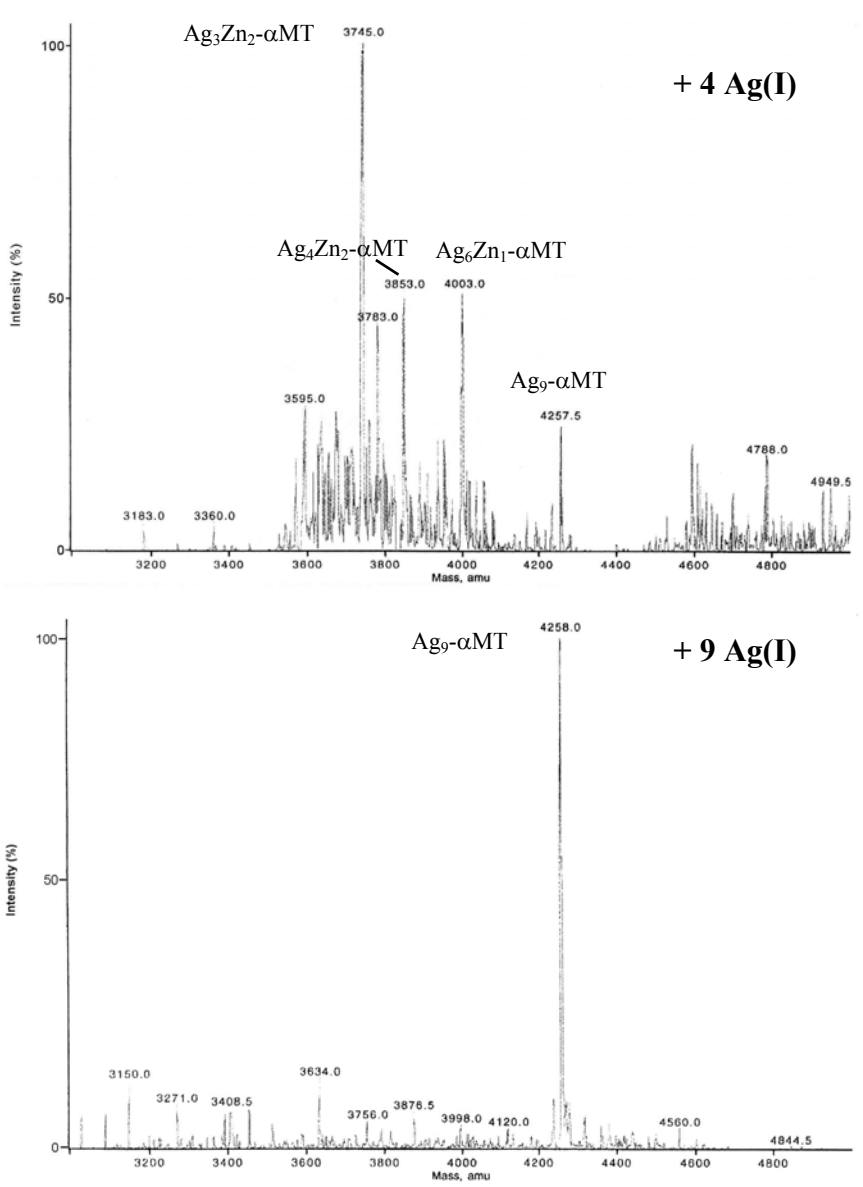

Figure S5. Deconvoluted mass spectra recorded after the addition of 4 and 9 Ag(I) eq to a solution of Zn_4-αMT at pH 7.5.

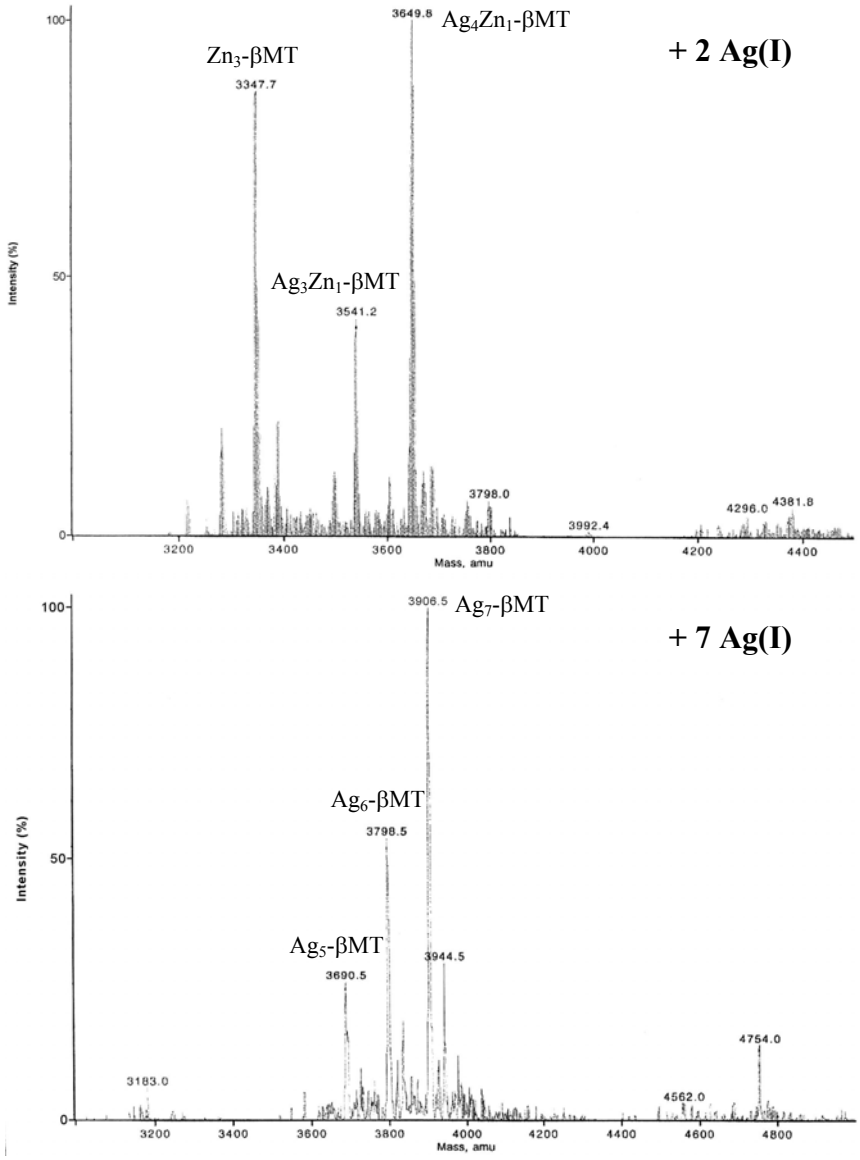

Figure S6. Deconvoluted mass spectra recorded after the addition of 2 and 7 Ag(I) eq to a Zn_3-βMT solution at pH 7.5.

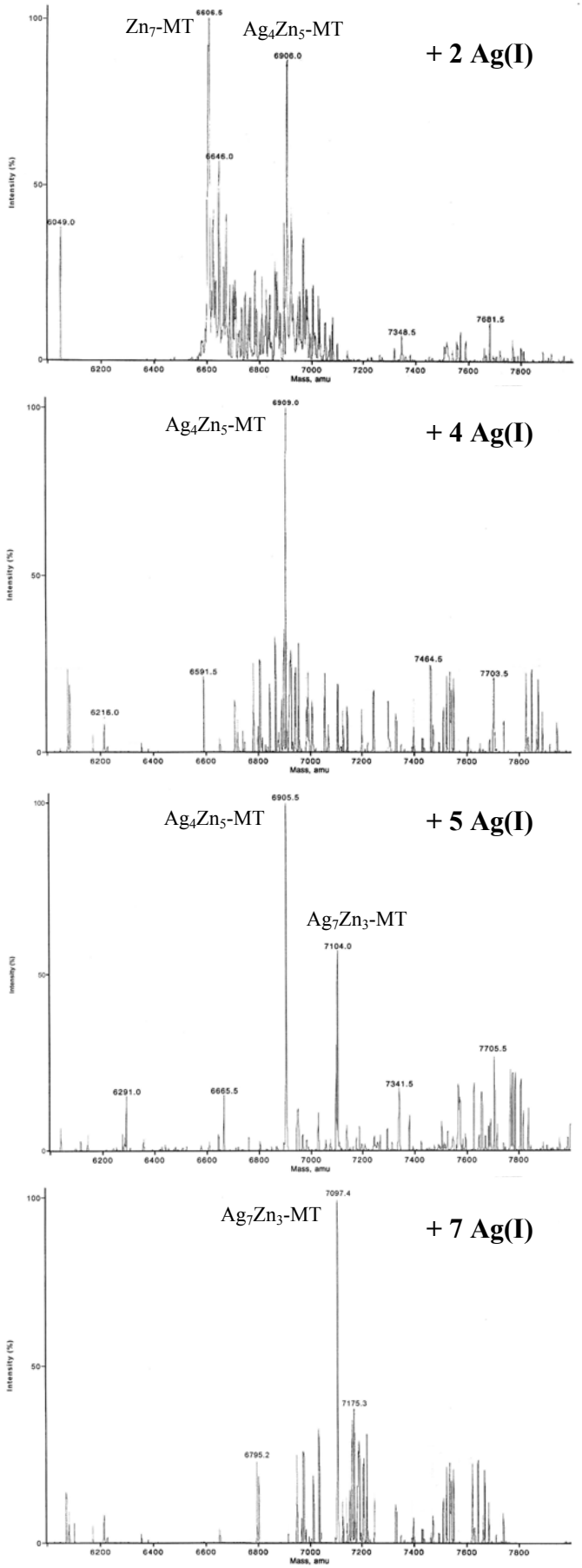

Figure S7. Deconvoluted mass spectra recorded after the addition of 2, 4, 5 and 7 Ag(I) eq to a Zn_7-MT solution at pH 7.5.

4. MTO de *Drosophila melanogaster*: contribució a una nova classificació de MT

4.1. Introducció

En condicions fisiològiques les MT es troben enllaçades als metalls essencials Cu i Zn. Donat que l'estructura terciària de les MT ve determinada per la seva coordinació als ions metàl·lics, ja que en forma demetal·lada presenta una estructura aleatòria, de *random coil*, i tenint en compte les relacions estructura/funció, sembla lògic proposar que la coordinació de MT a ions metàl·lics que presenten diferents propietats coordinants ha de donar lloc a agregats metall-MT d'estructures diferents, i per tant, amb funcions probablement diferents. Així, en base a la preferència de les MT per Zn o Cu, s'ha proposat la seva classificació com a Zn- o Cu-tioneïnes [15].

Seguint la mateixa metodologia de treballs anteriors per classificar les diferents MT estudiades com a Zn- o Cu-tioneïnes [14, 15, 16], en el treball que aquí es presenta s'estudia la isoforma MTO de *Drosophila melanogaster*. Així, un cop s'ha obtingut la proteïna mitjançant la tècnica de l'ADN recombinant en medis rics en Zn o Cu, s'ha procedit a la caracterització del contingut metàl·lic dels agregats biosintetitzats. Amb aquesta finalitat cal determinar la naturalesa dels agregats obtinguts *in vitro* per desplaçament dels ions Zn(II) en Zn-MTO per Cd(II) i per Cu(I), i comparar-los amb els agregats obtinguts *in vivo*. Aquestes dades, juntament amb l'estudi filogenètic de les relacions seqüencials d'aquesta MT amb d'altres relacionades, ha de portar a la seva classificació com a Zn o Cu-tioneïna. Així mateix, l'anàlisi de les dades espectroscòpiques i espectromètriques obtingudes al llarg de les valoracions de Zn-MTO amb Cd(II) i Cu(I) ha de permetre tenir un coneixement detallat de la capacitat coordinant d'aquesta MT envers els ions metàl·lics esmentats.

Cal destacar que a continuació de l'article publicat s'inclou com a material suplementari alguns dels espectres d'ESI-MS representatius de la valoració de Zn-MTO amb Cd(II) (Fig. 2) per tal de mostrar al lector dades que no han estat incloses a la publicació però que han resultat determinants per esbrinar el comportament de la MTO *in vitro* en presència de Cd(II).

Article 4

MTO: the second member of a Drosophila dual copper-thionein system

FEBS Letters, 2003, **533**, 72-78

MTO: the second member of a *Drosophila* dual copper-thionein system

J. Domenech[a,1], O. Palacios[b,1], L. Villarreal[b], P. González-Duarte[b], M. Capdevila[b], S. Atrian[a,*]

[a] *Departament de Genètica, Facultat de Biologia, Av. Diagonal 645, Universitat de Barcelona, E-08028 Barcelona, Spain*
[b] *Departament de Química, Facultat de Ciències, Universitat Autònoma de Barcelona, E-08193 Bellaterra, Spain*

Received 6 August 2002; revised 21 November 2002; accepted 22 November 2002

First published online 4 December 2002

Edited by Hans Eklund

Abstract ***Drosophila*** **MTO metal binding features were analyzed for comparison with MTN, the paralogous** ***Drosophila*** **metallothionein, and to classify MTO as either zinc- or copper-thionein. This was achieved by a combination of in vivo, in vitro and in silico methodologies. All the results unambiguously classified MTO as a second** ***Drosophila*** **copper-thionein, putting** ***Drosophila*** **forward as the only metazoan in which any zinc-thionein has still to be reported. Interestingly, experimental data only showed minor differences in the coordinative behavior of both MTs, but provided a characteristic spectroscopic fingerprint, revealing the possible binding of chloride anions in certain metal-MTO aggregates.**

Key words: *Drosophila* metallothionein; Cu(I) binding; Cd(II) binding; Zn(II) binding; Molecular evolution; Recombinant synthesis

1. Introduction

Metallothioneins (MT) are low molecular weight, cysteine-rich proteins with an exceptional heavy-metal coordination capacity [1]. They have been reported in all animal phyla and in most fungi and plants, and are usually associated with protection against toxic metals and with storage/transport of physiological zinc and copper. Other functions, such as free radical scavenging or oxidative stress protection, have also been proposed [2].

Among MTs, copper-thioneins constitute an interesting example of evolutionary convergence [3]. The yeast *Saccharomyces cerevisiae* CUP1, a 53-amino acid peptide binding seven Cu(I) ions within a monodominial cluster [4], can be considered the archetypical copper-thionein, together with other fungal MTs, from *Neisseria crassa* [5] and *Agaricus bisporus* [6]. Transcription of their corresponding genes is positively regulated by high copper concentrations, remaining almost uninduced by increased zinc levels. Since fungal MTs were the only Cu-thioneins known for a long time, MT preference for copper was only associated with primitive eukaryotes and was thus largely undervalued in higher organisms. Nevertheless, the Cu-thionein subfamily is at present the object of increasing interest, as new representatives are being reported in several animal phyla, including higher Metazoa. Two main features are used to identify a Cu-thionein. One of these is a gene induction criterion: MT forms recovered specifically from Cu-treated organisms are considered Cu-thioneins, as with *Helix pomatia* (Mollusca/Gastropoda) [7], *Callinectes sapidus* (Arthropoda/Crustacea) [8] and *Tetrahymena pigmentosa* (Protozoa/Ciliophora) [9]. The other is a protein characterization criterion, based on the features of recombinant metal-MT species and on the analysis of amino acid sequences [3]. Following this approach, the mammalian β-MT domain [10] and MTN, one of the two *Drosophila* (Arthropoda/Insecta) MTs [11], have been identified as Cu-thioneins.

To date, except for *Drosophila*, all Metazoa whose MT system has been studied exhibit both Zn- and Cu-thionein forms. Therefore, the characterization of the metal preference of MTO, the possible Zn-thionein counterpart of MTN, was of great interest. Although very preliminary MTO sequence analysis associated MTO with CUP1 [11], MTN and MTO are such distant paralogues (only 26% amino acid identity) that a similar metal binding preference cannot be taken for granted. For example, the Zn- and Cu-thioneins from *C. sapidus* share sequence levels of up to 40% identity. Furthermore, MTN and MTO are encoded by two genes that exhibit highly different regulation profiles: distinct tissue and ontogenic patterns of expression and distinct response to metals as expression inducer agents [12–15], which might be related to different metal preferences and thus to differential physiological roles.

Mto encodes a 43-amino acid peptide including 12 Cys, previously purified from flies [16] and from recombinant yeast [17], but never functionally characterized. In this work, we evaluated the character of Zn-thionein or Cu-thionein of MTO, and we compared its metal binding abilities with those previously reported for MTN. The significance of the Cu-thionein character of both *Drosophila* metallothioneins is then discussed in the context of the state of the art of the *Drosophila* MT system, as an essential clue to understanding the possible MT physiological roles and the gene expression regulation mechanisms in this model organism.

*Corresponding author. Fax: (34)-93-4110969.
E-mail address: satrian@ub.edu (S. Atrian).

[1] These authors made equal contributions to this study.

Abbreviations: CD, circular dichroism; ICP-AES, inductively coupled plasma atomic emission spectroscopy; ESI-MS, electrospray ionization mass spectrometry; MT, metallothionein; UV-vis, electronic absorption

0014-5793/02/$22.00
PII: S0014-5793(02)03754-7

2. Materials and methods

2.1. cDNA cloning and recombinant protein preparation

Drosophila melanogaster MTO cDNA was kindly provided by Dr. M. Wegnez. It was PCR-amplified using as primers: 5′-CCCGGATCCATGGTTTGCAAG-3′ (upstream primer) and 5′-GCGCCCGTCGACTTATTTGTTGCT-3′ (downstream primer), which introduced a *Bam*HI site immediately before the ATG initiation codon and a *Sal*I site just after the stop codon. Thereafter, the PCR product was directionally inserted (*Bam*HI–*Sal*I) into the multiple cloning site of the pGEX-4T-1 plasmid (Amersham-Pharmacia), to generate the expression vector pGEX-*Mto*. DNA sequencing of the *Mto* coding fragment was performed with the Amersham Dye Terminator Cycle Sequencing Kit in an ABI 370 automatic sequencer. pGEX-*Mto* was transformed into BL-21 for over-expression of the recombinant protein [18]. Expression and purification of the metal-MTO complexes were performed as described for MTN [11,19]. Culture media were enriched with 300 μM $ZnCl_2$ or with 500 μM $CuSO_4$ for the synthesis of Zn- or Cu-MTO complexes, respectively. Aliquots of the Superdex75 FPLC fractions containing MTO in Tris–HCl buffer, or alternatively Tris–$HClO_4$ buffer (50 mM, pH 7), were analyzed in 15% SDS–PAGE Coomassie blue-stained gels. Samples were pooled, aliquoted and stored at −80°C under argon atmosphere until further use.

2.2. Metal-MTO species characterization and spectroscopic analyses of the Cd(II) and Cu(I) titration of Zn-MTO

The characterization of the recombinantly synthesized Zn-MTO and Cu-MTO complexes was achieved through inductively coupled plasma atomic emission spectroscopy (ICP-AES) and Ellman's method as described elsewhere [10]. The electronic absorption and circular dichroism (CD) measurements recorded in parallel during the titrations of Zn-MTO with either Cd(II) or Cu(I) salts were carried out and corrected, as described in [3] for Cd(II) and in [20] for Cu(I). The Zn-MTO cadmium binding ability was tested with either Tris–HCl or Tris–$HClO_4$ buffer, using either $CdCl_2$ or $Cd(ClO_4)_2$ as titrating agent, respectively. Exceptionally, the preparation of $Cd(ClO_4)_2$ required determination of the Cd^{2+} concentration by atomic absorption spectrometry, using a Perkin-Elmer 2100 apparatus.

2.3. Electrospray ionization mass spectrometry (ESI-MS) measurements of MTO-metal complexes

Molecular mass measurements were performed on a Fisons Platform II Instrument, equipped with MassLynx software and calibrated with horse heart myoglobin (0.1 mg/ml). Conditions for the Zn and Cd species were: 20 μl of protein solution injected at 30 μl/min; the use of a HPLC Uptisphere C_4 33 mm×2 mm×5 μm column to separate analytes; capillary counterelectrode voltage, 4.5 kV; lens counterelectrode voltage, 1.0 kV; cone potential, 60 V; source temperature, 120°C; *m/z* range, 800–1950; scanning rate, 3 s/scan; interscan delay, 0.3 s. The running buffer was an appropriate mixture of acetonitrile and 5 mM ammonium acetate/ammonia, pH 7.5. Conditions for the Cu species were: 20 μl of protein solution injected at 30 μl/min; capillary counterelectrode voltage, 4.5 kV; lens counterelectrode voltage, 0.5 kV; cone potential, 40 V; source temperature, 90°C; *m/z* range, 800–1950; scanning rate, 3 s/scan; interscan delay, 0.3 s. The running buffer was a 5:95 mixture of acetonitrile and 5 mM ammonium acetate/ammonia, pH 7.5. The molecular mass of the apo-forms was determined as for the Cu species, except that for apo-MTO obtained from Zn-MTO the carrier was a 5:95 mixture of acetonitrile and ammonium formate/ammonia, pH 2.5; source temperature, 120°C; and for apo-MTO obtained from Cu-MTO, the carrier was a 1:1 mixture of acetonitrile and trichloroacetic acid, pH 1.5. In both cases, the capillary counterelectrode voltage was 3.5 kV, the lens counterelectrode voltage 0.5 kV and the cone potential 40 V. Masses for the holo-species were calculated as described in [21].

2.4. Protein sequence and evolution analyses

Protein sequence alignments were performed using the Pileup utility enclosed in the GCG Package, v.10, [22]. Protein sequences were aligned by ClustalW, v1.75, using Blosum62 as distance matrix [23]. The ClustalW alignments were the input for calculating protein distances through Protdist, which uses the Dayhoff–Pam matrix distance. The corresponding phylogenetic trees were constructed using Fitch, which uses the Fitch–Margoliash tree-building algorithm [24]. Protdist and Fitch are included in the Phylip software package [25].

3. Results and discussion

3.1. cDNA cloning and preparation of recombinant metal-MTO aggregates

DNA sequencing of the major PCR product (156 bp) confirmed the *mto* coding region [15] and ruled out the presence of any mutagenic nucleotide substitution. SDS–PAGE of total protein extracts from pGEX-*Mto*-transformed BL-21 cells grown in Zn- and Cu-supplemented media showed the presence of a band of the GST-MTO expected size (30.6 kDa). Homogeneous metal-MTO preparations (final concentration of 5.3×10^{-5} M for Zn-MTO and 3.7×10^{-5} M for Cu-MTO) were obtained from fermenter cultures. Acidification of the Zn-MTO and Cu-MTO complexes yielded the apo-form, with a molecular mass in accordance with the theoretical value for the polypeptide (Table 1). This confirmed both the identity and the integrity of the recombinant protein.

3.2. Characterization of the divalent metal binding abilities of MTO

The behavior of MTO in front of divalent metal ions was established through detailed analysis of the in vivo synthesized Zn(II)-MTO and of the Cd(II)-MTO species obtained in vitro by Zn/Cd replacement in Zn-MTO.

ESI-MS analysis of the Zn-MTO preparations revealed the presence of three species: a major Zn_4-MTO and two minor Zn_5-MTO and Zn_3-MTO forms (Table 1). The degree of Zn-MTO oxidation ranged from 16 to 52%, depending on culture

Table 1
Molecular masses and metal (Zn or Cu) to protein ratios found for in vivo synthesized Zn-MTO and Cu-MTO, eluted in Tris–HCl buffer

Metal supplemented in culture media	MW_{exp} (apo-MTO)[a]	MW_{exp} (M-MTO)[b]	MW_{calc} [c]	M/MTO[d]	M/MTO[e]
M = Zn	4667.1 ± 0.6	4922.2 ± 0.4 (S)	4922.86	4	3.7
		4988.5 ± 1.9 (s)	4986.24	5	
		4858.3 ± 0.3 (s)	4859.48	3	
M = Cu	4667.6 ± 1.0	5231.2 ± 0.5 (e)	5232.29	9	7.4–8.1
		5170.1 ± 2.1 (e)	5169.74	8	
M = Cu[f]	4667.6 ± 1.0	5231.2 ± 0.5	5232.29	9	8.9

[a]Experimental molecular masses for the apo-proteins. MTO calculated mass is 4669.34.
[b]Experimental molecular masses for the Zn- and Cu-MTO complexes. (S) denotes a major species, (s) denotes a minor species and (e) denotes equimolarity.
[c]Calculated molecular masses for neutral species with loss of two protons/Zn bound and one proton/Cu bound.
[d]Zinc or copper per MTO molar ratio calculated from the mass difference between holo- and apo-protein.
[e]Zinc per MTO molar ratio calculated from the Zn content (ICP-AES) and cysteine thiolates (Ellman's method), and Cu per MTO molar ratio calculated from the copper and total sulfur content.
[f]Small-scale cultures.

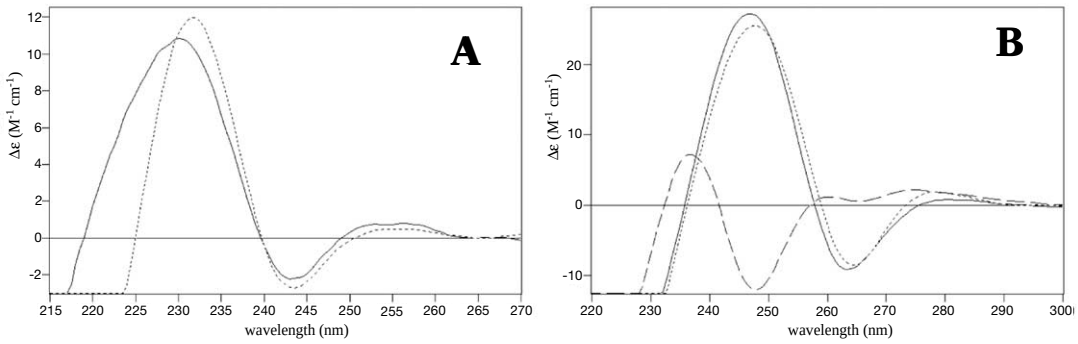

Fig. 1. A: CD spectra of recombinant Zn_4-MTO eluted in Tris–HCl (solid line) and in Tris–$HClO_4$ (dotted line). B: CD spectra of the Cd_4-MTO species in Tris–HCl buffer (solid line) and in Tris–$HClO_4$ (dotted line), and of the Cd_9-MTO aggregate (dashed line) obtained by Zn/Cd replacement of a 23.4 μM solution of Zn-MTO.

conditions [10]. These values agreed well with the ICP-AES data, indicating average ratios of Zn per reduced protein of 3.70 and 2.80, respectively. The weak intensity of the Zn-MTO CD spectrum (Fig. 1A) evidenced a low degree of chirality for the biosynthesized Zn-MTO aggregates in Tris–HCl, but still allowed identification of the Zn-thiolate chromophores by detection of an exciton coupling centered at ca. 240 nm. A new Gaussian-shaped band centered at ca. 230(+) nm was observed, with an intensity inversely related to the MTO oxidation degree. To investigate whether this absorption could be related to a non-standard zinc peptide chromophore, the spectroscopic features of Zn-MTO eluted in Tris–$HClO_4$ buffer were also analyzed (Fig. 1A). Since the absorption at 230 nm was red-shifted and narrowed, a possible role of the chloride anions in the folding of the Zn-MTO aggregates was inferred.

The in vitro formation of fully cadmium-loaded MTO as a result of Zn/Cd replacement in Zn-MTO proceeded in two stages, when using both $CdCl_2$ and $Cd(ClO_4)_2$ as titrating agent. The stoichiometric (ESI-MS) and spectroscopic (CD and UV-visible) data of the intermediate species are shown in Table 2 (detailed data are available upon request).

During the first step of the titration, although the Zn/Cd replacement increased the metal cluster organization, essentially the same mixture of species was found, i.e. $M(II)_4$-MTO (major) and $M(II)_5$-MTO (minor). Thus, the stoichiometric similarities and the parallelism of the CD spectra between the Zn- and Cd-MTO species pointed to an isomorphic Zn/Cd replacement. Consistently, $M(II)_4$-MTO should be considered the physiologically stable species, which can incorporate a fifth M(II) ion without significant alteration of the initial structure. In the second stage of the titration, the addition of Cd(II) caused an extensive rearrangement of the previous Cd_4- and Cd_5-MTO aggregates (Fig. 1B), which generated a final, unique Cd_9-MTO species. No intermediates were observed and no changes were introduced by further Cd(II) additions. In order to analyze the role of Cl^- ions in the formation of M(II)-MTO aggregates, the UV-vis difference spectra corresponding to the titrations of Zn-MTO with $CdCl_2$ or $Cd(ClO_4)_2$ were compared (Fig. 2). In addition to the red shift up to ca. 260 nm associated with the Zn/Cd substitution, an unprecedented absorption at ca. 240 nm was found for the binding of the fourth Cd(II) in the presence of chloride anions (Fig. 2A), absent when using $Cd(ClO_4)_2$ as titrating agent (Fig. 2B). Thus, the absorption at 240 nm would be in agreement with the presence of chloride ligands in the coordination environment of cadmium in MTO (i.e. $CdS_{4-x}Cl_x$), not observable for MTN (Fig. 2C). On the other hand, the apparent isostructural replacement of Zn by Cd in MTO called into question the possibility of assigning the 230-nm Gaussian band detected for Zn-MTO to $ZnS_{4-x}Cl_x$ chromophores. Unfortunately, ESI-MS of Cd- and Zn-MTO in Tris–HCl did not allow discrimination between the common ammonium adducts and possible species containing M(II)-Cl bonds. However, while the CD spectra of Zn-MTO show significant differences in the 220–240-nm region, depending on the elution buffer (Fig. 1A), those of Cd-MTO are very similar and thus indicative of structurally related metal–sulfur aggregates (Fig. 1B). Overall, the experimental results indicate the participation of Cl^- anions in both M(II)-MTO aggre-

Table 2
Analysis of the in vitro Zn/Cd replacement in Zn-MTO

Cd(II) eq./mol of Zn-MTO	Metal-MTO species obtained (ESI-MS and spectroscopic characterization)	Chiroptical features (CD spectroscopy, Fig. 1)
Step 1 (1–8)		
From 1 to 3	Mixture of all possible Zn_x,Cd_y-MTO aggregates ($x+y=4$), with predominance of those with $y=$ no. Cd(II) eq. added+1	Formation of Cd_4S chromophores
From 4 to 6	Mixture of species: Cd_4-MTO (S), Cd_5-MTO (s)	Development of a derivative-shaped profile (crossover point, 258 nm)
Up to 8	Equimolar mixture of species: Cd_4-MTO, Cd_5-MTO	Development of a Gaussian band at 245(+) nm
Step 2		
From 8 to 16	Final Cd_9-MTO, no intermediate species, no further transformation	Extensive rearrangement of the former Cd-thiolate clusters

(S) denotes a major species, (s) denotes a minor species.

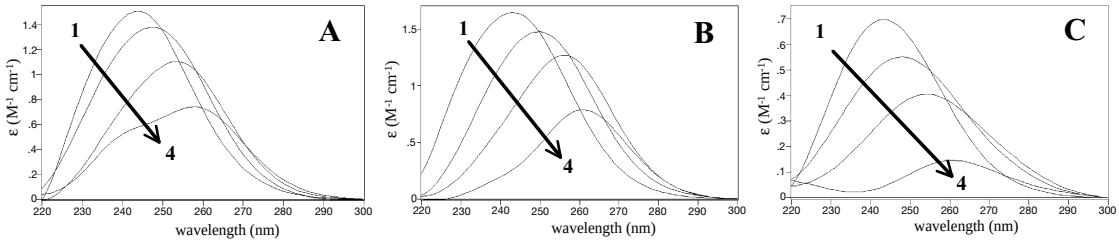

Fig. 2. Difference UV-vis absorption spectra corresponding to the titrations of recombinant (A) Zn-MTO in Tris–HCl buffer with $CdCl_2$ from 1 to 4 Cd(II) eq.; (B) Zn-MTO in Tris–$HClO_4$ buffer with $Cd(ClO_4)_2$ from 1 to 4 Cd(II) eq.; (C) Zn-MTN with $CdCl_2$ from 1 to 4 Cd(II) eq.

gates, M = Zn or Cd, but with higher structural significance in the Zn_4S_{12} than in the Cd_4S_{12} metal–cysteine clusters.

3.3. Characterization of the monovalent metal binding abilities of MTO

The analysis of the behavior of MTO in front of monovalent metal ions was achieved by characterization of the in vivo synthesized Cu-MTO aggregates and of the Cu-MTO species obtained in vitro by Zn/Cu replacement.

Mto-cDNA expression in *standard* copper-supplemented cultures yielded homometallic Cu-MTO species, with a total metal-per-sulfur content of 7.4–8.1 (ICP-AES results) and an approximate equimolar ratio of the Cu_8- and Cu_9-MTO species (ESI-MS analyses, Table 1). Small-scale synthesis yielded a unique Cu_9-MTO species according to ESI-MS, which corresponded well to an ICP-AES copper-to-MTO ratio of 8.9. Zn(II) absence in all Cu-MTO samples was systematically confirmed by ICP-AES. The high intensity and well-defined CD spectra of recombinant Cu-MTO (Fig. 3D) revealed a high metal cluster organization.

Zn/Cu exchange during titration of Zn-MTO with Cu(I) (Fig. 3) evolved in two distinct phases (Table 3), as for Zn/Cd replacement. At the end of the first step, 9 equivalents of Cu(I) added, Zn-MTO turned into the fully copper-loaded species Cu_8-MTO and Cu_9-MTO, which exhibited maximum chirality and was highly coincident with all the features of the in vivo synthesized Cu-MTO (Fig. 3D). The second step led to overloaded Cu_{15}- and Cu_{17}-MTO species.

3.4. Primary structure analysis of MTO, MTN and other Arthropoda MTs

The ClustalW-based analysis [3] of the MTO amino acid sequence included two *S. cerevisiae* proteins: CUP1 and CRS5, a MT-like peptide also associated with copper resis-

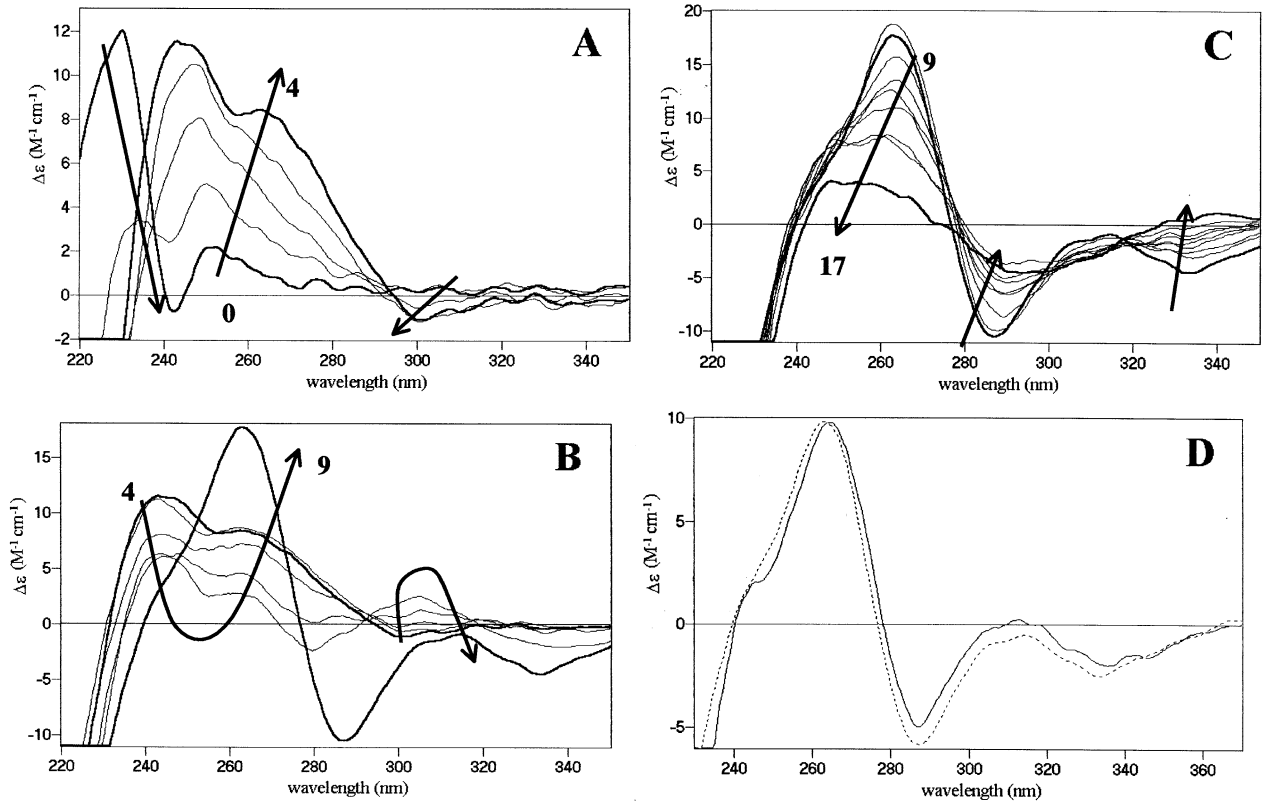

Fig. 3. CD spectra recorded during the titration of a 14.4 μM solution of Zn-MTO with Cu(I) at pH 7, shown in three stages: (A) from 0 to 4, (B) from 4 to 9, and (C) from 9 to 17 equivalents of Cu(I) added. Arrows indicate increasing Cu(I) equivalent amounts. Traces corresponding to the first and last spectrum of each stage are depicted in bold. D: Superimposition of the CD spectra of the recombinant Cu-MTO (solid line) and the Cu_9-MTO species generated in vitro by Zn/Cu replacement (dotted line).

Table 3
Analysis of the in vitro Zn/Cu replacement in Zn-MTO

Cu(I) eq./mol of Zn-MTO	Metal-MTO species obtained (ESI-MS and spectroscopic characterization)	Chiroptical features (CD spectroscopy, Fig. 3)
Step 1 (1–9)		
From 1 to 4	Cu_4,Zn_2-MTO (Chelex [26])	Formation of CuS chromophores
Up to 9	Cu_8-MTO, Cu_9-MTO	Red shift of the absorption indicative of Zn/Cu replacement
Step 2		
From 9 to 17	Overmetallated species[a]: Cu_{15}-MTO, Cu_{17}-MTO	Decrease in intensity of (+) and (−) bands: loss of the previous Cu–S chromophores

[a]Identified by CD results, non-detectable by ESI-MS, as repeatedly reported for homometallic Cu-MT aggregates of high nuclearity [26,27].

tance [28]. The generated alignment and the non-rooted neighbor-joining tree are shown in Fig. 4. MTO unquestionably came together with the known Cu-thionein sequences, with a significant bootstrap value of 999/1000 separating this cluster from that of the Arthropoda Zn-thioneins [3]. Strikingly, the two *Drosophila* MTs did not share the closest sequence similarity: the shortest Cu-thionein subset branch joined *Drosophila* MTN with *Callinectes* Cu-MT, while MTO was associated with both *S. cerevisiae* metallothioneins. This agrees with an MTN–MTO divergence preceding *Drosophila* differentiation, so that the branches from which MTO and MTN evolved could have split at an early stage of Arthropoda radiation. The opposite conclusion had previously been drawn [15], but only zinc-thioneins had been reported in Crustacea.

We unsuccessfully attempted to identify the sequence feature responsible for the clustering of Cu-thioneins. There are no Cys motifs or distribution patterns in Zn-thioneins that do not appear in one or other Cu-thionein, although it is true

A)

```
                    10        20        30        40        50        60        70        80
A.astacus     -----MPGP--CCND-VCECAAG---GCKTG--CVCTS------CRCSPCDKCTS--GCKCPSKEE-C-AKTCSKPCECCP--
C.sapidusI    -----MPGP--CCND-KCVCQEG---GCKAG--CQCTS------CRCSPCQKCTS--GCKCATKEE-C-SKTCTKPCSCCPK-
C.sapidusII   -----MPDP--CCND-KCECKEG---ECKTG--CKCKS------CRCPPCDKCSS--ECKCTSKEE-C-SKTCSKPCSCCP--
C.maenas      -----MPDP--CCID-KCECKEG---GCKAG--CKCTS------CRCTPCEKCSS--GCKCTTKED-C-CKTCTKPCSCCP--
H.americanus  ------PGP--CCKD-KCECAEG---GCKTG--CKCTS------CRCAPCEKCTS--GCKCPSKDE-C-AKTCSKPCKCCP-
S.serrataII   ------PDP--CCND-KCDCKEG---ECKTG--CKCTS------CRCPPCEQCSS--GCKCANKED-C-RKTCSKPCSCCP--
S.serrataI    ------PGP--CCND-KCVCKEG---GCKEG--CQCTS------CRCSPCEKCSS--GCKCANKEE-C-SKTCSKACSCCPT-
P.leniusculus -----MPGP--CCND-QCECAAG---GCKTG--CVCTS------CRCQPCDKCTS--GCKCPSKEE-C-AKTCSKPCRCCP--
P.potamios    ------PDP--CCAEGTCECEEG---KCKAG--CKCTS------CRCSPCEKCTS--ECECKSKEE-C-AKNCTKPCSCCP--
C.sapidus-Cu  -----MPCG--CGTS--CKCGSG---KCCCGSTCNCTTCPSKQSCSCND-GACGS--ACQCKTSCC-C-GADC--KCSPCPMK
Drosophila MTN -----MPCP--CGSG--CKCAS----QATKGS-CNCGS-----DCKCG--GDKKS--ACGCSE----------------------
Drosophila MTO -----MVCK--GCGT-NCQCSAQ---KCGDN-------------CACN--KDC----QCVCKNGP----KDQC---CSNK---
Yeast CUP1    MFSELINFQ--NEGH-ECQCQCG---SCKNNE--QCQK-----SCSCP--TGCNSDDKCPCGNKSEET-KKSC---CSGK---
Yeast CRS5    MTVKICDCEGECCKD-SCHCGSTCLPSCSGGEKCKCDHS-----TGSPQCKSCGE--KCKCETTCT-CEKSKCN--CEKC---
```

B)

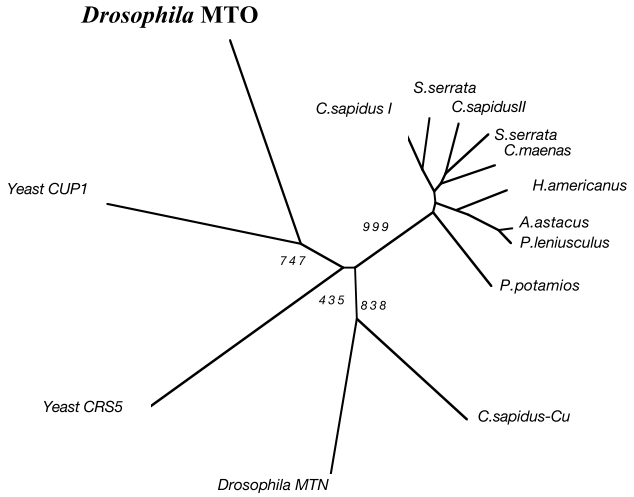

Fig. 4. A: ClustalW output of the multiple alignment of Arthropoda and yeast MT sequences, constructed using the Blosum62 weight matrix. The names of the organisms are: *Callinectes sapidus*, *Scylla serrata*, *Carcinus maenas*, *Astacus astacus*, *Pacifastacus leniusculus*, *Homarus americanus*, *Potamon potamios*, yeast (*Saccharomyces cerevisiae*) and *Drosophila melanogaster*. B: Consensus protein distance tree, constructed by the neighbor-joining method from the alignment shown in A, with a bootstrap value of 999. The mean bootstrap values for the longest tree branches are shown.

that no Cu-thionein shares the complete Cys arrangement with a Zn-thionein. Non-Cys residues also failed to reveal any regular pattern which which zinc or copper preference could be associated. MTO and MTN polypeptides differ not only in length (43 vs. 40 amino acids, respectively), but also in number of cysteines (12 vs. 10) and in their distribution. In MTN, Cys are arranged in five C-X-C motifs, while in MTO they are more randomly distributed, only eight of 12 arranged in C-X-C motifs. Taking the sequence similarities between MTO and CUP1 into account, it is difficult to explain the eight/nine Cu(I) ions bound to recombinant MTO if the two last C-terminal Cys were devoid of binding capacity, as has been postulated for the two consecutive Cys of the C-terminal tail of CUP1 by nuclear magnetic resonance studies [29,30].

4. Conclusions

Both the experimental and in silico results presented in this work unambiguously classify MTO as a second *Drosophila* Cu-thionein, according to the phylogenetic analysis method proposed in [3]. This signifies the unprecedented fact of an animal organism for which no Zn-thionein form has yet been reported. The in vivo and in vitro criteria used to assess the Cu-thionein character of MTO are the following. First, the high degree of folding and stability of Cu-MTO vs. the weak chirality and oxidation susceptibility of Zn-MTO, indicative of a low preference of MTO for Zn and of an intrinsic instability of Zn-MTO in intracellular environments, similar to those reported for MTN [11]. Second, the recovery of homometallic Cu-MTO species from recombinant synthesis on Cu-supplemented media. Particularly, although in vitro Zn/Cu replacement in Zn-MTO led to the formation of intermediate (the heterometallic Cu_4,Zn_2-MTO) and overloaded (Cu_{15}- and Cu_{17}-MTO) species, the structural and stoichiometric similarities between the biosynthesized Cu-MTO aggregates and those resulting from the addition of 9 Cu(I) to Zn-MTO pointed to Cu_9-MTO as the species produced in intracellular Cu-rich environments. It is worth noting here that the tree clustering of copper-thioneins identified by two independent criteria – copper gene inducibility for CUP1 [31] and *Callinectes* Cu-MT [8], and metal coordination studies for *Drosophila* MTN [11] and MTO (this work) – validates the protein sequence similarity approach and the coherence of the thus defined copper-thionein subfamily.

The proposed Zn-thionein/Cu-thionein classification concerns the evolutionary origin of the MTs, as well as the primordial *molecular function* of the chelating peptide, which, in the case of Cu-thioneins, would imply an intrinsic ability to form homometallic, biologically stable, copper aggregates. However, the *biological role* of MTs should be considered from a broader perspective than that of the optimal molecular function, since, by definition, MTs are proteins which do not exhibit specificity for metal chelation. Thus, the classification of a given MT as Cu-thionein does not imply its inability to react towards metals ions other than copper, especially in metal stress conditions. The case of *Drosophila* MTs, and particularly MTO, could yield a good example of the duality of an MT's metal binding behavior, if physiological or metal poisoning situations are considered.

In physiological conditions, the two metal ions to be taken into account are Cu(I) and Zn(II). From the results presented here, the optimal reactivity of MTO towards copper vs. the poor behavior towards Zn is clear. Therefore, the MTO Cu-thionein nature has to be considered when trying to understand its normal biological role and its basal gene regulation patterns. It has recently been reported that a Cu-MT complex in the midgut *copper cells* could be involved in *Drosophila* digestive acid secretion [32], and the putative demands imposed by copper-oxygen transporters (hemocyanins) in insects are well known [33]. With respect to gene regulation, although *Mto* and *Mtn* follow different temporal and tissue patterns, it remains true that both genes exhibit the highest expression levels after copper induction, while remaining poorly induced by zinc [12–17]. In fact, the analysis of *Mto* and *Mtn* molecular control mechanisms reveals a puzzling situation: a transcription factor homologous to mammalian MTF-1 [34], dMTF, has been reported, which binds upstream of *Mto* and *Mtn* to several MRE boxes upon zinc coordination, while MT synthesis in flies as a response to this metal remains very poor [35], as would be expected when considering the copper-thionein character of the encoded peptides.

In metal stress conditions, it is worth considering the behavior of MTO towards cadmium, as a paradigm of a xenobiotic divalent metal ion. Previous results clearly showed the involvement of MTO in *Drosophila* Cd resistance [15], and *Mto* inducibility by cadmium, although lower than by copper, is far more pronounced than by zinc [12–17]. In fact, our results are in full agreement with the hypothesis that MTO, although a Cu-thionein by origin, plays an important role in Cd detoxification in *Drosophila*. First, the degree of folding of the *canonical* Cd-MTO species (Cd_4- and Cd_5-MTO) is considerably higher than that of Zn-MTO, which would ensure a good stability of the cadmium-MTO aggregates in intracellular environments. Second, under excessive Cd(II) concentrations, we show that MTO can rearrange its peptide chain to accommodate extra metal ions, yielding an equally stable, overmetallated aggregate, namely Cd_9-MTO. And finally, it is worth noting that MTN and MTO exhibit only a few differences in metal binding behavior, although the spectroscopic results have provided evidence for the possible binding of chloride anions in the M_4-MTO, M = Zn(II), Cd(II), aggregates. However, the contribution of the chloride ions in M-MTO complexes has been found to be less significant for M = Cd(II) than for M = Zn(II). This would point to the MTO polypeptide's higher capacity for association with cadmium than with zinc, a metal ion that would require extra ligands to maintain the corresponding MTO aggregate.

Further study is needed to reveal whether the coexistence of MTN and MTO is maintained by differential gene expression programs or by any of the slight differences in metal coordination highlighted in this work. Moreover, the search for new MT forms by in silico *Drosophila* genome screening and the elucidation of the MT gene transcriptional activation pathways ensure that the *Drosophila* MT system is an intriguing model for which many questions still remain unanswered.

Acknowledgements: We are grateful to Dr. M. Wegnez (CNRS, University of Paris XI, France) who kindly provided a *D. melanogaster Mto* cDNA clone, and to Prof. W. Schaffner (Zürich University, Switzerland) for fruitful discussions. This work was supported by projects BIO2000-0910 and BQU2001-1976 from the Spanish Ministerio de Ciencia y Tecnología. O.P. and L.V. are indebted to the Spanish Ministerio de Educación, Cultura y Deporte and to the Departament de Química of the Universitat Autònoma de Barcelona, respectively, for pre-doctoral scholarships. We acknowledge the Ser-

veis Científico-Tècnics, Universitat de Barcelona (DNA sequencing, ICP-AES and ESI-MS) and the Servei d'Anàlisi Química, Universitat Autònoma de Barcelona (AAS, CD, UV) for allocating instrument time.

References

[1] Kägi, J.H.R. (1993) in: Metallothionein III. Biological Roles and Implications (Suzuki, K.T. Imura N. and Kimura, M., Eds.), pp. 29–55, Birkhäuser Verlag, Basel.
[2] Fisher, E.H. and Davie, E.W. (1998) Proc. Natl. Acad. Sci. USA 95, 3333–3334.
[3] Valls, M., Bofill, R., González-Duarte, R., González-Duarte, P., Capdevila, M. and Atrian, S. (2001) J. Biol. Chem. 276, 32835–32843.
[4] Bertini, I., Hartman, H.-J., Klein, T., Liu, G., Luchinat, C. and Weser, U. (2000) Eur. J. Biochem. 267, 1008–1018.
[5] Lerch, K. (1980) Nature 284, 368–370.
[6] Münger, K. and Lerch, K. (1985) Biochemistry 24, 6751–6756.
[7] Dallinger, R., Berger, B., Hunziker, P. and Kägi, J.H.R. (1997) Nature 388, 237–238.
[8] Syring, R.A., Hoexum-Brouwer, T. and Brouwer, M. (2000) Comp. Biochem. Physiol. C 125, 325–332.
[9] Santovito, G., Irato, P., Palermo, S., Boldrin, F., Sack, R., Hunziker, P. and Piccinni, E. (2001) Protist 152, 219–229.
[10] Cols, N., Romero-Isart, N., Bofill, R., Capdevila, M., González-Duarte, P., González-Duarte, R. and Atrian, S. (1999) Protein Eng. 12, 265–269.
[11] Valls, M., Bofill, R., Romero-Isart, N., González-Duarte, R., Abián, J., Carrascal, M., González-Duarte, P., Capdevila, M. and Atrian, S. (2000) FEBS Lett. 467, 189–194.
[12] Latowski-Perry, D., Otto, E. and Maroni, G. (1985) J. Biol. Chem. 260, 1527–1530.
[13] Durliat, M., Bonneton, F., Boissonneau, E., André, M. and Wegnez, M. (1995) Biometals 8, 339–351.
[14] Maroni, G., Wise, J., Young, J.E. and Otto, E. (1987) Genetics 117, 739–744.
[15] Mokdad, R., Debec, A. and Wegnez, M. (1987) Proc. Natl. Acad. Sci. USA 84, 2658–2662.
[16] Silar, P., Theodore, L., Mokdad, R., Erraiss, N.E., Cadic, A. and Wegnez, M. (1990) J. Mol. Biol. 215, 217–224.
[17] Silar, P. and Wegnez, M. (1990) FEBS Lett. 269, 273–276.
[18] Studier, F.W. and Moffatt, B.A. (1986) J. Mol. Biol. 189, 113–130.
[19] Capdevila, M., Cols, N., Romero-Isart, N., González-Duarte, R., Atrian, S. and González-Duarte, P. (1997) Cell. Mol. Life Sci. 53, 681–688.
[20] Bofill, R., Palacios, O., Capdevila, M., Cols, N., González-Duarte, R., Atrian, S. and González-Duarte, P. (1999) J. Inorg. Biochem. 73, 57–64.
[21] Fabris, D., Zaia, J., Hathout, Y. and Fenselau, C. (1996) J. Am. Chem. Soc. 118, 12242–12243.
[22] GCG (1994) Program Manual for the Wisconsin Package, v. 10, Wisconsin Genetics Computer Group, Madison, WI.
[23] Thompson, J.D., Higgins, D.G. and Gibson, T.J. (1994) Nucleic Acids Res. 22, 4673–4680.
[24] Fitch, W.M. and Margoliash, E. (1967) Science 155, 279–284.
[25] Felsenstein, J. (1989) Cladistics 5, 164–166.
[26] Bofill, R., Capdevila, M., Cols, N., Atrian, S. and González-Duarte, P. (2001) J. Biol. Inorg. Chem. 6, 405–417.
[27] Zaia, J., Fabris, D., Wei, D., Karpel, R.L. and Fenselau, C. (1998) Protein Sci. 7, 2398–2404.
[28] Culotta, V.C., Howard, W.R. and Liu, X.F. (1994) J. Biol. Chem. 269, 25295–25302.
[29] Narula, S.S., Winge, D.R. and Armitage, I.M. (1993) Biochemistry 32, 6773–6787.
[30] Peterson, C.W., Narula, S.S. and Armitage, I.M. (1996) FEBS Lett. 379, 85–93.
[31] Butt, T.R., Sternberg, E.J., Gorman, J.A., Clark, P., Hamer, D., Rosenberg, M. and Crooke, S.T. (1984) Proc. Natl. Acad. Sci. USA 81, 3332–3336.
[32] McNulty, M., Pujlung, M., Jefford, G. and Dubreuil, R.R. (2001) Cell Tissue Res. 304, 383–389.
[33] Brouwer, M., Syring, R. and Hoexum-Brouwer, T. (2002) J. Inorg. Biochem. 88, 228–239.
[34] Heuchel, R., Radtke, F., Georgiev, O., Stark, G., Aguet, M. and Schaffner, W. (1994) EMBO J. 13, 2870–2875.
[35] Zhang, B., Egli, D., Georgiev, O. and Schaffner, W. (2001) Mol. Cell. Biol. 21, 4505–4514.

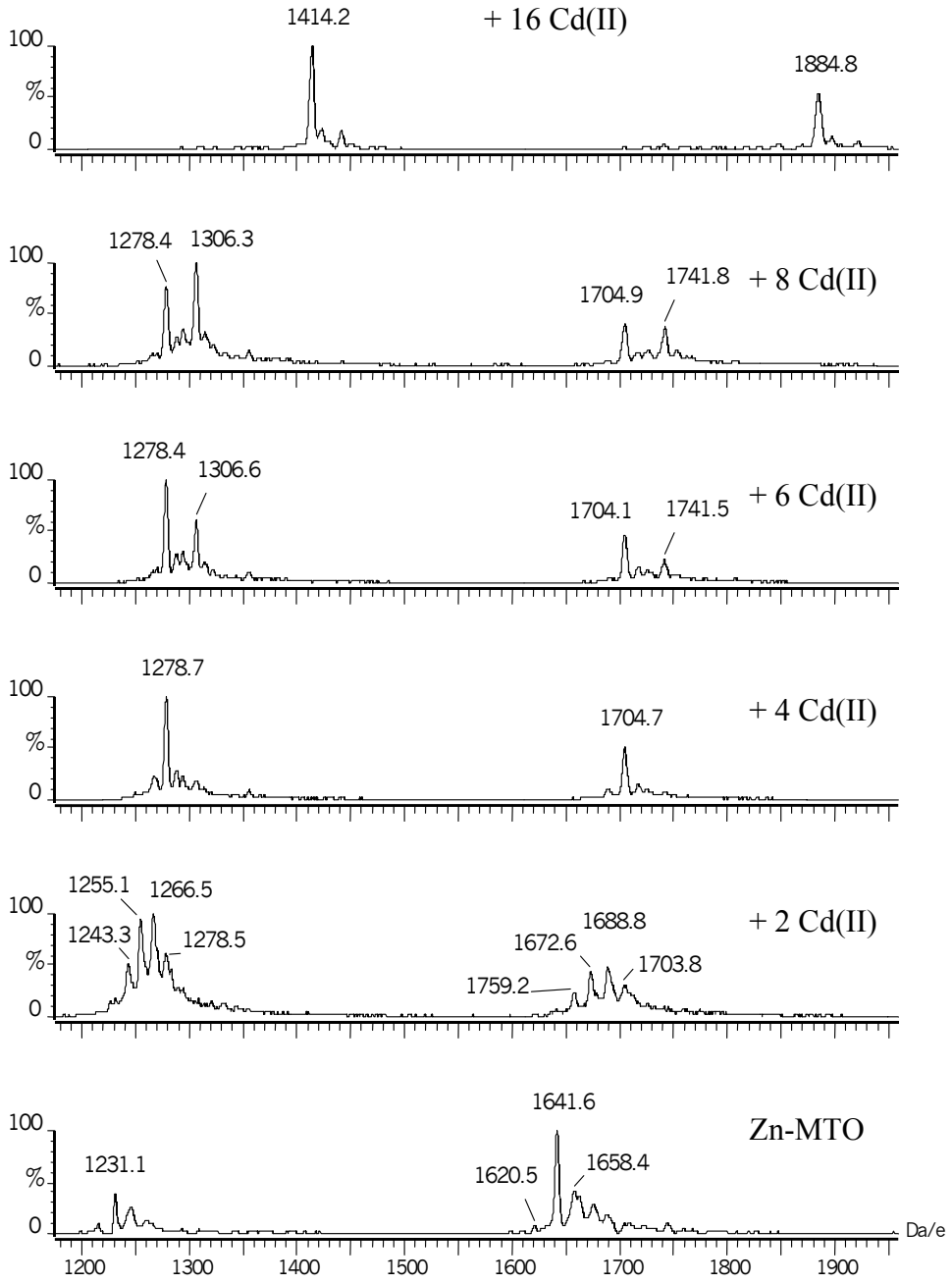

Figura 2. Espectres d'ESI-MS corresponents a la valoració de Zn_4-MTO amb Cd(II) a pH 7. Els pics obtinguts corresponen a les masses de les espècies amb càrrega +3 i +4 (veure taula adjunta).

	M	(M+3)/3	(M+4)/4
Zn_4-MTO	4922.9	1641.97	1231.73
Zn_5-MTO	4986.29	1663.10	1247.57
Zn_3-MTO	4859.51	1620.84	1215.88
Cd_1Zn_3-MTO	4969.91	1657.64	1243.48
Cd_2Zn_2-MTO	5016.92	1673.31	1255.23

	M	(M+3)/3	(M+4)/4
Cd_3Zn_1-MTO	5063.93	1688.98	1266.98
Cd_4-MTO	5110.94	1704.65	1278.74
Cd_5-MTO	5221.34	1741.45	1306.34
Cd_9-MTO	5662.94	1888.65	1416.74

5. Resum global i discussió de resultats

En aquest capítol es dóna una visió global del treball, exposant de manera resumida els resultats obtinguts i fent una discussió general dels mateixos.

Anàlogament a l'estructuració que s'ha seguit en la presentació de les diferents parts que conformen aquesta memòria, aquest capítol s'ha dividit en tres apartats, relatius als resultats dels capítols 2, 3 i 4, i que segueixen el mateix ordre.

5.1. Aplicació de l'espectrometria de masses a l'estudi de MT amb Cd

La CZE, per les seves excel·lents qualitats com a tècnica separativa, es presenta com a una bona alternativa a d'altres mètodes de separació convencionals per a l'estudi de MT mitjançant espectrometria de masses en presència d'elevades concentracions de tampó. Però les dificultats tècniques que presenta l'acoblament CZE-ESI-MS recomanen, encara avui, la participació d'equips especialitzats en la mateixa. Per aquest motiu s'ha col·laborat amb el grup del Dr. Lobinski, que disposa d'una interfase per aquest sistema, i que ha estat particularment interessat en poder treballar amb MT recombinant, d'elevada puresa. Aquests dos factors han permès iniciar l'aplicació del sistema CZE-ESI-MS a l'estudi de les reaccions de substitució metàl·lica de les MT.

L'estudi de la coordinació del Cd(II) a l'espècie Zn_7-MT 1 recombinant de ratolí mitjançant els acoblaments CZE-ESI-MS i CZE-ICP-MS tenia com a objectius validar la utilització d'aquests sistemes analítics per a l'estudi del bescanvi metàl·lic en MT.

El grup del Dr. Lobinski ha estat el responsable d'establir les condicions òptimes de treball pels dos acoblaments, CZE-ICP-MS i CZE-ESI-MS, tant els paràmetres de la separació com els de la detecció, amb la finalitat d'aconseguir una resolució separativa comparable amb l'obtinguda mitjançant el sistema CZE-UV.

Les condicions de separació òptimes pels dos acoblaments (article 1, *J. Anal. At. Spectrom.*, table 1, pag. 24) són comparables, ja que les lleugeres diferències (el tampó utilitzat com a tampó electroforètic (*running buffer*) i la seva concentració, la quantitat de mostra injectada, i el tipus de líquid recobridor (*sheath liquid*) i el seu fluxe) han estat imposades pels sistemes acoblats amb la CZE, o sigui, ESI-MS i ICP-MS. Això implica que la separació realitzada mitjançant la CZE en ambdós acoblaments es pot considerar pràcticament la mateixa, la qual cosa permet comparar els resultats obtingut mitjançant CZE-ESI-MS i CZE-ICP-MS.

L'estudi de la substitució del Zn pel Cd en l'espècie Zn_7-MT ha permès observar que tant en l'espècie de partida com en les posteriors addicions de Cd(II), els electroferogrames obtinguts mitjançant els acoblaments CZE-ESI-MS i CZE-ICP-MS són similars, tant en el nombre de pics com en els temps de retenció dels mateixos. En tots els casos la separació del tampó i la proteïna ha estat satisfactòria, permetent una bona detecció per ESI-MS de les espècies formades. Els electroferogrames s'han caracteritzat per un pic intens, que contenia Zn i/o Cd, precedit d'un pic menor causat per la

	Eq. Cd(II) addicionats					
Espècie	0	2	4	7	9	11
Zn_7-MT	**X**					
Cd_1Zn_6-MT		x				
Cd_2Zn_5-MT		**X**	x			
Cd_3Zn_4-MT		**X**	x			
Cd_4Zn_3-MT		x	**X**			
Cd_5Zn_2-MT		x	**X**	x	x	x
Cd_6Zn_1-MT			x	x	x	x
Cd_7-MT			x	**X**	**X**	**X**
Cd_6Zn_2-MT					x	x
Cd_7Zn_1-MT					x	x
Cd_8-MT					x	x

X: espècie majoritària x: espècie minoritària

Taula 1. Distribució de les espècies Cd-MT detectades mitjançant l'acoblament CZE-ESI-MS durant la valoració de Zn_7-MT recombinant de ratolí a pH 7 en funció del nombre d'equivalents de Cd(II) afegits.

presència de Cu, tal i com mostra la detecció per ICP-MS. La presència de Cu prové molt probablement de la contaminació del sistema, la qual és difícil d'eliminar. Els espectres d'ESI-MS han mostrat com l'addició de Cd a l'espècie Zn_7-MT provoca el desplaçament seqüencial i no cooperatiu del Zn pel Cd (veure Taula 1) amb una elevada tendència a desplaçar tot el Zn, fins a obtenir-se l'espècie Cd_7-MT, que s'ha presentat com a majoritària a partir de 7 equivalents de Cd(II) afegits, indicant la seva elevada estabilitat. Cal destacar, d'una banda, la presència de l'espècie Cd_6Zn_1-MT fins i tot en presència d'un gran excés de Cd. La dificultat que presenta la substitució total del Zn per Cd suggereix un important paper estructural del Zn en l'espècie Cd_6Zn_1-MT [14]. Aquest fet concorda amb el que s'havia observat, mitjançant simulacions semiempíriques, en l'estudi de les preferències de Zn(II) i Cd(II) pels llocs de coordinació de la MT de mamífer [48]. D'altra banda, el fet que l'addició de més de 7 equivalents de Cd(II) provoqui el mateix efecte, la formació majoritària de l'espècie Cd_7-MT amb presència de quantitats menors d'espècies amb diferent metal·lació (Cd_5Zn_2-MT, Cd_6Zn_1-MT, Cd_6Zn_2-MT, Cd_7Zn_1-MT i Cd_8-MT), obtenint-se els mateixos electroferogrames, indica que un excés de Cd(II) en el medi no altera significativament els senyals electroforètics.

Cal remarcar que els resultats obtinguts mitjançant CZE-ESI-MS són complementaris als obtinguts mitjançant RMN [47]. Però, si bé l'estudi de l'enllaç de Cd(II) a l'espècie Zn_7-MT mitjançant RMN de ^{113}Cd va aportar informació significativa referent a la distribució metàl·lica entre els dos dominis de MT, la complexitat dels espectres presentats no va fer possible l'obtenció de informació referent al nombre i estequiometria de les espècies presents en solució [47].

48. C. C. Chang, P. C. Huang. *Protein Eng*., 1996, **9**, 1165-1172.

D'altra banda, donat que el Cu és un contaminant no desitjat freqüent en els sistemes on s'analitzen mostres biològiques, i que la seva eliminació és molt difícil, es va estudiar l'addició de Cu(I) a l'espècie Cd_7-MT 1 recombinant de ratolí i també a dues isoformes comercials de MT 1 i MT 2 (Sigma-Aldrich). L'addició de Cu(I) de manera controlada a les diferents mostres de Cd-MT ha provocat el desplaçament gradual del Cd(II). Els electroferogrames obtinguts han mostrat pics amb diferents temps de retenció que varien en nombre i en intensitat, en funció de la quantitat de Cu present a la mostra i de l'espècie de partida. Els espectres d'ESI-MS obtinguts han permès observar la coexistència d'un gran nombre d'espècies Cu-MT de diferents estequiometries per cada addició de Cu(I). Aquestes observacions permeten concloure que en l'estudi de MT mitjançant CZE, la presència de Cu, que és un contaminant freqüent a les mostres biològiques, provoca l'aparició de diversos pics als electroferogrames, i per tant, aquest fet posa en dubte algunes de les conclusions extretes utilitzant el sistema CZE-UV, ja que en diverses publicacions s'ha considerat que cada pic que apareix als electroferogrames correspon a una isoforma diferent i no a possibles espècies diferents de la mateixa isoforma.

Així doncs, la interfase utilitzada en l'acoblament CZE-ICP-MS ha permès aconseguir que la resolució separativa d'aquest sigui comparable a la del sistema CZE-UV, el qual presenta la màxima resolució separativa possible mitjançant la CZE, a més a més de disposar d'un sistema de detecció selectiu. Així, aquests avantatges que ofereix l'acoblament CZE-ICP-MS demostren que és una eina d'anàlisi elemental a tenir en compte per a l'estudi d'intercanvis metàl·lics en metal·lotioneïnes.

De la mateixa manera, l'acoblament CZE-ESI-MS ha demostrat ser un bon sistema de separació i detecció per a l'estudi de sistemes metall-MT que contenen un elevat contingut en tampó i en ions metàl·lics, permetent determinar l'estequiometria de les espècies formades en les reaccions de substitució metàl·lica en MT i aportant informació complementària a la obtinguda mitjançant les tècniques d'espectroscòpia òptica.

5.2. El catió Ag^+ com a model en l'estudi de Cu-MT

Durant força temps s'ha considerat que els ions Ag(I) podien ser uns bons substituts de Cu(I) per a l'estudi de les MT que contenen Cu atès que el catió Ag(I) és estable a l'oxidació, presenta isòtops actius a l'RMN i propietats coordinants properes a les de Cu(I). Tot i així, darrerament s'han publicat diversos treballs que posen en dubte la idoneïtat en la substitució de Cu(I) per Ag(I) per a l'estudi de les MT esmentades [18].

El procediment seguit en el nostre estudi sobre la idoneïtat dels ions Ag(I) com a sonda per a l'estudi de les MT que contenen Cu, ha consistit en valorar les formes Zn-MT i apo-MT de les tres proteïnes amb Ag(I) a pH 7.5 i 2.5, i seguir aquestes valoracions mitjançant

l'espectroscòpia òptica i l'espectrometria de masses. Posteriorment s'ha realitzat la comparació del comportament de Ag(I) i Cu(I) enfront aquestes proteïnes.

La utilització de l'acoblament CZE-ESI-MS ha proporcionat per primer cop dades espectromètriques dels sistemes Ag-MT. Aquestes no només han confirmat l'existència de les espècies postulades per espectroscòpia òptica, sinó que també han permès detectar un major nombre d'espècies, determinar la seva estequiometria i alhora posar de manifest una important coexistència d'espècies en pràcticament tots els punts de les valoracions. Com a conseqüència, la tècnica de l'ESI-MS s'ha revelat com una metodologia imprescindible si es pretén assolir un coneixement profund dels sistemes Ag-MT i sempre que sigui possible, dels sistemes metall-MT.

La coordinació de Ag(I) a la MT sencera i als seus fragments α i β dóna lloc a la formació d'un gran nombre d'espècies, entre les quals cal destacar diverses espècies heterometàl·liques Ag,Zn-MT que no havien estat descrites amb anterioritat.

Anàlogament al que s'havia descrit pel Cu(I), la comparació entre les valoracions de les tres proteïnes amb Ag(I) realitzades a pH 7.5 i 2.5 ha fet palès el paper estructural del Zn quan aquestes enllacen Ag(I). Les dades de DC indiquen les diferències estructurals entre les espècies Ag-MT formades a partir de les formes apo- i les formades a partir de les Zn-MT, tot i la coincidència en algunes estequiometries, i en conseqüència, es pot concloure que el Zn exerceix un efecte plantilla en els agregats Ag(I)-MT.

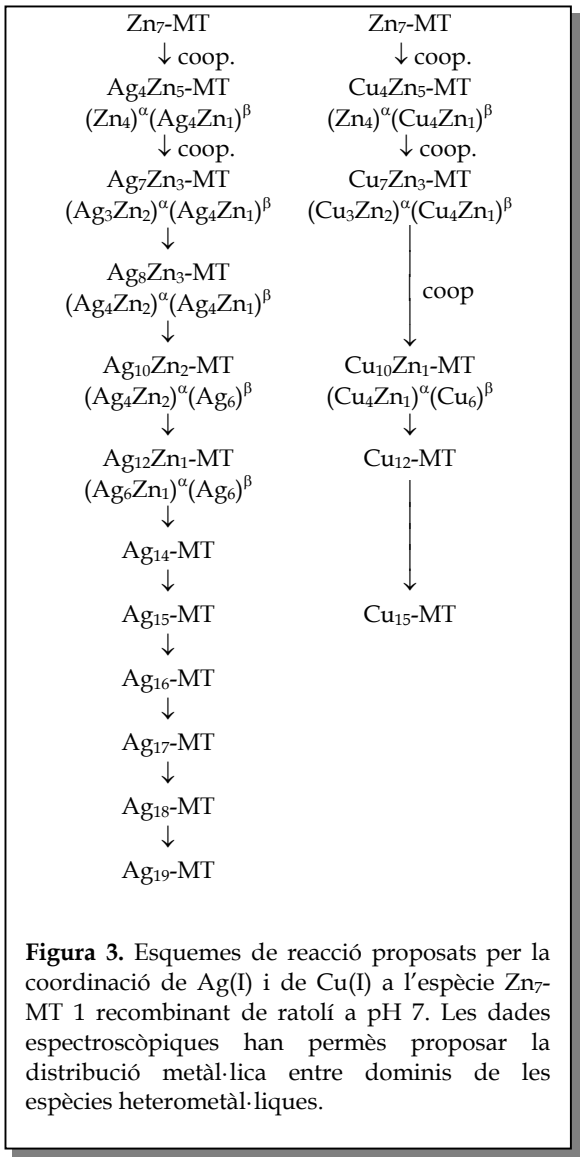

Figura 3. Esquemes de reacció proposats per la coordinació de Ag(I) i de Cu(I) a l'espècie Zn_7-MT 1 recombinant de ratolí a pH 7. Les dades espectroscòpiques han permès proposar la distribució metàl·lica entre dominis de les espècies heterometàl·liques.

El conjunt de les dades òptiques i espectromètriques obtingudes en les valoracions dels fragments α i β ha permès proposar la distribució metàl·lica entre dominis d'algunes de les espècies que es formen al llarg de la valoració de Zn_7-MT amb Ag(I). Aquesta distribució revela que únicament a l'inici de la valoració hi ha una preferència coordinativa del catió Ag^+ pel domini β. També s'ha observat que el comportament dels fragments per separat no reprodueix exactament el que manifesta la MT sencera, la qual cosa indica que els dos dominis de la MT no actuen de manera completament independent. Una

conclusió important és que l'estructura bidominial de la MT sencera es manté mentre hi ha Zn coordinat a la proteïna. Un cop els ions Ag(I) desplacen l'últim Zn(II) coordinat, l'agregat evoluciona cap a una estructura presumiblement monodominial, com la que ja s'havia descrit en el cas del Cu(I).

Estudis anteriors referents a la coordinació de Ag(I) a apo-MT [31, 34] i a Zn_7-MT [22, 33] a pH 7 van proposar la formació de Ag_{12}-MT i $Ag_{17\text{-}18}$-MT en ambdues valoracions, si bé també es formava Ag_6-MT a partir de l'apo-MT i M_4Ag_6-MT en valorar M_7-MT (M = Zn, Cd) [21, 22, 33]. De la mateixa manera, les valoracions amb Ag(I) de les espècies apo-αMT [7, 28, 31], Zn_4-αMT [33], apo-βMT [7, 28, 31] i Zn_3-βMT [33] van indicar la formació de Ag_6-αMT i Ag_6-βMT, mentre que a partir de les apo-formes també s'havien format les espècies Ag_3-αMT i Ag_3-βMT. Probablement, les diferències observades entre les dades bibliogràfiques i les obtingudes en el treball que aquí es presenta siguin degudes a diversos factors, com pot ser el fet d'utilitzar proteïnes de diferent naturalesa (natives i recombinants), les condicions en que s'han realitzat els diferents experiments (pH, concentració de la proteïna, temperatura) i la possibilitat d'avaluar el contingut en Zn de les espècies Ag-MT. Tot i així, les dades espectroscòpiques i espectromètriques que s'han presentat en aquest treball referents a l'enllaç de Ag(I) tant a les apo-MT com a les Zn-MT evidencien la necessitat d'un control rigorós del pH i la necessitat de diverses tècniques complementàries per assolir un coneixement profund del sistema Ag-MT.

En comparar els comportaments de Ag^+ i Cu^+ enfront les diverses proteïnes estudiades s'observa una elevada similitud entre ambdós ions metàl·lics però restringida als primers estadis de la substitució del Zn(II) per Ag(I), el que s'evidencia en l'inici de les valoracions a pH 7.5 de MT sencera i del seu fragment α. El paral·lelisme observat en les empremtes espectrals de les espècies M_4Zn_5-MT i M_7Zn_3-MT (M = Ag, Cu) suggereix la seva isoestructuralitat, cosa que permet anticipar la possible determinació de l'estructura tridimensionals de les espècies anteriors de Cu(I) mitjançant la seva substitució per Ag(I).

En les formes apo de les tres proteïnes i en el fragment β a ambdós valors de pH no s'ha trobat cap similitud de comportament entre Ag i Cu. El fet que el fragment Zn_3-βMT enllaci Ag(I) i Cu(I) de manera diferenciada és molt probablement degut a que en el cas del Cu, a diferència del de la Ag, no s'observa un efecte plantilla del Zn. Pel que fa a les apo-proteïnes, les diferències coordinatives que presenten les tres proteïnes envers Ag(I) i Cu(I) podrien justificar-se en base a les diferents afinitats i preferències coordinatives d'aquests dos ions metàl·lics envers els lligands tiolat (Ag(I) digonal, Cu(I) trigonal).

La comparació entre Ag(I) i Cu(I) aquí presentada indica doncs que, si bé aquests cations poden presentar un comportament similar en coordinar-se a les MT, tal i com havien postulat alguns autors anteriorment [24, 25, 26], aquesta similitud només es dóna en les primeres espècies heterometàl·liques Ag,Zn-MT procedents de la substitució Zn/Ag de les formes Zn-MT, i en el cas de MT de mamífers, només per la MT sencera i el fragment α. Aquests resultats en part

justifiquen que alguns autors hagin qüestionat el possible reemplaçament isomorf de Cu(I) per Ag(I) en MT [18].

5.3. MTO de *Drosophila melanogaster*: contribució a una nova classificació de MT.

Fins a la presentació d'aquest treball, només s'havien descrit dos gens que codifiquen per a la síntesi de MT en *Drosophila melanogaster*: *Mtn* i *Mto*, que determinen les proteïnes MTN (40 aa, 10 Cys) i MTO (43 aa, 12 Cys), respectivament. L'estudi de la capacitat coordinant de MTN envers diferents ions metàl·lics tant *in vivo* com *in vitro* juntament amb l'anàlisi de les relacions filogenètiques amb d'altres MT evolutivament properes, va conduir a la classificació de la MTN com a Cu-tioneïna [16].

L'estudi de MTO de *Drosophila* contempla dos objectius principals: la determinació de les seves propietats coordinants tant *in vivo* com *in vitro* enfront de Zn i de Cu a fi de poder-la classificar com a Zn- o Cu-tioneïna; i la comparació del seu comportament coordinatiu amb el de MTN per tal de trobar els motius que justifiquen la presència d'ambdues proteïnes en *Drosophila*.

L'expressió de MTO en medis enriquits en Zn ha donat lloc a la formació majoritària de l'espècie Zn_4-MTO que, en funció de les condicions de síntesi, presenta uns graus d'oxidació considerables, mentre que en medis enriquits amb Cu s'obté una barreja equimolar de Cu_8- i Cu_9-MTO, que en cultius a petita escala es redueix únicament a Cu_9-MTO.

Les dades presentades en aquest treball han permès establir que en presència de metalls divalents, les espècies d'estequiometria M_4-MTO (M = Zn, Cd) són les més estables. També s'ha pogut apreciar una certa capacitat dels agregats M_4-MTO per coordinar un cinquè M(II) sense alteració significativa de la seva estructura. Cal destacar que s'ha pogut descriure per primer cop unes característiques espectroscòpiques que indiquen la participació dels ions Cl^- en l'estructura dels agregats M_4-MTO, si bé el seu paper estructural és més important en el cas del Zn que en el del Cd. Aquesta participació dels clorurs en la coordinació metàl·lica s'ha revelat com un tret diferencial entre MTN i MTO. Així mateix, l'espècie Cd_4-MTO dóna lloc a l'agregat Cd_9-MTO en presència d'excessos importants de Cd(II) en el medi.

La substitució *in vitro* de Zn(II) per Cu(I) en l'espècie Zn_4-MTO ha mostrat la formació d'un conjunt d'espècies, entre les quals cal destacar l'espècie Cu_4Zn_2-MTO com a única espècie heterometàl·lica determinada en aquesta valoració, i l'espècie Cu_9-MTO que presenta una empremta espectral pràcticament idèntica a l'obtinguda en la síntesi *in vivo* en medis rics en Cu. Aquests resultats han permès demostrar que l'espècie homometàl·lica Cu_9-MTO és la que es biosintetitza en entorns cel·lulars rics en Cu, si bé, aquesta espècie presenta una certa tendència a alliberar un catió Cu(I) per donar lloc a l'espècie Cu_8-MTO sense variar pràcticament la seva estructura. L'addició de més Cu(I) a la solució proteica un cop s'ha

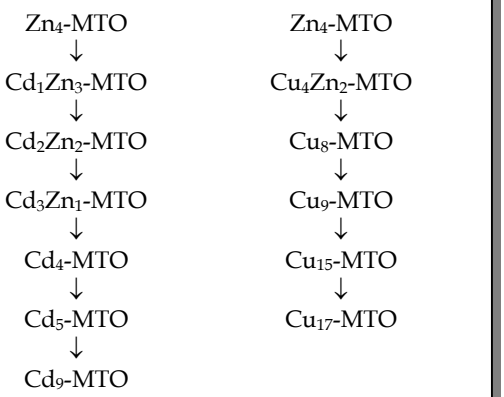

Figura 4. Esquemes de reacció proposats per a la valoració de Zn_4-MTO a pH 7 amb Cd(II) (A) i amb Cu(I) (B).

format l'espècie Cu_9-MTO dona lloc a la coordinació de més cations Cu(I) fins arribar a la saturació per 17 Cu(I).

Aquest conjunt de resultats ha permès classificar MTO com una segona Cu-tioneïna de *Drosophila*, cosa que implica que *D.melanogaster* és l'únic metazou conegut que no presenta cap Zn-tioneïna.

L'anàlisi de l'estructura primària de MTO i la seva comparació amb la d'altres MT ha indicat que la MTO està relacionada seqüencialment amb les Cu-tioneïnes analitzades i clarament diferenciada de les Zn-tioneïnes. Alhora, la seva seqüència és més propera a CUP 1 de *S.cerevisiae* que a MTN, la qual cosa sembla indicar que la diferenciació entre MTO i MTN ha estat prèvia a la diferenciació de *Drosophila* de la resta d'artròpodes.

La comparació entre MTO i MTN ha permès observar que, si bé l'anàlisi seqüencial d'ambdues proteïnes revela certes diferències, el seu comportament envers Cu(I), Cd(II) i Zn(II) és significativament proper, amb l'excepció que la capacitat coordinant de l'MTO és superior donades les seves 2 Cys addicionals. Conseqüentment, amb les dades de què actualment es disposa, no és possible justificar la presència de dues Cu-tioneïnes en *D.melanogaster*, i per tant, caldran estudis més profunds per determinar si són els patrons d'expressió, les petites diferències coordinatives o algun altre factor, els responsables de la presència de dues Cu-tioneïnes en aquest organisme, així com la possible existència d'alguna Zn-tioneïna.

6. Conclusions

El treball realitzat en el marc d'aquesta tesi doctoral permet arribar a un conjunt de conclusions que s'exposen a continuació agrupades d'acord amb els objectius proposats.

6.1. Aplicació de l'espectrometria de masses a l'estudi de MT amb Cd

- L'acoblament CZE-ESI-MS permet la separació del tampó present en les solucions metall-MT i en conseqüència la determinació acurada del nombre i de l'estequiometria de les espècies proteiques presents en solució. Aquesta metodologia amplia substancialment la informació obtinguda habitualment mitjançant espectroscòpia òptica.
- La nova interfase utilitzada en l'acoblament CZE-ICP-MS permet aconseguir una resolució separativa òptima, comparable a la del sistema CZE-UV, la qual cosa permet disposar de les elevades prestacions de la CZE, que combinades amb l'especificitat de l'ICP-MS, fan de l'acoblament CZE-ICP-MS una eina a tenir en compte per a l'estudi de l'intercanvi metàl·lic en les MT.
- Els avantatges de l'acoblament CZE-ESI-MS queden substancialment alterats quan el sistema analític està contaminat per traces de Cu, el que sovint és difícil de subsanar, ja que provoca l'alteració dels electroferogrames obtinguts. En aquest cas, es fa necessària la utilització prèvia d'un sistema de detecció selectiu pels elements o les molècules en estudi, com per exemple l'ICP-MS. D'aquesta manera la determinació per ESI-MS es pot restringir als senyals electroforètics que corresponen exclusivament a la mostra en estudi.
- L'acoblament CZE-ESI-MS ha permès ampliar les dades existents sobre la substitució de Zn per Cd en Zn_7-MT. Així, en la valoració de Zn_7-MT amb Cd(II) a pH 7 s'ha observat el desplaçament seqüencial i no cooperatiu del Zn pel Cd fins donar lloc a la formació de l'espècie Cd_7-MT, la qual, si bé és majoritària, coexisteix amb d'altres espècies, entre les quals cal destacar Cd_6Zn_1-MT. La dificultat de substitució de tot el Zn inicialment coordinat a la proteïna podria ser atribuïda a un paper estructural de l'ió Zn(II) en les espècies Cd-MT.

6.2. El catió Ag^+ com a model en l'estudi de Cu-MT

- La coordinació dels ions Ag(I) a Zn_7-MT, Zn_4-αMT i Zn_3-βMT, així com a apo-MT, apo-αMT i apo-βMT, provoca la formació d'un gran nombre d'espècies, tan homo- (Ag_x-MT) com heterometàl·liques (Ag_xZn_y-MT), fins arribar al punt de saturació de les diferents proteïnes estudiades, que és proper a una relació $Ag:S_{Cys}$ de 1 (veure Fig. 5).
- La distribució metàl·lica entre dominis per a les espècies formades en la substitució Zn(II)/Ag(I) en l'espècie Zn_7-MT ha revelat que l'estructura bidominial inicial només es manté mentre hi ha Zn coordinat a la proteïna, i un cop els ions Zn(II) han estat totalment desplaçats per Ag(I), l'estructura esdevé presumiblement monodominial.

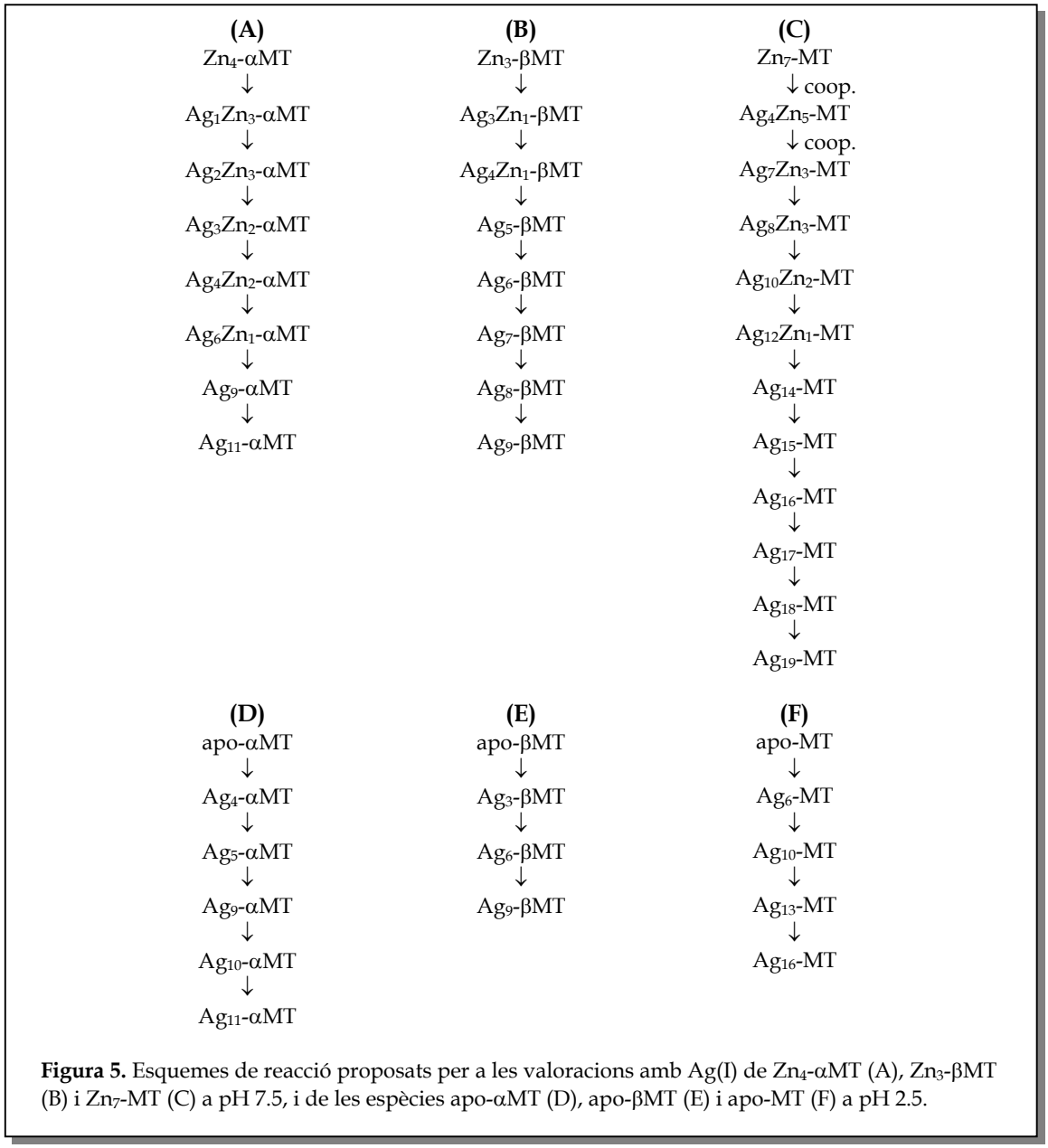

Figura 5. Esquemes de reacció proposats per a les valoracions amb Ag(I) de Zn_4-αMT (A), Zn_3-βMT (B) i Zn_7-MT (C) a pH 7.5, i de les espècies apo-αMT (D), apo-βMT (E) i apo-MT (F) a pH 2.5.

- En presència de Ag(I), tant la MT sencera com els seus fragments per separat, donen lloc a un conjunt d'espècies més nombrós que en presència de Cu(I), especialment quan es parteix de les espècies Zn-MT, indicant una complexitat coordinativa superior dels sistemes Ag-MT.
- Quan es substitueix el Zn, tant de la MT sencera com del seu fragment α, el grau de metal·lació assolit és molt superior en presència de Ag (Ag_{19}-MT, Ag_{11}-αMT) que en presència de Cu (Cu_{15}-MT, Cu_9-αMT), mentre que en el fragment β les diferències no son tan importants (Ag_9-βMT *vs*. Cu_{10}-βMT).
- En el cas del fragment β no hi ha cap similitud significativa entre Ag i Cu, probablement degut a que el Zn no realitza cap efecte plantilla en el cas del Cu però sí ho fa en cas de la Ag.
- El comportament de la MT sencera i el seu fragment α enfront de Ag(I) i Cu(I) és molt similar en les primeres fases de les valoracions. En el cas de MT sencera s'ha observat la formació cooperativa de les espècies M_4Zn_5-

MT i M_7Zn_3-MT (M = Ag, Cu), amb una distribució metàl·lica entre dominis idèntica i unes empremtes espectrals comparables, indicant així la seva possible isoestructuralitat. D'aquesta manera, hauria de ser possible determinar l'estructura de Cu_7Zn_3-MT, que és la que s'expressa in vivo en un medi enriquit amb Cu, mitjançant RMN de Ag.

- El comportament de Ag i Cu envers les apo-formes estudiades és significativament diferent, la qual cosa suggereix que les similituds observades en MT i el seu fragment α per les primeres espècies M, Zn-MT (M = Ag, Cu) formades a pH 7.5 es deuen molt probablement a la presència de Zn i a l'efecte plantilla que aquest exerceix en la coordinació de Ag(I) a MT.
- La Ag és un bon model del Cu en MT sencera i el seu fragment α únicament quan es parteix de les Zn-MT corresponents i només per a les espècies heterometàl·liques Cu,Zn-MT que es formen a l'inici de les valoracions.

6.3. MTO de *Drosophila melanogaster*: contribució a una nova classificació de MT.

- Les síntesis *in vivo* de la isoforma MTO de *Drosophila* en medis rics en Cu dóna lloc a la barreja equimolar de les espècies homometàl·liques Cu_8-MTO i Cu_9-MTO en condicions standard de cultiu i únicament Cu_9-MTO en cultius a petita escala sota un major control. La síntesis *in vivo* de MTO en medis enriquits en Zn dóna lloc a la formació majoritària de l'espècie Zn_4-MTO, acompanyada de petites quantitats de les espècies Zn_3-MTO i Zn_5-MTO.
- Els estudis *in vitro* a partir de Zn-MTO tant amb Cd(II) com amb Cu(I) a pH 7 han permès observar la formació successiva d'un conjunt d'espècies (veure apartat 5.3, Fig. 4) entre les quals cal destacar l'espècie Cd_4-MTO per ser la més estable en la valoració amb Cd(II), mentre que en la valoració amb Cu(I) destaca la formació d'una espècie inicial heterometàl·lica Cu_4Zn_2-MTO i posteriorment d'altres espècies homometàl·liques Cu-MTO fins assolir un grau màxim de 17 Cu(I) coordinats.
- Les dades experimentals (síntesis *in vivo* en medis rics en Cu i substitució *in vitro* de Zn(II) per Cu(I) en l'espècie Zn_4-MTO) i la comparació de seqüències permeten classificar MTO com una segona Cu-tioneïna de *Drosophila melanogaster*, que es biosintetitza com a Cu_9-MTO en medis rics en Cu, tot i tenir una certa tendència a perdre un catió Cu(I) per donar lloc a l'espècie Cu_8-MTO.
- En presència de metalls divalents, les espècies M_4-MTO (M = Zn, Cd) són les més estables, si bé poden incorporar un cinquè M(II) sense una alteració significativa de la seva estructura.
- Per primer cop en l'estudi de les MT, s'han obtingut evidències experimentals (bandes d'absorció en la zona de l'UV diferents de les atribuïdes als enllaços M-S_{Cys}) de la participació dels ions Cl^- en l'estructura dels agregats metall-MT i en concret pels complexos M_4-MTO (M = Zn, Cd).
- Si bé MTO presenta una capacitat superior per coordinar ions metàl·lics, tan monovalents com divalents, MTO i MTN es comporten de

manera similar en presència d'aquests ions, el que de d'un punt de vista biològic deixa oberta la cerca de Zn-tioneïnes en *Drosophila*.